University of Catania

International PhD in
Translational Biomedicine
XXVIII cycle

Coordinator: Prof. Daniele Filippo Condorelli

Giorgia Spampinato

Genomic analysis in human solid tumours: Copper Homeostasis Genes in Colorectal cancer

PhD Thesis

Tutor:
Prof. Vincenza Barresi

2013-2015

INDEX

1.1INTRODUCTION

1.1.1 COPPER: AN ESSENTIAL TRACE NUTRIENT

Metals are integral components of nearly all biological processes. Paradoxically, some metals are essential in trace amounts and toxic at elevated levels, some are simply toxic, while others are tolerated at excessively high levels by living cells. Uranium, arsenic, copper, and lead have all recently been implicated in novel biological roles [**Yannone *et al.,* 2012**]. It is common knowledge that the elemental building blocks of life as carbon, hydrogen, oxygen and nitrogen are considered, always as the elements essential to life. Really these fundamental components are predominate only in terms of mass in fact it is important to note that all life forms have an absolute requirement for a number of metals that are considered 'trace' elements and that play a key role to most biological processes.

Copper (Cu), zinc (Zn), and iron (Fe) are essential micronutrients for maintenance of life. These micronutrients are involved in many complex enzyme systems functioning in various biological processes. The metals are defined as essential when they are needed for the life of the cell and for the proper functioning of the physiological processes; The iron, for example, is an enzyme cofactor in higher eukaryotes that ensures normal functioning of hemoglobin, also the copper acts as a cofactor for many enzymes (eg. Superoxide dismutase, cytochrome oxidase, etc..) allowing their activity within the cell. Copper is required for respiration, connective tissue formation, iron metabolism, and many others processes. In human cells, copper is utilized in several cells compartments, and the intracellular distribution of copper is regulated in response to metabolic demands and changes in cell environment [**Lutsenko 2010**].

However even if the copper and the iron are involved in various physiological processes important to the cell at high concentrations, can lead to the formation of free radicals and promote lipid peroxidation, leading to a rapid decline in the integrity of biological membranes but can also cause damage DNA and RNA, for this reason the concentration of free copper in the cell is maintained at ≤ 10^{-18} M [**Howell *et al.,* 2010**]. The life-supporting properties of Cu incur a significant challenge to cells that must not only exquisitely balance intracellular Cu concentrations, but also chaperone this redox-active metal from its point of cellular entry to

its ultimate destination so as to avert the potential for inappropriate biochemical interactions or generation of damaging reactive oxidative species (ROS) [**Nevitt *et al.,* 2012**].

For these important characteristics the ability of an organism to accumulate in appropriate concentrations these metal species, considered therefore as essential trace elements, is critical to your health.

1.1.2 COPPER HOMEOSTASIS

Copper (Cu), a transition metal with two redox states, is an essential trace element in living organisms that acts as a catalytic cofactor for a number of enzymes involved in critical biological processes including protection against free radicals (superoxide dismutase), oxidative phosphorylation (cytochrome c oxidase), pigmentation (tyrosinase) collagen maturation (lysyl oxidase) and neuropeptide and peptide hormone production (peptidylglycine alpha amidating mono-oxygenase, PAM). [**Mufti *et al.,* 2007**]

Copper functions as the active centre of cuproenzymes, such as cytochrome c oxidase (CCO), Cu,Zn-superoxide dismutase (Cu,Zn-SOD, SOD1), ceruloplasmin, lysyl oxidase, tyrosinase, and dopamine β-hydroxylase. However, free copper is very toxic due to its ability to react with hydrogen peroxide and generate highly reactive hydroxyl radicals [**Mufti *et al.,* 2007**] (Fig. 1). Other possible molecular events that contribute to the toxicity of copper in vivo include inappropriate insertion of copper into metalloproteins (so-called protein hijacking), copper-dependent perturbation of membrane potential, and inhibition of membrane ATPases.

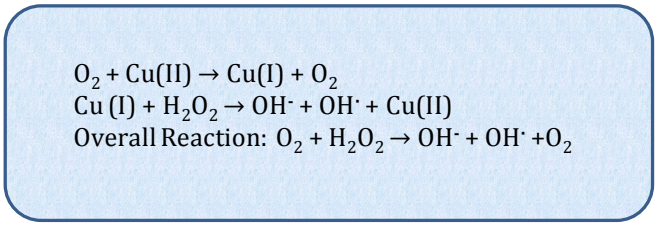

Figure 1. Chemical reactions of copper.

Consequently, free copper in the cell is almost undetectable and complex homeostatic mechanisms have evolved to regulate intracellular copper distribution and excretion (Fig. 2). Copper (Cu^+) is transported into the cell via the high affinity Copper transporter (Ctr) proteins, which are highly conserved from yeast to humans. [**Lee *et al.,* 2001**] All Ctr proteins

contain three transmembrane domains, and most possess extracellular methionine rich motifs (MxxM, MxM) at the amino terminal and an additional MxxxM motif in the second transmembrane domain. [**Guo *et al.,* 2004**] These domains are essential for binding extracellular copper and facilitating transport into the cell.

Metalloreductases, Step2, bound to the plasma membrane, and Steap3-4 located on membrane of intracellular vesicles. Both are responsible for reducing of Cu^{2+} to Cu^{1+} prior to transport through the membrane. [**Puing *et al.,* 2002**]

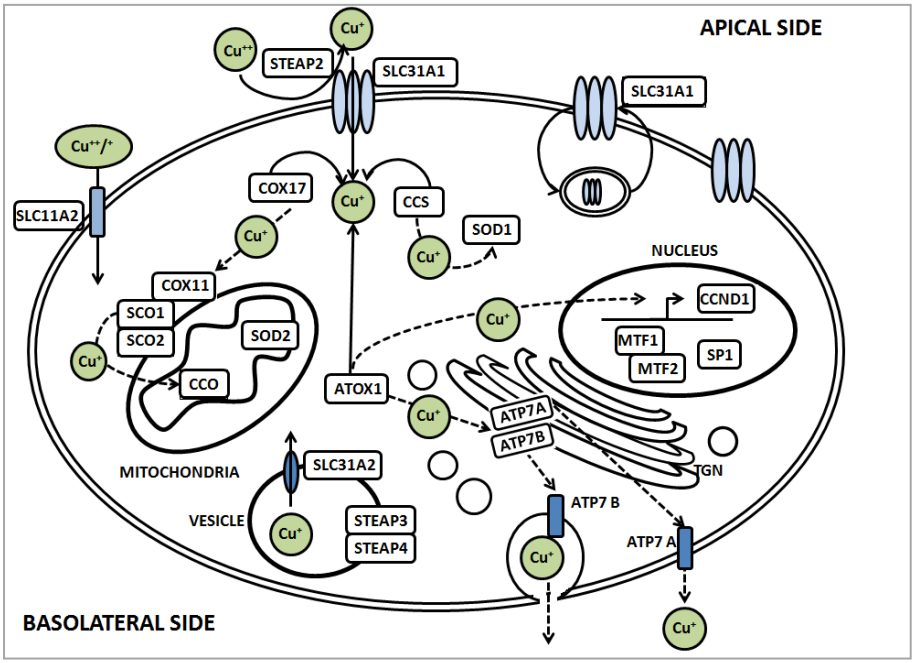

Figure2. Copper distribution pathways in a generalized mammalian cell.

Two Ctr homologs, Ctr1 (SLC31A1 gene) and Ctr2 (SLC31A2 gene), have also been identified in vertebrates, and of these, Ctr1 is the main protein responsible for intracellular copper transport. The exact function of Ctr2 in vertebrates remains unclear. [**Rees *et al.,* 2004**] Due to its toxicity, intracellular copper trafficking is very tightly regulated and evolutionarily conserved pathways have evolved for the handling of copper upon entry into the cell involving proteins, known as chaperones, whose function is the delivery of copper to specific targets (Fig. 2). [**Mufti *et al.,* 2007**] Delivery of copper to superoxide dismutase (SOD1), a zinc and copper containing protein, occurs via the Copper Chaperone for SOD (CCS), which is found in both the cytoplasm and the intermembrane mitochondrial space (IMS). SOD1 is an important enzyme, which catalyzes the conversion of superoxide anion to hydrogen peroxide and oxygen (Fig. 3).

$$SOD\text{-}Cu(II) + O_2^{\cdot} \leftrightarrow SOD\text{-}Cu(I) + O_2$$
$$SOD\text{-}Cu(II) + O_2^{\cdot} \leftrightarrow SOD\text{-}Cu(II) + H_2O_2$$

Figure 3. SOD catalytic mechanism.

Mutations in SOD1 are associated with amyotrophic lateral sclerosis (ALS), a neurodegenerative disorder characterized by the loss of upper and lower motor neurons and muscle atrophy. [**Rowland *et al.,* 2002**]

Another example of intracellular copper handling involves copper delivery to Cytochrome c Oxidase (CcO), the terminal enzyme in the respiratory chain (Fig. 2). CcO enzyme in mammals is located within the mitochondrial inner membrane needs three copper ions to perform its function. The CcO and is constituted by 13 subunits, two of which contain two copper centres. One, called CuB, is a monocopper site in subunit I, and the other, called CuA, is a binuclear site in subunit II. [**Banci *et al.,* 2008**] A number of proteins are required for the metallation of these sites. For copper insertion into the CuA site, Cox17, Sco1, and Sco2 proteins have been proposed to have essential non-overlapping roles within the mitochondrial intermembrane space (IMS), the first working as a metallochaperone to Sco1 and Sco2 [**Horng *et al.,* 2004. Leary *et al.,* 2004**], whereas the other two have a cochaperone function during the copper insertion in the CuA site.

Antioxidant protein 1, or Atox1, is a cytosolic copper chaperone , like CCS and / or small thiol molecules such as glutathione, binds the ‘‘Labile’’ Cu pool, entered in the cytosolic environment by SLC31A1 transporter, coordinating its further intracellular destination while the excess copper is sequestered by metallothioneins to avoid build-up to toxic levels (‘‘Immobilized’’ copper pool). [**Hatori and Lutsenko 2013**]. Atox1 is responsible for the shuttling of Cu^{1+} to the export pumps ATP7A/B (Fig. 4). These are the main transporters responsible for copper excretion from cells, and are both found in the trans-Golgi network, contain six MxCxxC metal binding domains (MBDs) at their amino termini and each MBD is capable of binding one atom of copper [**Lutsenko *et al.,* 2002**]. Following binding to copper and under normal or low copper conditions, ATP7A/7B translocate Cu^{1+} into the lumen of the secretory vesicles for integration into cuproenzymes such as ceruloplasmin and tyrosinase [**Miyayama *et al.,* 2009**]. The exact manner in which copper is loaded onto cuproenzymes in the secretory compartment is not known.

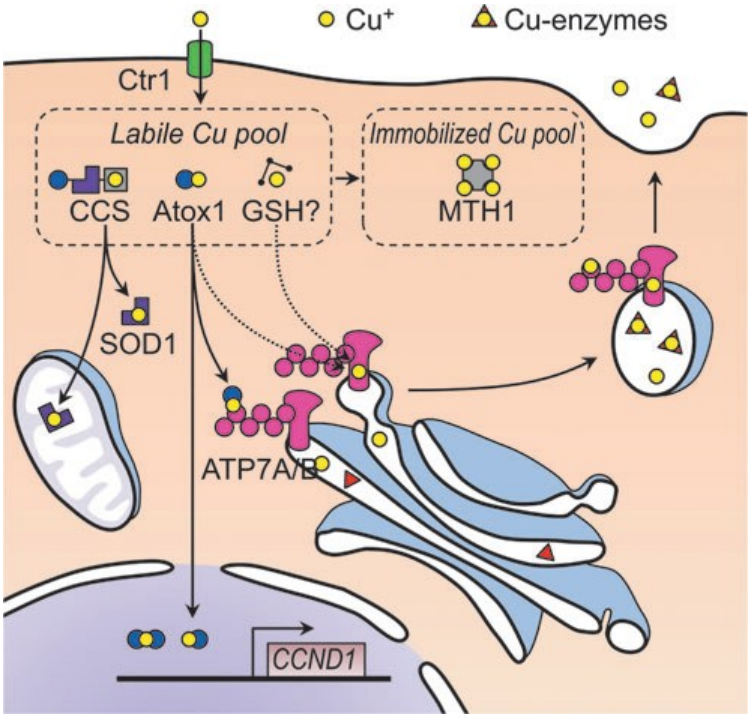

Figure 4. Atox1 role in cellular copper trafficking pathways, taken from Hatori *et al.,* 2013.

ATP7A is present in most tissues of the body and is highly expressed in intestinal epithelial cells but is absent in hepatic tissue. In the intestinal epithelium, ATP7A is required to mediate delivery of copper from the cell to the systemic circulation and thus it is essential for the systemic absorption of copper from the gastrointestinal tract. [**Voskoboinik *et al.,* 2002**] In the presence of elevated copper levels, ATP7A translocates to the plasma membrane and pumps excess copper out of the cell.

Like ATP7A, in elevated copper states, ATP7B moves from post-Golgi vesicles to the plasma membrane, specifically the biliary canalicular membrane allowing copper excretion into bile. This constitutes the main pathway for copper efflux from the body. Because of mutations in the gene ATP7B, the copper accumulates in the liver. First inducing the production of metallothioneins (MTs), a family of small proteins (7 kDa) containing a high proportion of cysteins. SH groups of MTs can bind metal ions with high affinity acting as a buffer system or a reservoir for essential copper and zinc ions. [**Zalewska *et al.,* 2014**] These proteins are able to sequester toxic metal ions and exchange them for zinc [**Aicha Ba *et al.,* 2009**] or can apparently maintain copper in a relatively harmless state. Subsequently, this accumulation of copper causes damage to mitochondria initially, and eventually leads to destruction of the hepatocyte. In Wilson's disease, the copper is also deposited in renal tubules, and kidney damage occurs to varying degrees. A combination of copper accumulation

in the blood as well as impaired expression of *ATP7B* in the brain, leads to neurological disease, by mechanisms not entirely explained.

X-linked inhibitor of apoptosis (XIAP), known primarily for its caspase inhibitory properties, has recently been shown to interact with and regulate the levels of COMMD1, a protein associated with a form of canine copper toxicosis.

It was recently reported that COMMD1, copper metabolism (Murr1) domain containing 1, interacts with ATP7B (Fig. 5), to mediate the efflux of copper from the cell [**Tao *et al.*, 2003**], although, the functional role of this interaction remains to be elucidated. COMMD1 is the prototypical member of a family of ten homologous and highly conserved proteins known as COMMD1 to 10 [**Burstein *et al.*, 2005**]. The defining characteristic is the presence of a unique carboxy-terminal domain termed the COMM domain (copper metabolism gene MURR1).

In addition to its role in copper homeostasis, COMMD1 and other COMMD proteins also function as negative regulators of the transcription factor NF-κB.

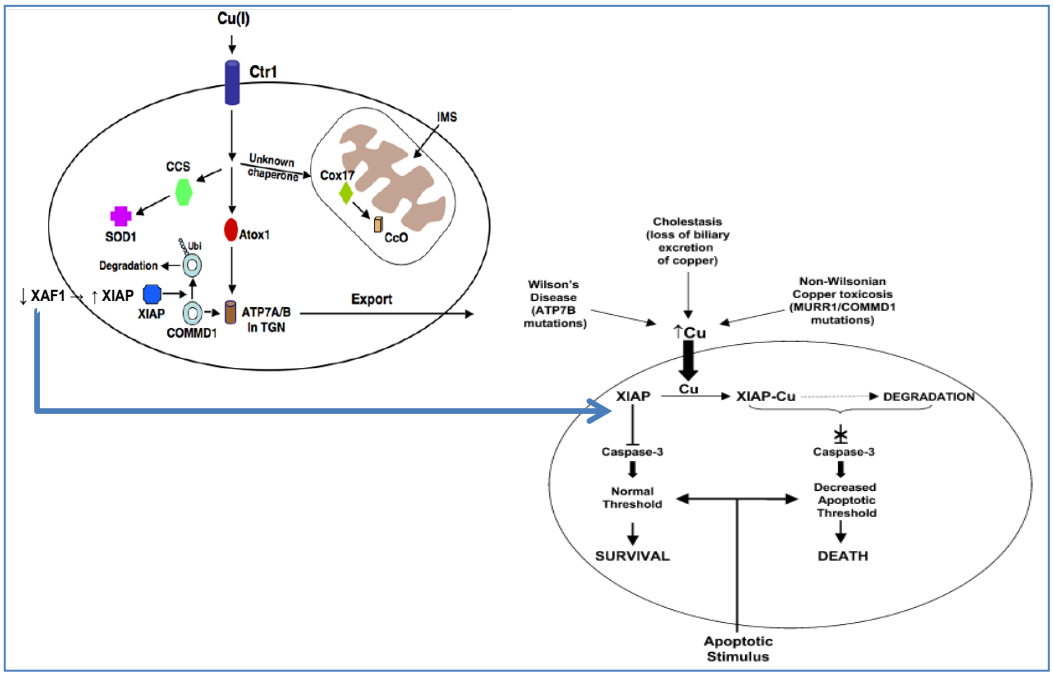

Figure 5. Model of copper uptake and metabolism taken from Mufti et al., 2007.

XIAP-associated factor 1 (XAF1) has been identified as an X-linked inhibitor of apoptosis (XIAP) binding partner (**Mufti *et al.*, 2007**). XAF1 interacts with endogenous XIAP and results in XIAP sequestration in nuclear inclusions. XAF1 mRNA is expressed ubiquitously in all normal adult and fetal tissues, in contrast to very low or undetectable levels in various cancer

cell lines. Reduced or absent XAF1 expression seems to be a frequent event in human cancer tissues. Transient over expression of XAF1 sensitizes tumour cells to the proapoptotic effects and antagonizes the XIAP-mediated inhibition of caspase 3 activity. Moreover, loss of XAF1 expression correlates strongly with tumour staging, implicating loss of XAF1 function in tumour progression [**Shui Ping Tu *et al.,* 2010**].

1.1.3 ATOX1: COPPER CHAPERONE ANTIOXIDANT-1

One of the human copper chaperones is HAH1 (also called human Atx1 or Atox1), a small soluble protein [**Klomp *et al.,* 1997**] which is capable of delivering copper(I) both to the Menkes and the Wilson disease proteins (ATP7A and ATP7B, respectively). [**Petris *et al.,* 1996**]

The Atox1 gene is located on chromosome 5 and contains 4 exons and 3 introns. Atox1 encodes for a ubiquitously expressed protein of 68 amino acids and it is characterized by a fold *βαββαβ*. Antioxidant-1 (Atox1) contains a single N-terminal copy of the conserved MXCXXC copper binding motif (Fig. 6A) suggesting an interaction between Atox1 and ATP7A or ATP7B, in fact has been demonstrated that Atox1 in which the Cys residues, Cys12 and Cys15, of the MBS were mutated was unable to interact with ATP7B, indicating that the MBSs coordinate these interactions (Fig. 6B). [**Strausak *et al.,* 2003**] Another conserved lysine-rich region (KKTGK) is localized at C-terminus is (Fig. 6A), several data show that this domain represents the potential NLS (nuclear localization signal) and is involved in recruiting Atox1 to the nucleus, data confirmed *in vitro* [**Itoh *et al.,* 2008. Hamza *et al.,* 1999**] and *in vivo* [**Ozumi *et al.,* 2012**]. In these studies, it has been tested the hypothesis that, in mouse embryonic fibroblast cells (MEFs), nuclear Atox1 may be involved in regulating copper-induced cell proliferation and that copper stimulates cell proliferation in an Atox1-dependent manner, demonstrating also that the copper induces Atox1 nuclear translocation, binding to DNA at novel cis elements (GAAAGA; Atox1-responsive elements)(Atox1-RE) in the promoter of the cyclin D1 promoting cellular proliferation. [**Itoh *et al.,* 2008. Muller and Klomp, 2009**]

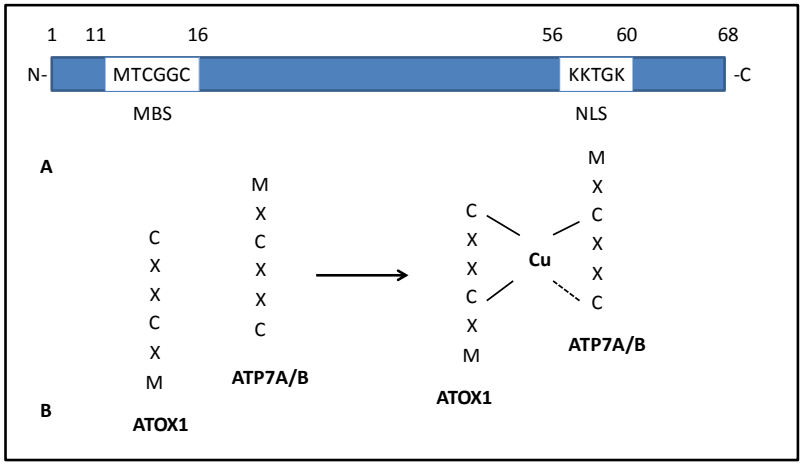

Figure 6 Structure of ATOX1 and homo / heterodimerization.

Tetrathiomolybdate (TTM) is a copper chelator, which blocks Atox1 function [**Alvarez *et al.,* 2010**], preventing tumor progression in clinical trials [**Brewer *et al.,* 2005**]

X-ray crystallography and biochemical analyses also revealed copper-dependent ATOX1 homodimerization. [**Wernimont *et al.,* 2000**] In these homodimers, two Cys residues of each monomer formed a three-coordinate Cu^{1+} complex with a loose interaction with the fourth Cys residue. These studies propose that Atox1 can function as a copper chaperone that delivers copper to the export pumps ATP7A or ATP7B and, alternatively, it can function as a copper-dependent transcription factor in which homodimerization copper-induced of Atox1 drives the expression of CCND1 and possibly other genes. In conclusion, Atox1 might shuttle between the nucleus and might form homodimers to activate transcription (Fig. 7). [**Muller and Klomp, 2009**]

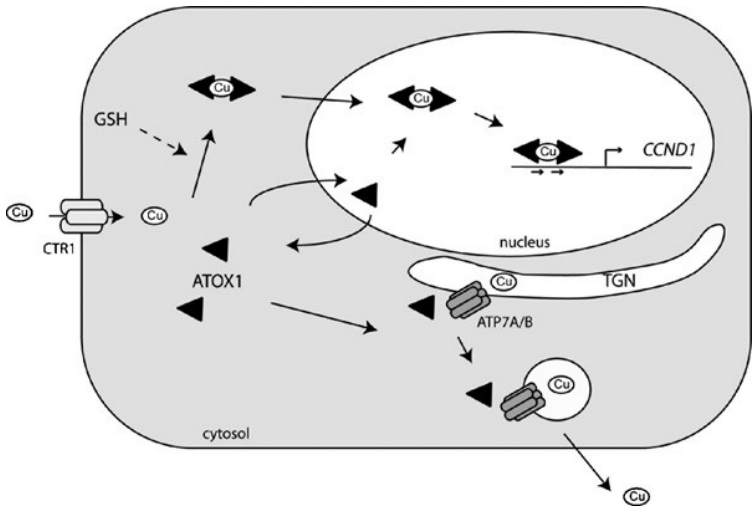

Figure 7. Cellular model of Atox1 function taken from Muller and Klomp, 2009.

CTR1: COPPER TRANSPORTER

The high-affinity copper transporter (Ctr1) (SCLC31A1 gene) is the main copper influx transporter and plays an important role in regulating copper homeostasis because Cu deficiency is detrimental to many important cellular functions while its excess is toxic.

The SLC31A1 gene is localized on long arm of 9 chromosome coding for the human Ctr1 protein. The Ctr1 proteins are integral membrane proteins have a length of 190 amino acids with a ~67 aa extra-cellular amino-terminal (ecto) domain and a ~15 aa carboxyl-terminal cytosolic tail. These transporters harboring three trans-membrane domains (TMD) and multiple copper-binding ligands (predominantly methionine, histidine or cysteine) within the extracellular amino-terminus, at the extracellular boundary of TMD2 and in the cytosolic carboxyl-terminus (Fig. 8). [**Puing *et al.*, 2002. Klomp *et al.*, 2003**]

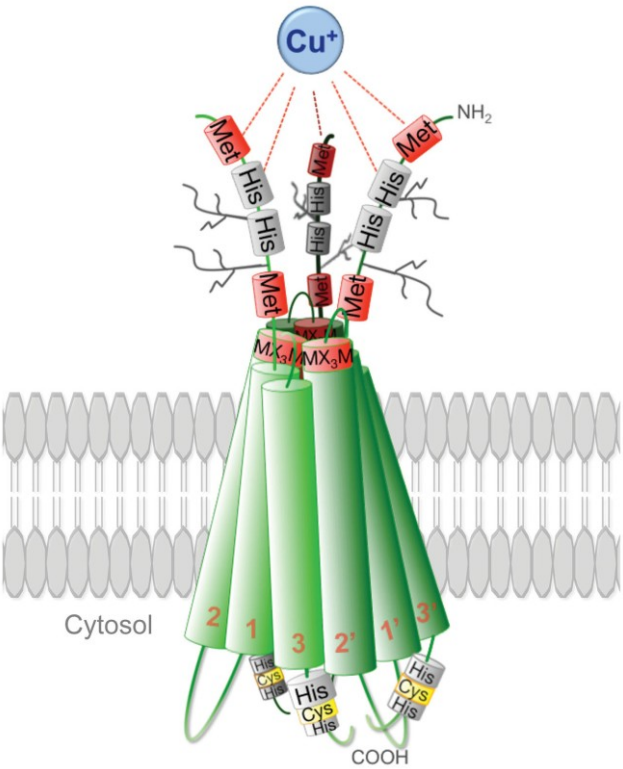

Figure 8. Structural model of three Ctr1 monomers in a lipid bilayer taken from Ohrvik and Thiele, 2014.

Recent insights into the 3D structure of human Ctr1 revealed a homo-trimeric complex arranged in a tail-to-tail orientation in which the carboxy-termini face each other within the cytosol, generating a cone-like pore that is narrow at the extracellular face (approximately 8 Å across) and wide at the intracellular aqueous exit (approximately 22 Å across). [**De Feo *et al.*,**

2009] Additionally, the position of the conserved M-X_3-M Cu-binding motif on TM2 along the pore interface of the symmetric Ctr1 trimer, suggests that Cu^+ moves through the Ctr1 pore by a series of ligand exchange reactions between distinct binding sites and that these reactions induce conformational changes that mediate Cu^+ movement through the pore up to the HCH-motif near the carboxyl terminus of the protein. The higher stability of Cu^+-cysteine interactions when compared to those between Cu^+-methionine, would thus favor cation enrichment (in the form of a thermodynamic sink) at the wider aqueous intracellular exit, thereby obviating the energetic requirement for ATP hydrolysis to drive Cu transport.

Ctr1 is an important regulator in response to environmental Cu stresses. Recently, it has been demonstrated that Cu deficiency induced by treating human cancer cells with Cu chelators up-regulates hCtr1 expression; whereas Cu sufficiency achieved by treating cells with $CuSO_4$, down-regulates endogenous hCtr1 expression. [**Liang *et al.*, 2012. Song *et al.*, 2008**] Moreover, it has been revealed that human Cu homeostasis is tightly controlled by interregulatory circuitry involving Cu, Sp1 and hCtr1. This circuitry uses Sp1 transcription factor as a Cu sensor in modulating hCtr1 expression which in turn controls cellular Cu and Sp1 levels in a three-way mutual regulatory loop. [**Kuo *et al.*, 2012**] Not only hCtr1, but also Sp1 itself, is regulated by Cu bioavailability (Fig.9).

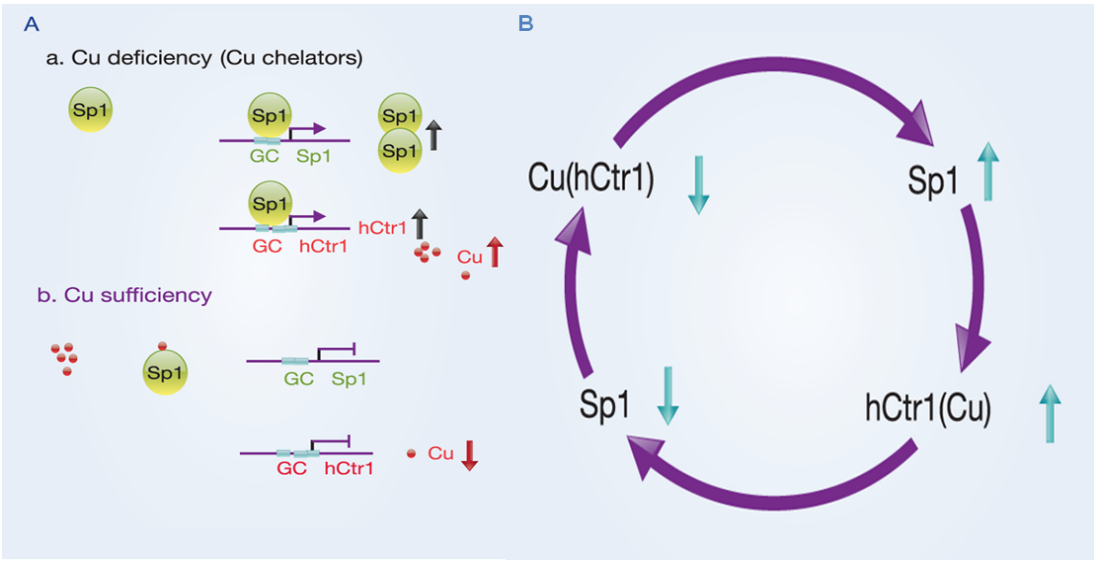

Figure 9. Regulation of hCtr1 and Sp1 expression by Cu bioavailability, taken from Kuo *et al.*, 2012.

1.1.4 THE RELATIONSHIP BETWEEN TRACE METALS AND CANCER

The roles of metals in the development and inhibition of cancer have a complex character and have risen many questions because of their essential and toxic effects on human health. Question of whether trace metal concentrations in tissues are increased or decreased in cancerous patients in comparison with noncancerous patients has not been answered yet, due to the fact that the data known in this field is rare and have contradictory results. Although Zn and Cu concentrations in serum and tissues of cancerous patients have been extensively studied, the precise role of these metals in carcinogenesis is not clearly understood. The differences in literature on the increases or decreases in trace metal concentrations of cancerous tissues in comparison with non-cancerous tissues may be attributed to a few reasons such as the tissue basis-dry or wet weight, different sensitivities and basis of analysis methods that affect the accuracy, and the difficulties in taking of the sample representing the cancerous or non-cancerous area. [**Mehmet Yaman 2006**]

Epidemiological studies have found that many metals and metal-containing compounds may be potent mutagens and carcinogens. In the last three decade, the metals including cadmium, nickel, arsenic, beryllium and chromium (VI) have been recognized as human or animal carcinogens by International Agency for Research on Cancer (IARC).

Carcinogenesis is caused by mutations of the genetic material of normal cells, which upsets the normal balance between proliferation and cell death. This results in uncontrolled cell division and the evolution of those cells by natural selection in the body. The uncontrolled and often rapid proliferation of cells can lead to benign tumours; some types of these may turn into malignant tumours (cancer).

It is considered that carcinogenesis is occurring in four stages:

- Initiation;
- Promotion;
- Progression;
- Metastasis.

The mechanisms of metal-induced carcinogenesis are believed to be involved in all stages of cancer development. The cells that can cause malignant tumors have several properties that distinguish them from cells of healthy tissue:

- Resistance to apoptosis (programmed cell suicide);
- Division uncontrolled (or die) and proliferation more frequently than normal;
- Self-sufficiency in growth factors;
- Resistance to inhibition by contact;
- Defective cell differentiation.

Some studies suggest that the ratio Cu / Zn is a good indicator of extension and prognosis of various tumors, in particular, has been observed that the serum levels of copper are significantly higher in patients with prostate cancer compared to healthy individuals, while the levels of zinc in serum are lower in patients with cancer, therefore, the ratio of Cu / Zn in the serum showed a gradual and significant increase. [**Gupta *et al.,* 2005**]

The mechanism for these alterations in serum trace element levels are not well understood. Increased ceruloplasmin level, increased uptake from the gut, diminished urinary excretion, and tissue breakdown as a result of tumor necrosis with consequent release of copper stores have been suggested as the possible causes for increased serum copper level.

Over the past two decades, chemical and cellular studies have contributed enormously to broaden the understanding of the mechanisms and pathophysiological processes induced by metals. In particular, has focused attention on ways of signal transduction induced by carcinogenic metals, such as:

- NF-kB activation;
- apoptosis;
- cell cycle progression.

Reactive oxygen species (ROS) are indispensable factors in signal transduction pathways. Under physiological conditions, ROS level is controlled by SOD1 and other antioxidative systems. However, in presence of copper and/or zinc dyshomeostasis, metal-induced ROS accumulation may induce various diseases, including cancer [**Formigari *et al.,* 2013**]. As reported by **Ba and colleagues** (**2009**), one of the most devastating events caused by ROS is the oxidation of ligands and subsequent metal ion release. Metals released during oxidative stress include the redox active iron and copper ions, which amplify ROS levels through Fenton chemistry. It is generally believed that oxidative stress, resulting from metal-induced generation of reactive oxygen species (ROS), is a critical mediator for the malignant

transformation but targets of these metals can be regulatory proteins or signaling proteins involved in cell growth, in apoptosis, in cell cycle regulation, in DNA repair, and in differentiation [**Bartsch *et al.,* 2000].** However, much more information and research are essential to elucidating the role, mechanisms and factors relating to zinc (and copper) in cancers. [**Franklin and Costello, 2009**]

1.2 CRC: COLORECTAL CANCER

Colorectal cancer (CRC) is the third most common cancer worldwide. (Jemal et al., 2011). The incidence of CRC is higher in countries in the developed world, where it is the second most common form of cancer among women (after breast cancer) and third among men (after prostate and lung). The predominant localization of CRC is rectum (50–60%) and sigmoid colon (15–25%).

Several study estimate that approximately 90% of colorectal cancer cases are sporadic without family history or genetic predisposition while less than 10% of all CRC cases have a true inherited predisposition to CRC. In most of these cases, the causative genetic event has been identified. However, up to 25% of cases have a family history of CRC (familial CRC), but are not consistent with one of the known inherited syndromes, they have a higher risk of developing CRC in comparison with the general population, although not as high as in the inherited syndromes. [**Bogaert and Prenen 2014**]

CRC arises as a consequence of the accumulation of genetic alterations (gene mutations, gene amplification, and so on) and epigenetic alterations (aberrant DNA methylation, chromatin modifications, and so on) that transform colonic epithelial cells into colon adenocarcinoma cells (Fig. 10).[**Grady and Carethers 2008**]

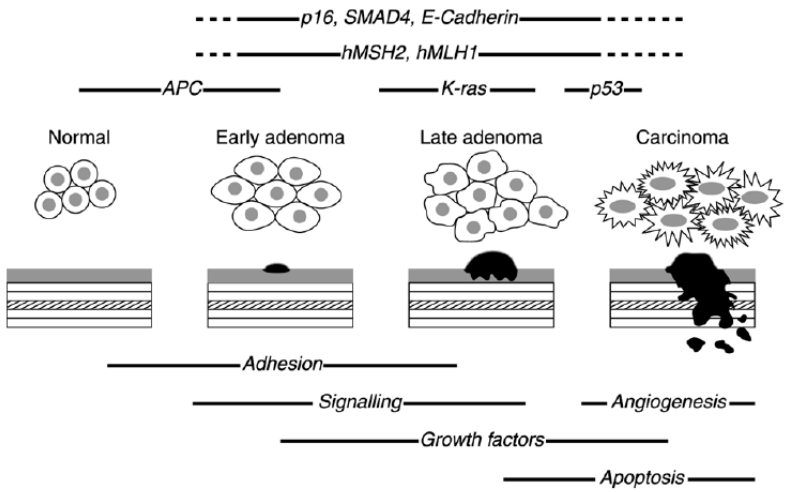

Figure 10. Basic outline of the adenoma to carcinoma sequence. Taken from Earnhead *et al.,* 2002. The time-line in which key genes may be affected is shown above the histological stages of disease during which they are thought to occur.

The sequential process of gene mutations and epigenetic alterations is widely believed to drive the initiation and progression of benign adenomas to malignant adenocarcinomas because these mutations affect signaling pathways that regulate hallmark behaviors of cancer. [**Hanahan *et al.,* 2000. Fearon *et al.,* 1990**] The earliest genetic change associated with adenomatous polyps is most frequently mutation and/or loss of the APC gene. The exact sequence of commonly acquired genetic changes accumulated subsequent to inactivation of APC is variable. K-ras mutations are found in ~50% of colorectal cancers and are thought to be relatively early events that correlate histologically with early to late adenomas. There is good evidence to suggest that p53 mutations occur more frequently in high-grade dysplastic polyps and are thought to mark the transition from adenoma to carcinoma. [**Fearon E.R. *et al.,* 1990. Rodrigues N.R. *et al.,* 1990**]

These mutations create a clonal growth advantage that leads to the outgrowth of progressively more malignant cells, which ultimately manifests itself as invasive adenocarcinoma. The acquisition of these mutations is facilitated by the loss of genomic stability, which appears to be a key molecular step in cancer formation. [**Lengauer *et al.,* 1998. Grady *et al.,* 2004. Gollin *et al.,* 2005**]

The loss of genomic stability and resulting gene alterations are key molecular pathogenic steps that occur early in tumorigenesis; they permit the acquisition of a sufficient number of alterations in tumor suppressor genes and oncogenes that transform cells and promote tumor progression. Three predominant forms of genomic instability that have been identified in

colon cancer: chromosome instability (CIN), microsatellite instability (MSI) and CpG island methylator phenotype.

- ✓ The first form is the 'chromosomal instability' (CIN) with karyotype changes that occurs in 80-85% of colorectal carcinomas;
- ✓ Microsatellite instability (MSI) is a hypermutable phenotype caused by the loss of DNA mismatch repair activity and it is characterized by deletions and amplifications of short sequences of nucleotides. MSI is detected in about 15% of all colorectal cancers; 3% are of these are associated with Lynch syndrome and the other 12% are caused by sporadic, acquired hypermethylation of the promoter of the MLH1 gene, which occurs in tumors with the CpG island methylator phenotype [**Sheffer *et al.,* 2009**].
- ✓ The third form is the CpG island methylator phenotype (CIMP) which was originally grouped together with MSI tumors. The islands are CpG rich regions within the genome and especially found in promoter sequences. In carcinogenesis, methylation of CpG islands (so-called type C methylation) leads to transcriptional silencing of genes involved in tumor suppression, apoptosis, DNA repair, and cell-cycle control. [**Goel *et al.,* 2007**] Genes that are frequently affected by this non-covalent epigenetic modification are *p16*, *MGMT*, and *hMLH1*.

MSI tumours are usually euploid, while CIN tumours are aneuploid; these genetic differences are reflected in a different pathological and clinical behaviour.

1.2.1 Inherited predisposition to colorectal cancer

Inherited forms of CRC account for as much as 30% of all CRC cases and between 2% to 5% of all colon cancers arise in the setting of well defined inherited syndromes, including Lynch syndrome (also called hereditary nonpolyposis colorectal cancer [HNPCC]), familial adenomatous polyposis (FAP), MUTYH-associated polyposis (MAP), and certain hamartomatous polyposis conditions. All of these conditions are inherited, autosomal dominant disorders, except MAP, which is autosomal recessive.

Colorectal cancer results from the progressive accumulation of genetic and epigenetic alterations that lead to the transformation of normal colonic epithelium to colon

adenocarcinoma, which is called the polyp → cancer progression sequence (Fig. 11). [**Grady et *al.,* 2008]**

The tumor initiates from a normal colonocyte stem cell that has sustained genetic damage over time due to the local environment or has inherited a germline genetic mutation. The damaged DNA drives tumor progression up to the formation of carcinoma. In FAP, tumor initiation is accelerated with the inheritance of a germline APC mutation; in Lynch syndrome, tumor initiation might be normal to slightly accelerated, but the true driving force to the tumor progression is due to the hypermutable phenotype that occurs with loss of DNA MMR.

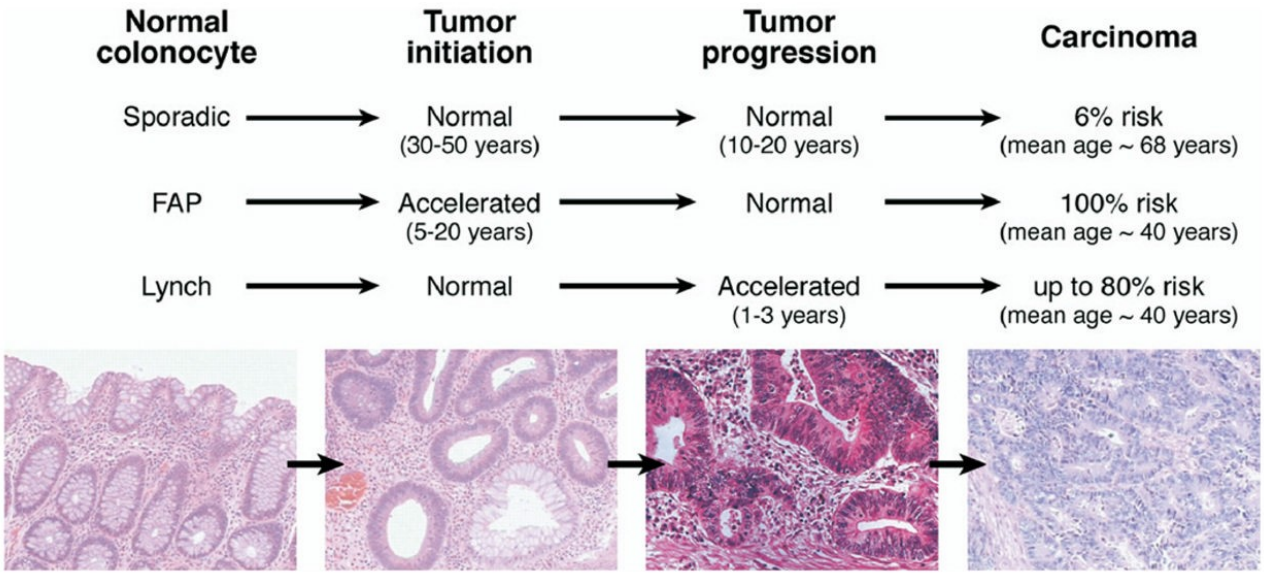

Figure 11. Depiction of colorectal tumor progression in sporadic and high-risk genetic syndromes. Taken from Grady et al., 2008.

1.2.2 Lynch Syndrome (LS)

The syndrome accounts for 2%–4% of all CRCs [**Hampel *et al.,* 2008**] and individuals with Lynch syndrome are predisposed to various types of cancers, especially colon-rectum and endometrial, [**Lynch *et al.,* 2003**] other cancers associated with Lynch syndrome are gastric, ovarian, biliary, urinary tract, small bowel, brain and pancreatic tumors. Although affected individuals can develop colonic adenomas with greater frequency than the general population, polyposis is rare. The lifetime CRC risk is estimated to be 50%–80%. [**Stoffel *et***

***al.,* 2005**] Histologically, cancers are often poorly differentiated, mucinous, and have large numbers of tumor-infiltrating lymphocytes.

Lynch syndrome is the result of a autosomal dominant heterozygous germline mutations in a class of genes involved in DNA MMR, including hMSH2, hMLH1, hMSH6, and hPMS2. The MMR system is necessary for maintaining genomic stability by correcting single-base mismatches and insertion-deletion loops that form during DNA replication. Mutations in hMSH2 and hMLH1 account for the up to 90% of Lynch syndrome cases; mutations in hMSH6 account for approximately 10% and mutations in hPMS2 are detected on rare occasions. [**Rustgi 2007. Kastrinos *et al.,* 2009. Peltomaki P *et al.,* 2004**] They are also characterized by a high level of microsatellite instability (MSI-H), a molecular phenotype that is a direct consequence of impaired MMR activity. Of interest is that colon cancers with MSI-H overall have a better prognosis compared to those without MSI. [**Ribic *et al.,* 2003**] Several tools are available to assist clinical diagnosis of Lynch syndrome, including analyses of family histories, tumor testing, mutation prediction models, and genetic testing.

1.2.3 MSI AS A MARKER OF DEFECTIVE MMR

The human DNA MMR system is an evolutionarily conserved system that involves a number of proteins that recognize and direct repair of nucleotide mismatches and is responsible for maintaining replicative fidelity of DNA. [**Marra *et al.,* 1996. Fishel R. 1998**] Parsons and colleagues [**Parson *et al.,* 1993**] demonstrated that LS cancer cells lacked the ability to repair small insertions or deletions in tandem repeat sequences, as well as single-base mispairs, which is consistent with defective MMR (Fig. 12). These findings provided the first evidence that LS was a disease of defective MMR. Approximately 90% of Lynch syndrome-associated CRCs will have MSI-H and loss of MMR protein expression it was quickly shown that inactivation of members of the human DNA MMR gene family was the cause of microsatellite unstable colorectal cancer, on the contrary mechanism(s) responsible for causing CIN and CpG island methylator phenotype (CIMP) remain to be identified.

Following the recognition that genome-wide MSI was a key characteristic of LS tumours. Thus, MSI is a marker for loss of DNA MMR activity. In the analysis of tumor DNA, it has become clear that in some tumors, genetic sequences with short repetitive nucleotide sequences such as A_n or CA_n (termed microsatellites, where *n* is the number of repeats) can become shorter or longer in length when compared with non tumor DNA from the same

individual. [**Grady and Carethers 2008**] A microsatellite may lengthen in a daughter cell if there is nucleotide-pairing slippage (looping) along the newly synthesized strand during DNA synthesis or may shorten if the template strand microsatellite has slippage during DNA replication. This alteration in microsatellite length in genomic DNA defines MSI. Although the DNA MMR system recognizes and directs repair of single nucleotide mispairs (see the following text), this aspect is not usually tested when examining tumors for MSI. Multiple point mutations as well as MSI are observed in these tumors, providing the basis for the term "hypermutable" phenotype, and this increase in the spontaneous mutation rate appears to be the mechanism for the apparent rapid neoplastic progression in Lynch syndrome and sporadic tumors that exhibit MSI. [**Aaltonen *et al.,* 1993; Tsao *et al.,* 2000**]

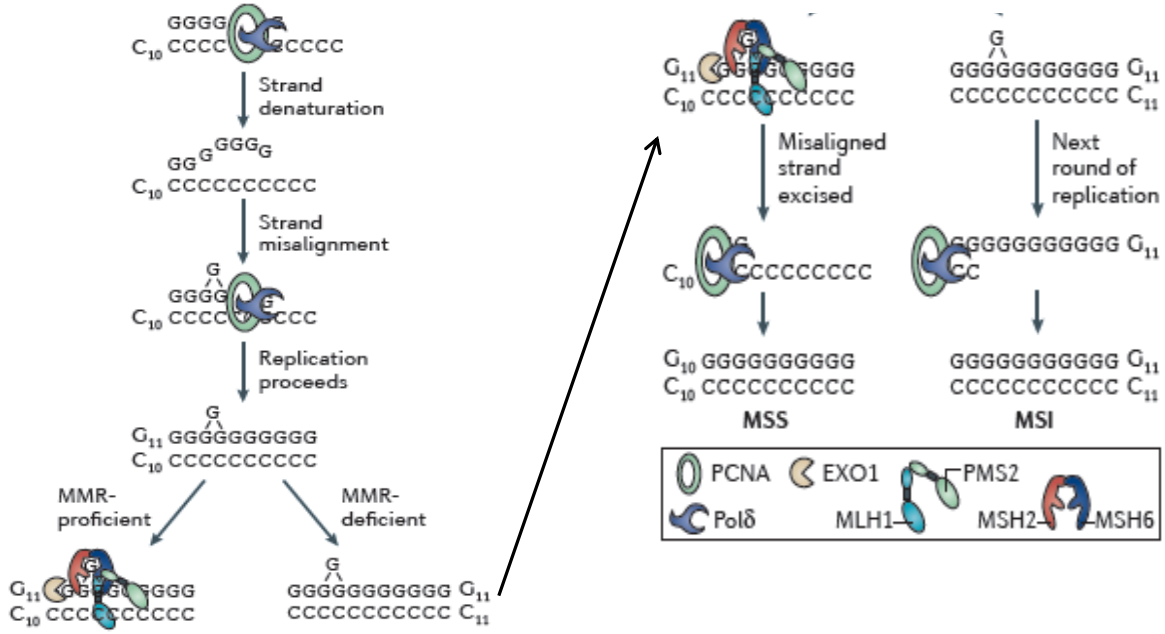

Figure 12. Molecular mechanism of MSI, taken from Henry T. Lynch *et al*., 2015. During replication of tandem repeat sequences (C10), DNA strand denaturation may occur, resulting in strands reannealing 'out of register' (that is, becoming misaligned). This may lead to the addition (or subtraction) of one or more nucleotides during replication (G11). Moreover, in the absence of MMR activity, the extra nucleotide remains. During the next round of DNA replication, the G11 strand becomes the template strand. Successful replication of this errant strand results in permanent fixation of the additional nucleotide and the generation of a new allele (C11). EXO1, exonuclease 1; MSI, microsatellite instability; MSS, microsatellite stability; PCNA, proliferating cell nuclear antigen; Polδ, DNA polymerase-δ.

1.2.4 THE MUTATOR PHENOTYPE AND CANCER DEVELOPMENT

The normal colonic epithelium in carriers of a heterozygous germline mismatch repair (MMR) gene mutation is MMR-proficient and thus microsatellite stable (MSS). Hemminki [**Hemmininki *et al*., 1994**] showed that loss of the remaining wild-type allele of the mutated MMR gene was a feature of LS tumours, which is consistent with Knudson's [**Knudson 1985**] two-hit model of carcinogenesis, according to this the combination of a germline mutation in an MMR gene with inactivation of the remaining normal allele, results in loss of MMR function and accumulation of mutations in microsatellites. The loss of function of both alleles in somatic cells results in loss of MMR function and the establishment of a mutator phenotype [**Fishel and Kolodner 1995**].

The idea of a mutator phenotype was first proposed in 1974 by Loeb who argued that defects in DNA replication or repair would enhance the mutation frequency in cancer cells and increase the chances of a mutation in an important oncogene or tumour suppressor gene. Loss of MMR would result in DNA polymerase errors remaining intact. Upon the next round of DNA replication, an incorrectly inserted base or an extra repeat sequence bulge would be replicated and permanently fixed in the genome (Fig. 13). This phenomenon underlies the presence of MSI and the several hundred-fold increase in mutation frequency observed in MMR-deficient cells85.

The recognition that microsatellite sequences were particularly susceptible to a mutator phenotype led researchers to search for mutations within tandem repeat sequences in the coding region of cancer genes. Further evidence for a mutator phenotype in MMR-deficient cancer cells came recently from The Cancer Genome Atlas (TCGA) colon cancer study, which showed that MMR-deficient tumours contain hundreds to thousands of somatic point mutations, including both frameshift and nucleotide substitutions, well in excess of those observed in MMR-proficient tumours. [**Cancer Genome Atlas Network 2012**] This accelerated accumulation of mutations in MMR-deficient cells may underlie the rapid progression observed in LS tumours .

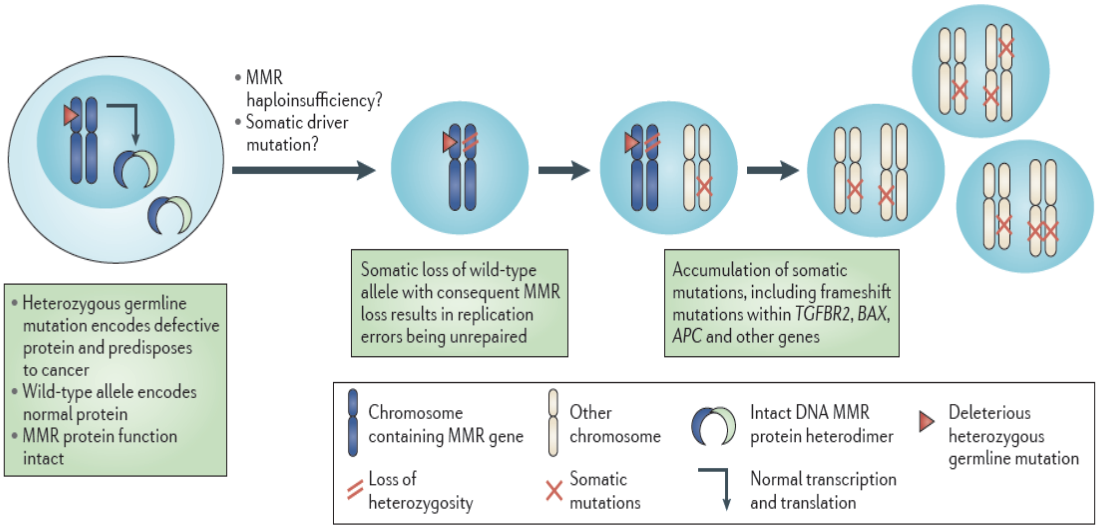

Figure 13. CRC development in individuals with LS , taken from Henry T. Lynch *et al.*, 2015. A schematic representation of the molecular mechanism of development of colorectal cancer (CRC) via pre-malignant colorectal polyps in individuals with Lynch syndrome (LS)

1.2.5 FAMILIAL ADENOMATOUS POLYPOSIS (FAP)

Familial adenomatous polyposis (FAP) is the second-most common inherited CRC syndrome with a prevalence of 1 in 10,000 individuals. Characteristic features of FAP include the development of hundreds to thousands of colonic adenomas, beginning in early adolescence, and inevitable CRC in untreated individuals. The genetic basis for FAP lies in germline (inherited) mutation of the adenomatous polyposis coli (*APC*) gene which encodes a tumor suppressor that is part of the WNT signaling pathway (**OMIM 175100**). Approximately one-quarter of all cases are caused by new mutations that maintain the incidence of FAP [**Bisgaard *et al.*, 1994**], despite the strong selective disadvantage of the disease. Germline mutations in the *APC* gene have been demonstrated in most FAP patients. [**Cottrell *et al.*, 1992**] The vast majority (95%) of *APC* mutations are nonsense or frameshift mutations that result in a truncated protein product with abnormal function.

1.2.6 MUTYH-ASSOCIATED POLYPOSIS (MAP)

MAP is characterized by the presence of adenomatous polyposis of the colorectum and an increased risk of CRC. MAP is caused by biallelic mutations in *MUTYH* (also referred to as

MYH). The *MUTYH* gene product is part of the base-excision repair pathway, which is involved in defending against oxidative DNA damage. Functionally, MUTYH helps prevent G:C to T:A transversions caused by oxidative stress to highly mutagenic DNA bases. Colonic polyposis typically occurs by the time patients reach their 40s although polyps and cancer can occur at earlier ages. Biallelic *MUTYH* mutations have also been found in individuals with early onset CRC and few-to-no polyps [**Cleary *et al.,* 2009**].

1.3 ANTICANCER ACTIVITY OF THE COPPER COMPLEXES

Copper assumes a critical role in various biochemical reactions including signaling, catalytic, regulatory and structural functions, for this reason is fundamental importance is to maintain the correct concentration inside the cells (free divalent metals approximatively 10^{-18} M) in order to guarantee normal physiological functions. In humans, disruption of this tightly regulated cellular copper homeostasis affects normal tissue development and a growing number of reports indicate an alteration of essential metal ion homeostasis (metallostasis) in tumors. [**Harrison *et al.,* 2000. Robinson and Winge 2010]** In particular, copper is crucial to the angiogenic process that sustains tumor and metastasis development, and its sequestration underlies an anticancer strategy aimed at preventing establishment of the tumor.

Alternatively, copper complexes have shown antibacterial and anticancer activity, whereby the organic component (the ligand) is responsible for directing the metal to different molecular targets [**Tardito *et al.,* 2012**]. For this reason, organic-copper compounds are systems of great interest in the field of inorganic and bioinorganic chemistry. Several small molecules able to bind metals, such as copper and zinc, have been proposed as anticancer agents [**Ding *et al.,* 2005. Ding and Lind 2009**]. It has been suggested the such molecules can be distinguished in two classes: *metal chelators* able to remove metals from biologically active site, such as TPEN (Zn), and *metal ionophores* capable of transferring multiple metal ions across biological membranes such as hydroxyquinolines (Zn, Cu, Pb) [**Ding *et al.,* 2005. Ding and Lind 2009**].

The effects of "metal chelator" can be contrasted by an increase in metal concentration while the metal-ionophore's effect is potentiated in manner metal-dose-dependent by increasing the metal concentration inside the cells. In the last years some researchers are investigating the possibility to hint the homeostasis of transition metals inside the cells to kill cancer cells. In the present study we wanted to investigate if the copper dyshomeostasis induced by metal chelators and ionophores (compounds used are reported in Table n1) can address the tumor cells to programmed death and if the expression of components of the copper homeostasis functional network can modify the sensitivity to the cytotoxicity of copper and copper-binding compounds.

Table n1

Clioquinol CQ 5-chloro-7-iodo-8 hydroxyquinoline	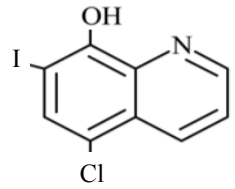
Chloro-hydroxyquinoline ClHQ 5-chloro-8-hydroxyquinoline	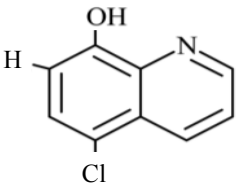
Hydroxyquinoline OHQ 8-hydroxyquinoline	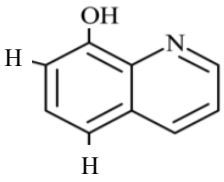
TPEN N,N,N',N-tetrakis (2-pyridylmethyl) ethylenediamine	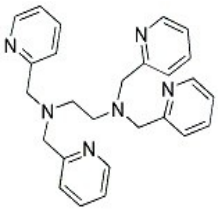

Clioquinol (5-chloro-7-iodo-8-hydroxyquinoline, CQ) is a member of 8-hydroxyquinoline family with metal-ionophore function, it is known to exhibit a variety of biological activities such as antibacterial [**Margalioth *et al.,* 1983**] and anticancer [**Dìez *et al.,* 1989**] activities. CQ displays an anticancer effect *in vitro* [**Mao and Schimmer 2008. Mao *et al.,* 2009**] and *in vivo* [**Chen *et al.,* 2007**] preclinical models. CQ induces apoptosis in breast cancer cells through a caspase-dependent apoptotic pathway. [**Daniel *et al.,* 2005. Ding *et al.,* 2006**] Moreover, Clioquinol induces apoptosis in leukemia and myeloma cells by inhibiting histone Deacetylase activity. [**Cao *et al.,* 2013]** In addition, Zhai and collaborators (2010) [**Zhai *et al.,* 2010**] demonstrated that both 8-OHQ and CQ/copper complexes are able to inhibit the proteasome activity resulting in proliferation suppression and apoptosis in cultured breast cancer cells before cell death (Fig. 14). Recently a new mechanism, called parapoptotic, was described in Hela cells treated with the CQ-copper complex at 14

μM. [**Sperandio *et al.,* 2000. Tardito *et al.,* 2012**] This phenomena is characterized by a massive cytoplasmic vacuolization due to accumulation of unfolded proteins in endoplasmic reticulum. [**Sperandio *et al.,* 2000**] Conversely, the activation of the caspase-3 during the apoptotic process was observed in Hela Cells treated with CQ at the highest concentration 50 μM. [**Tardito *et al.,* 2012**]

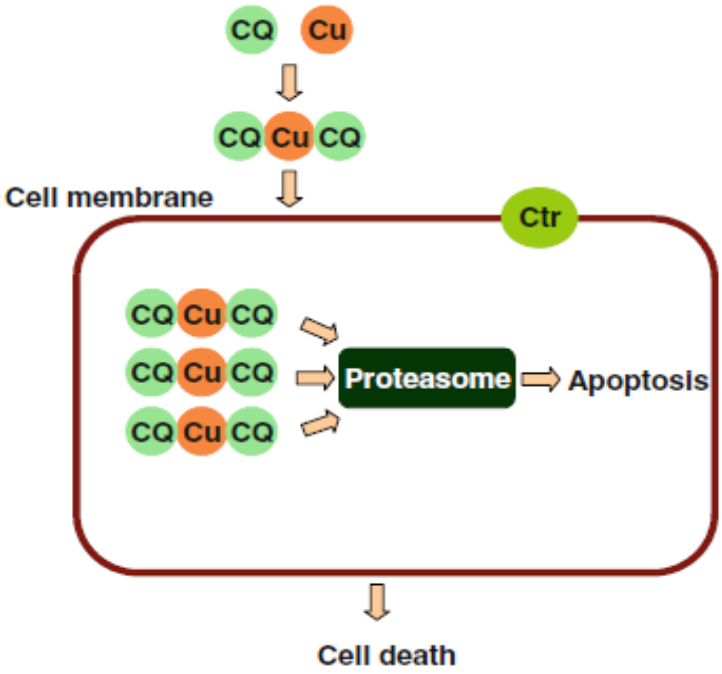

Figure 14. Probable model for clioquinol-induced apoptosis. The CQ binds the extracellular copper and the copper-clioquinol complex induces apoptosis by the inhibition of proteasome activity.

On the contrary of 8-hydroxyquinoline derivatives, TPEN (N,N,N',N-tetrakis (2-pyridylmethyl) ethylenediamine) is a cell permeable, high-affinity zinc and copper chelator. Different studies demonstrated that TPEN, at concentration higher than 1 μM induces apoptosis. In particular, was demonstrated that exposure of PC3 and DU 145 prostate cancer cells to TPEN (2-20 μM) activated caspase 3/7 activity. [**Carraway *et al.,* 2012**] Same results was obtained in cultured hippocampal neurons through inhibition of ERK signalling pathway and activation of caspase-3. [**Pang *et al.,* 2013**]

Although TPEN can chelate all the endogenous transition metals such as zinc, iron, and copper, TPEN-induced apoptosis is most likely caused by chelating and thus depleting intracellular zinc, and possibly copper. This conclusion was deduced from the result that addition of equimolar copper or zinc, but not iron, blocked TPEN-induced apoptosis, and from the affinities of metals with TPEN (copper > zinc >iron). [**Hyun *et al.,* 2001**] Recently it has been demonstrated that, in HCT116 colorectal cells,

TPEN induces cell death by chelating intracellular copper to produce TPEN-copper complex that engage in redox cycling and selectively induce the cell death. [**Fatfat *et al.,* 2014**] In particular TPEN's ability to extract essential metals, particularly copper from mitochondrial electron carriers facilitated the generation of superoxide and H_2O_2.

1.4 HIGH DENSITY OLIGONUCLEOTIDE ARRAYS

The microarray technology is based on the hybridization between target nucleic acids and probe nucleic acids (we call "target" the nucleic acid that is the object of the analysis and "probe" the known nucleic acid that is used as a tool for the analysis). The peculiarity of microarray is that millions of hybridization reactions to different probes are performed simultaneously. This technology is evolving rapidly and different platforms and several different solutions to processing and labeling the biological samples are commercial available.

The Affymetrix GeneChips platform is most frequently used by scientists to detect practically every known human gene that is expressed and eventually turned into a protein [**Auer *et al.,* 2009**]. This platform helps researchers learn more about different diseases such as heart diseases, mental illness, infectious disease and especially the study of cancer. Until recently, different types of cancer have been classified on the basis of the organs in which the tumors develop. Now, with the evolution of microarray technology based on GeneChip probe, it will be possible for the researchers to further classify the types of cancer on the basis of the patterns of gene activity in the tumor cells. This will tremendously help the pharmaceutical community to develop more effective drugs as the treatment strategies will be targeted directly to the specific type of cancer.

The highly-automated manufacture process used by Affymetrix, combines chemistry and photolithography to build vertically (on each feature of the chip's quartz surface) specific 25 nucleotides-long DNA probes, in a predetermined spatial orientation. The process is miniaturized (a typical glass chip is about 1.28 cm^2 in size) to generate high-density arrays of oligonucleotide probes.

The GeneChip array is high-resolution array, is formed by approximately 500 thousand probe cells with size of 5 μm^2 each, contains >6.0 million distinct probes covering coding and non-coding transcripts. 70% of the probes on this array cover exons for coding transcripts, and the remaining 30% of probes on the array cover exon-exon splice junctions and non-coding transcripts [**Affymetrix**] (Fig.15). On average, 109 probes per gene are used. Since oligonucleotide probes are synthesized in known locations on the array, the hybridization patterns and signal intensities

can be interpreted in terms of gene identity and relative expression levels by Affymetrix GeneChip Operating Software.

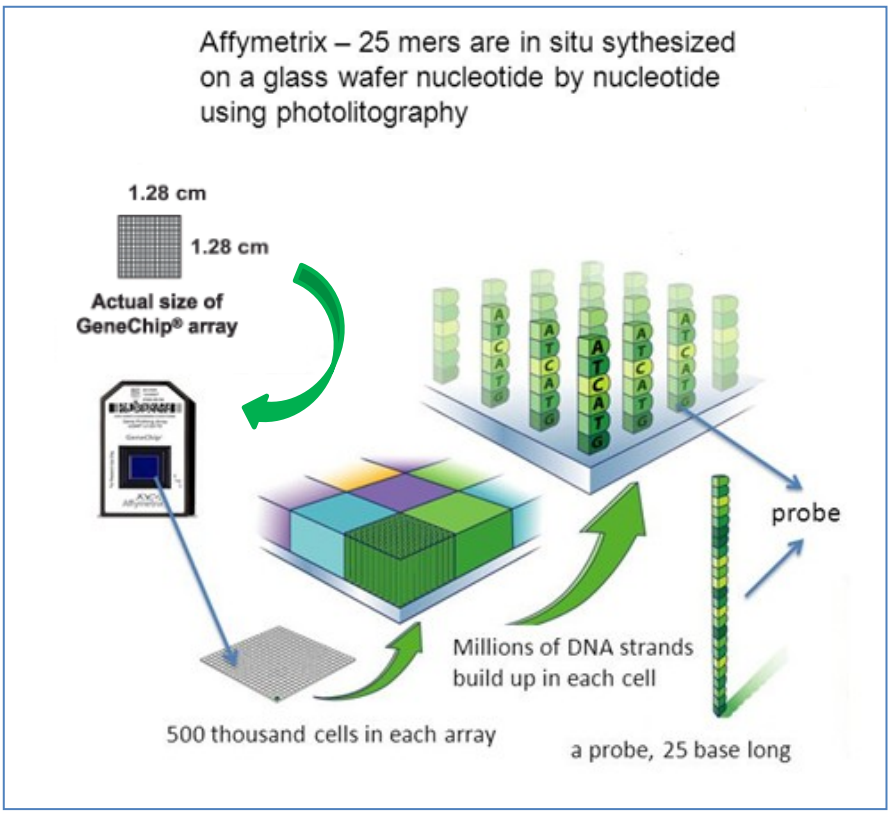

Figure 15. Microarray Affymetrix Chips

1.4.1 THE GENECHIP HUMAN TRANSCRIPTOME ARRAY 2.0

The entire procedure can be subdivided in five main steps:

A) Extraction of RNA;
B) Preparation and labeling of target cDNA;
C) Hybridization of target cDNA to oligonucleotide probes on microarray surface;
D) Fluorimetric scan of the array;
E) Processing of hybridization signals and analysis of gene expression.

The **first phase** is the extraction of RNA form the biological sample. In this training the starting biological samples is a frozen colon cancer sample. We will extract total RNA by a method based on adsorption to a silica gel matrix.

The **second phase** is the preparation and labeling of target nucleic acid. The target nucleic acid is the nucleic acid that we want to analyze in our procedure. In this case we want to determine the levels of entire repertoire of cellular mRNAs and a large number of non-coding RNAs. However we must convert RNA in a form useful for the hybridization reaction. The protocol depends on the type of microarray used. The procedure for "Human Transcriptome Array 2.0" is summarized in the following in Figure 16.

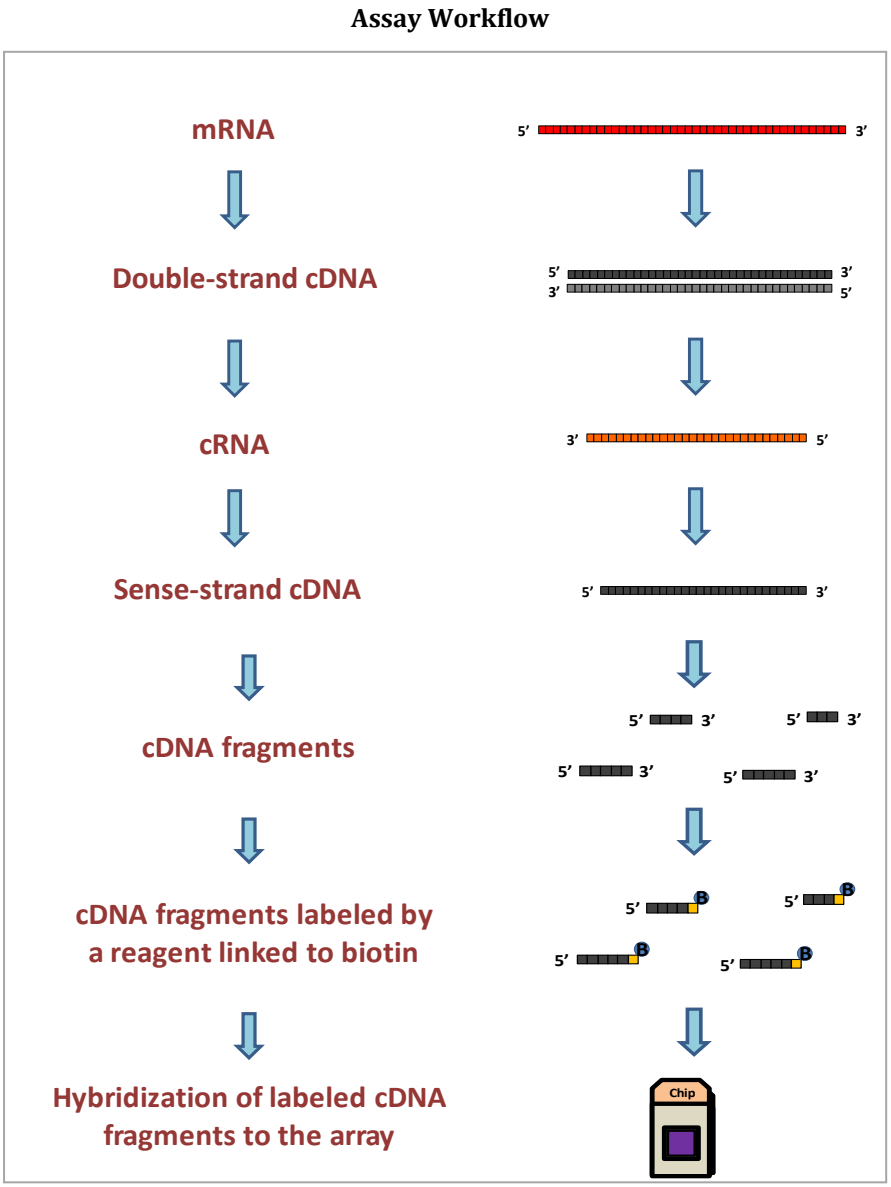

Figure 16. Human Transcriptome Array 2.0 workflow.

In this protocol total RNA is first reverse transcribed to double-cDNA. The cDNA is converted in antisense cRNA by in vitro transcription. cRNA is then reverse-transcribed in single strand sense cDNA. Sense cDNA is then fragmented and labeled with biotin and

represents the target DNA. In the **third phase** labeled target cDNAs are hybridized to oligonucleotide probes on the microarray surface. The chip probe array consists of a square glass (1.28 cm for side) mounted in a plastic cartridge. The array of oligo probes is fixed on the inner glass surface. A plastic chamber is under the glass and act a reservoir where hybridization occurs. After loading microarrays are incubated in an hybridization oven at 45°C for 16 hours with rotation at 60 rpm. During incubation sense target cDNAs will hybridize to the corresponding antisense oligoprobes. Then the Fluidic station will perform the staining to amplify the signal by three consecutive incubations: (the first incubation will be with streptavidin-phycoerythrin, the second incubation with biotinylated antibody against streptavidin and the third again with streptavidin-phycoerythrin). The fluidics station mix the staining solution by alternately draining and filling the cartridge. At the end the fluidic station expel the staining solution to the waste line and fill the cartridge with holding buffer for the fluorimetric scan by *GeneChip Scanner 3000*, that is an epifluorescent confocal microscope that uses a solid-state YAG laser (532 nm) to excite phycoerythrin bound to hybridized nucleic acids at 1.56 μm pixel resolution (**www. affymetrix. com**). In the **fourth phase** raw fluorescence signals are processed in order to perform an analysis of gene expression.

1.4.2 PROCESSING OF HYBRIDIZATION SIGNALS AND ANALYSIS OF GENE EXPRESSION

The software AGCC (Affymetrix GeneChip Command Console) represents the fluorescence intensity values from each pixel on the array in a grayscale or pseudocolor mode and creates Image data files (.DAT). Then the AGCC software superimposes a grid on the image to delineate the probe cells (features) and summarizes probe cell intensity data (CEL file generation).

The Expression Console software will use CEL files to create summarized expression values (.CHP file) by the Gene Level-SST-RMA analysis, that looks at the expression of the gene overall, giving us a RMA (Robust Multiple-Array) value for each Probe Set perfectly matched. Finally dedicated software will perform comparison of gene expression between different samples.

For instance, “Transcriptome Analysis Console” (TAC) by Affymetrix performs statistical analysis to obtain a list of differentially expressed genes and alternative splicing events. It provides the visualization of genes, exons, junctions and transcript isoforms. TAC software reports a Fold Change number (FC) that describes how much the signal changes from an first

group (for example CRC samples) to a second group (for example Mu samples). Moreover it gives us the relative FDR (false discovery rate) control, a statistical method used to reduce the number of false positives and to increase the chances of identifying all the differentially expressed genes.

The Transcriptome Analysis Console uses rma.alt-splice-sst.chp files, generated by Expression Console, for exon-level analysis estimating the alternative splicing events. The Splicing Index algorithm (SI) normalizes the exon and junction expression values by the level of gene expression and creates a ratio of normalized signal: The Splicing Index value. This value shows the normalized fold change (in linear space) of Condition1 vs. Condition2. High value of SI indicates that a particular Probe Selection Region (PSR) is preferentially included in a condition, but not in the other.

TAC software provides a series of Differential Expression Analysis Graphics such as: Scatter Plot, Chromosome Summary, WikiPathways and Hierarchical Clustering. The Scatter Plot (Fig. 17), for example, is a standard scatter plot graph of the comparison between two conditions. The two conditions that are compared are reported respectively in the Y and in the X axis. In this case we compare colon cancer samples with their matched normal colon mucosa. The gray point are the ones filtered out by the table, because their differential value between cancer and normal tissue is lower that a predetermined threshold (2 fold difference). The green points are genes up-regulated in colon cancer. The red points are genes down-regulated in colon cancer.

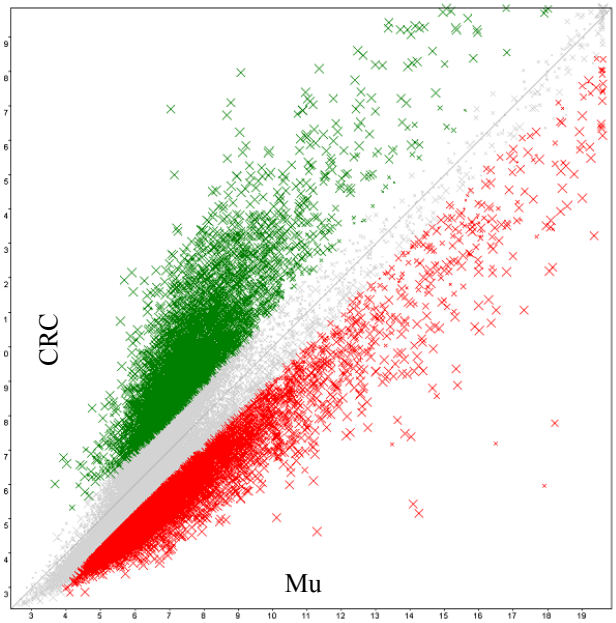

Figure 17. Scatter Plot Graph

AIM OF THE WORK

Copper, a catalytic cofactor required for the normal function of many enzymes involved in biological processes, is highly cytotoxic when in excess. Therefore its homeostasis and distribution is strictly regulated by a network of transporters (SLC31A1, SLC31A2) and intracellular chaperones (ATOX1, CCS and COX11) encoded by a group of genes that can be collectively called Copper-Homeostasis Genes (CHGs). Recent advances reveal that an alteration of copper homeostasis is very frequent in tumors supporting the hypothesis that can play an essential role in cancer angiogenesis.

The mutational and gene expression profiles associated to cancer are excellent analysis tools to identify target genes sensitive to drug therapy. Therefore, a first aim of this work was to investigate the presence of somatic mutations in CHGs in colorectal cancer, consulting the public database Cancer Genome Atlas Network. Such analysis, performed on 228 colorectal tumor samples, has revealed that inactivating mutations are extremely rare in CHGs.

The collection of whole transcriptome profiles by oligonucleotide microarrays was the second aim of the thesis. CHGs mRNA levels have been measured in 37 colorectal carcinoma samples and in their matched normal colonic mucosae. The transcriptome analysis offers the most advanced and comprehensive gene expression profiling tool for whole-transcript coverage available on any microarray platform. In this thesis, the use of the last Human Transcriptome Array (HTA 2.0, Affymetrix) allowed to analyze simultaneously 40.000 coding transcripts and 20.000 non-coding transcripts and to reveal variations of mRNA levels between colorectal cancer and normal colonic mucosa.

The alternative splicing is a biological phenomenon that determines the generation of several distinct transcripts, and consequently proteins, from a single gene and these alternative transcripts affect phenotypes. The transcriptome analysis by the last generation on oligonucleotide microarrays gives a possibility to analyse gene expression levels and single exon expression levels. In the 37 human colorectal samples, the exon-level expression analysis has been performed for the CHGs, such as SLC31A1 and SCO1, more expressed in colorectal cancer samples in comparison to normal colonic mucosa, in order to estimate the presence of alternative transcripts prevalent in a condition respect to other.

A third aim of the thesis was the evaluation of the role of the copper chaperone ATOX1 in sensitivity to copper chelating or ionophore drugs. In the last years, the research has been

focused on the possibility to use a class of a drugs, called “metal ionophores and chelators” with the aim to create an intracellular copper dyshomeostasis. “Metal ionophores” are molecules able to transfer a single metal ions across biological membranes in order to increase intracellular free metals while, in opposite sense, “metal chelators” are an another class of molecules that remove copper from biological active site in the intracellular proteins .

In this thesis we have analyzed the effects of copper addition on the toxic effects of some copper binding compounds, in particular, the ionophore copper-ionophore 5-chloro-8-hydroxyquinoline (ClHQ) and the copper chelator (N,N,N'N',-tetrakis (2-pyridylmethyl)ethylenediamine (TPEN) in two human colorectal cancer cell lines (Caco-2 and HT29).

ATOX1 expression was attenuated by treatment with short interfering RNAs in a colorectal cell line, Caco-2, showing a strong chromosomal aneuploidy, but a normal copy number and gene expression for ATOX1. Indeed, ATOX1 silencing enhanced the toxic effects of copper-ClHQ complexes and TPEN in Caco-2 cells confirming that the inhibition of copper chaperone Atox1 could be a good strategy to attenuate the cancer cell proliferation and to increase the anticancer effects of some copper binding drugs.

2. Material and methods

2.1. Human Cancer Cell Cultures

The following human cancer cell lines have been used:

- ✓ Human colon adenocarcinoma Caco-2
- ✓ Human colon adenocarcinoma HT29
- ✓ Human colon cancer HCT116
- ✓ Human mammary adenocarcinoma MCF7
- ✓ Human prostate cancer PC3

Human colon cancer Caco-2 (ATCC number: HTB-37) and HT29 (ATCC number: HTB-38) cell lines were maintained in D-MEM medium (Dulbecco's Modified Eagle Medium 1X; GIBCO, COD. 31965-023 containing 4.5g/L of D-glucose), supplemented with 10% FBS (Fetal Bovine Serum) and 100 U/ml of antibiotics (Penicillin-Streptomycin). The HCT116 (ATCC number: CCL-247) cell line was cultured in McCoy 5A+ (McCoy's 5A Medium 1X GIBCO, COD. 36600021 containing 3 g/L of D-glucose) supplemented with 10%FBS (Fetal Bovine Serum), 1.5 mM L-glutamine and 2200 mg/L of sodium bicarbonate. Human mammary adenocarcinoma MCF7 (ATCC: HTB-22) were grown in Dulbecco's MEM (DMEM), 1.0 g/l D-glucose. Each medium was supplemented with 10% (vol/vol) heat-inactivated fetal bovine serum, 2mM L-Alanyl-L-Glutamine, penicillin-streptomycin (50 units-50 □g for ml). Human prostate cancer cells PC3 (ATCC number: CRL-1435) were grown in DMEM/F12 (GIBCO, Cod. 21331) supplemented with 10%FBS (Fetal Bovine Serum). The cell cultures were grown in dishes (100 mm) and incubated at 37 °C in humidified atmosphere with 5% of CO2 and 95% of air. The culture medium was changed twice a week.

2.2 RNA Interference

Caco-2 cells were plated on 96/6-well plates (Nunclon TM Microwell TM" (Nunc)) in D-MEM with 10% FBS(fetal bovine serum) and 100 U/ml of antibiotics (Penicillin-Streptomycin). At 60% confluence, 25nM of small interfering RNA (siRNA) targeted to the copper chaperone Atox-1 was added, according to manufacturer's guidelines, in transfection medium (Opti-MEM I, Ca.Nu. 51985-026 Gibco®) containing the transfection reagent, Lipofectamine™ RNAiMAX (Cat. 13778 INVITROGEN) for 24 and 48h. Nonspecific siRNA was used as control under identical conditions.
The silencing of Atox1(NM_004045) was performed with small interfering RNA (siRNA), this molecule and its scramble were designed using siRNA Design Tool (MWG).
The targeted sequence of Atox1 and its scramble were as follows:

siRNAAtox1 206 MWG: CAAGAAGGUCUGCAUUGAA (19bp)
scrRNAAtox 206 MWG: CAACGGUACGGAUUAAUAG (19bp)

The siRNA206 was designed on exon 3 to 110 bp from ATG site and to 96bp from TAG site (Fig.18).

```
  1 gcgcactctc ggaagcgcag ccgaacccgc cctccgaatc cagagaggcg ctgctgacac
 61 cgccgccaca ccgccgccac accgccgctg cctcagtcAT Gccgaagcac gagttctctg
121 tggacatgac ctgtggaggc tgtgctgaag ctgtctctcg ggtcctcaat aagcttggag
181 gagttaagta tgacattgac ctgcccaaCA AGAAGGTCTG CATTGAAtct gagcacagca
241 tggacactct gcttgcaacc ctgaagaaaa caggaaagac tgtttcctac cttggccttg
301 agTAGcaggg gcctggtccc cacagcccac aggatggacc aaaggggca ggatgctgat
361 cctcccgctg gcttccagac agacctggga cttggcagtc atgccgggtg atggtgttcc
421 tgcggagacc ctcagttgtc ctattccttc ctagcttccc tgcaataaaa tcaagctgct
481 tttgttggaa aaaaaaaa
```

Figure 18. ATOX1 mRNA sequence. NCBI Reference Sequence:NM_004045.3
Highlighted in black the primers for quantitative amplification by PCR.

The cell line Caco-2 was transfected with siAtox1 and scrAtox1 following the forward transfection procedure by protocol Stealth ™ RNAi or siRNA by Lipofectamine™ RNAiMAX reagent (Cat. 13778 INVITROGEN). The cells were seeded on six-well plastic plates at a density of $7.0x10^4$ cells/well, for the RNA extraction that was performed using the commercial RNeasy Mini Kit (Qiagen), and on ninety-six well plastic plate at a density of $2.5\text{-}3x10^3$ cells/well, to test cell viability by MTT (3-(4,5 dimethylthiazol-2-yl)-2,5-diphenyltetrazolium bromide) colorimetric assay.

2.3 MTT Proliferation Assay

Caco-2 cell line (2.5-3x10^3 cells/0.33cm^2) were plated in a 96-well microplates "Nunclon TM Microwell TM" (Nunc) and were incubated at 37 °C. After 24 hours cells (60% confluence) were transfected with 25nM siRNA or scrRNA in 100 µl Opti-Mem (Opti-MEM I, Cat. No. 51985-026 Gibco®) containing the transfection reagent, Lipofectamine™ RNAiMAX (Cat.No. 13778 Invitrogen, Carlsbad CA) for 10 hours. At 24 hours from transfection (time line experimental condition) cells were treated with Copper(II) nitrate, [$Cu(NO_3)_2$] at increasing concentrations (0.01-0.1-1-10-50-100 µM) and/or with the copper-ionophore 5-chloro-8-hydroxyquinoline (ClHQ, Sigma Aldrich Inc) and/or the copper chelator (N,N,N'N',-tetrakis (2-pyridylmethyl)ethylenediamine (TPEN), Santa Cruz Biotechnology). Short incubations (2 hours) with copper and/or drugs were performed in 100 µl of PBS (Phosphate-buffered saline) supplemented with 0.9 mM Calcium Chloride (FLUKA Cat. No. 21014), 0.5 mM Magnesium Chloride (MERCK Cat. No. TA575835) and 5.5 mM D-glucose (SIGMA Cat. No. G-7528). This copper complexes were been premixed and subsequently were added to the cells. After 2 hours of incubation the PBS was removed and replaced by fresh standard growth medium (DMEM+10% FBS). Cells treated with 0.1% of DMSO were used as controls.

Time-line for silencing experimental condition

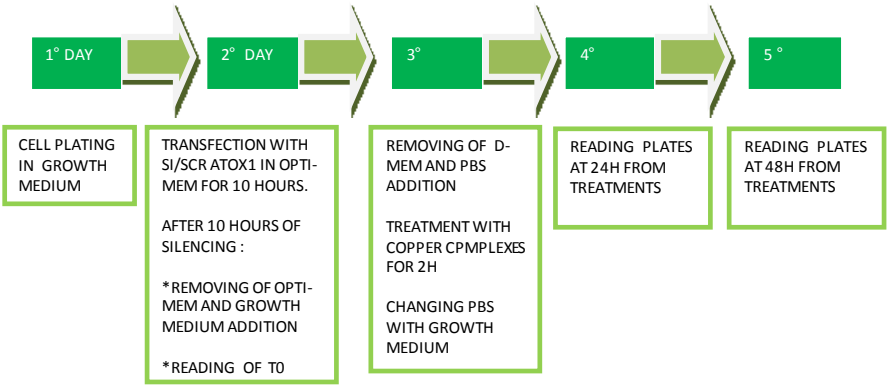

Microplates were incubated at 37 °C in humidified atmosphere of 5% CO_2, 95% air and the cellular growth inhibition and/or the cellular cytotoxicity has been valuated after 48 hours from the treatment by colorimetric assay based on the use of tetrazolium salt MTT (3 (4,5 dimethylthiazol-2-yl),-2,5-diphenyl tetrazolium bromide) [**Mosmann 1983**]. Solubilization of the converted purple formazan dye was accomplished by adding 150ul/well of DMSO

(dimethyl sulfoxide). The results were read on a multiwell scanning spectrophotometer (Multiscan reader), using a wavelength of 570 nm.

Each value was the average of 8 wells (standard deviations were less than 10%). The IC_{50} values were calculated by the nonlinear regression analysis, using the GraphPad Prism 6.0 software. Dose-response curves were obtained by the equation: log (inhibitor) vs. normalized response and the statistically significant results have been calculated by GraphPad Prism 6.0 software that has reported "95% Confidence Intervals" values. The cytotoxicity effect was calculated according to NCI when the optical density of treated cells was lower than the T0 value using the following formula: 100x (T-T0)/T0<0. (T is the optical density of the test well after a 24-48 h period of exposure to test compound; T0 is the optical density at time zero). When the optical density of treated cells was lower than the T0 value the following formula was used: 100 x (T-T0)/T0. The percentage of controls was calculate to determine cell viability and proliferative effect after a 24-48 h period of exposure to test compound.

2.4 Analyze of RNA expression by qRT-PCR

2.4.1 Purification of total RNA and reverse transcription

Caco-2 cells were plated on six-well plates at a density of 7.0x104 cells/well and siRNA transfection was performed as described in the previous section. Total RNA was extracted from control cells and treated cells with siAtox1 of colorectal carcinoma cell line (Caco-2), the extraction was performed using the commercial RNeasy Mini Kit (Qiagen) according to manufacturer's recommendations. Total RNA recovered from each sample (Ctrl, siAtox, scrAtox1) was quantified by means of a double reading performed by the NanoDrop spectrophotometer. Reverse transcription was performed using total RNA, RNaseH reverse transcriptase (Superscript II, Gibco BRL, Life Technologies, Gaithersburg, MD) and random primer hexamers.

2.4.2 Quantitative Real Time –PCR

Quantitative real-time PCR analysis was performed using StepOne™ Real-Time PCR System by Applied Biosystems(Applied Biosystems, Foster City, CA,USA). Three sequence-specific oligonucleotides (Table 2) were designed using the qPCR Probe design software (Eurofins MWG Synthesis GmbH, Ebersberg) based on the sequence of target genes: Atox1, CCND1 (NCBI

accession number: NM_053056.2) and GAPDH (NCBI accession number: NM_002046). Two of them were forward (Fw) and reverse (Rv) primers used for PCR amplification. The third sequence (TaqMan Probe, MWG) was a fluorogenic probe labelled with a fluorescent reporter dye (6-FAM, VIC) and a quencher dye (TAMRA) attached at the 5' and 3' end, respectively. The probe was designed to hybridize the portion of PCR amplicon between the Fw and Rv primers.

Table n2

CCND1 F-Exon3	5´-AGAGGCGGAGGAGAACAAAC-3´
CCND1 PROBE	5´-FAM-AGATCATCCGCAAACACGCGCAGA-TAMRA-3´
CCND1 R-Exon4	5´-AGGGCGGATTGGAAATGAAC-3´
ATOX1 F-Exon2	5´-TGTGCTGAAGCTGTCTCTC-3´
ATOX1 PROBE	5´-FAM-AGTTAAGTATGACATTGACCTGCCCAACAAGA-TAMRA-3´
ATOX1 R-Exon3	5´-GCTCAGATTCAATGCAGACC-3´
GAPDH F-Exon1	5'-TCTATAAATTGAGCCCGCAGCC-3'
GAPDH PROBE	5'-FAM-CCTCCTGTTCGACAGTCAGCCGCATCTTCTTT-TAMRA-3'
GAPDH R-Exon2	5'-TTGACTCCGACCTTCACCTTCC-3'

The 25 µL reaction mixtures contained TaqMan Universal PCR Master Mix (Applied Biosystems), 900 nM of forward and reverse primers, 250 nM of TaqMan probe.
The reaction (25 µL) was performed using 25 ng of cDNA. Each sample was analysed in triplicate and the average was normalized to human GAPDH expression. Amplification conditions included a cycle at 50 °C for 2 minutes; a cycle at 95 °C for 10 minutes followed by 50 cycles at 95 °C for 15 seconds and a cycle at 60°C for 1 minute. As a negative control, reaction without cDNA was performed (no template control, NTC).

The relative RNA expression level for each sample was calculated using the $2^{-\Delta\Delta CT}$ method [**Livak and Schmittgen 2001**]. This method relies on two assumptions. The first is that the reaction is occurring with 100% efficiency; in other words, with each cycle of PCR, the amount of product doubles. In the initial exponential phase of PCR, substrates are not limiting and there is no degradation of products. In practice, this requires setting the crossing threshold C_T this is the number of cycles that it takes each reaction to reach an arbitrary amount of fluorescence.

The second assumption of the $2^{-\Delta\Delta CT}$ method is that there is a gene (or genes) that is expressed at a constant level between the samples. This endogenous control will be used to correct for any difference in sample loading. The comparative differences between the gene of interest and an endogenous control for each sample enable a relative quantitative comparison between the samples.

2.5 The Cancer Genome Atlas Dataset

228 tumours and normal pairs from TCGA were analysed to search point mutations in genes related to copper homeostasis.

2.6 Gene Expression Analysis by GeneChip Human Transcriptome Array 2.0

Whole Transcript Expression analysis has been performed using 100 ng of total RNA to produce amplified, and targets labeled in sense orientation for hybridization to the "GeneChip Human Transcriptome Array 2.0" (Cat. No. 902310, Cat. No.900720, Affymetrix, Inc., Santa Clara, CA, USA).

The entire procedure consists of following steps:

1. RNA Extraction
2. Preparation and labeling of target cDNA
3. Hybridization of target cDNA to oligonucleotide probes on microarray surface and fluorimetric scan of the array
4. Processing of hybridization signals and analysis of gene expression.

2.6.1 RNA extraction

Total RNA was extracted from 10 colorectal tumors, matched normal colonic mucosa ("*Centro Clinico Diagnostico G.B. Morgagni*" Catania) and 5 human cell line cultures ("The European Collection of Cell Cultures –*ECACC"and* "*American Type Culture Collection* –ATCC") using RNeasy Mini Kit (Qiagen, Milan – Italy) according to the manufacturer's instructions. The concentration and the quality of the RNA were determined using a ND-1000 spectrophotometer (NanoDrop, Thermo Scientific, USA) by measuring the absorbance at 260 nm. The ratio between the absorbance values at 260 and 280 nm gives an estimate of RNA purity. A260/A280 ratio should be in the range of 1.7 to 2.1.

2.6.2 Patients

27 patients underwent surgical resection for primary invasive colorectal cancer at the "*Centro Clinico Diagnostico G.B. Morgagni*" in Catania. Tumors were staged according to the tumor-node-metastasis (TNM) staging system of UICC**.** The mean age was 66.61 years (SD 16.31) for 18 male patients and 68.67 (SD 15.63) for 9 female patients The tumors were mainly in stage II or III. In 19 patients a sample of the matched unaffected normal colonic mucosa was also taken at distance of 3-6 cm from the tumor. All CRC specimens were frozen and stored at -80°C until to RNA extraction. Informed consent was obtained from all patients involved in this study. This project was approved by the Ethics Committee of ASL3 of Catania (Italy).

2.6.3 Preparation and labeling of target cDNA

RNA must be converted into cDNA in a reverse transcription (RT) reaction using random primers containing the sequence of the T7 polymerase promoter. The reverse transcriptase synthesizes single-strand cDNA with T7 promoter sequence at the 5' end (2.1). Then, single-strand cDNA is converted to double-strand cDNA. The reaction uses RNA. RNA must be converted into cDNA in a reverse transcription (RT) reaction using random primers containing the sequence of the T7 polymerase promoter. The reverse transcriptase synthesizes single-strand cDNA with T7 promoter sequence at the 5' end (2.1). Then, single-strand cDNA is converted to double-strand cDNA. The reaction uses RNaseH. RNAseH degrades RNA and DNA polymerase synthesizes the second-strand of cDNA (2.2). In this step, the second-strand of cDNA is the template and T7 RNA polymerase binds to its promoter and synthesizes antisense RNA (also called complementary RNA or cRNA). This reaction is known as in vitro transcription (IVT). This step is also a form of amplification because many molecules of cRNAs are synthesized on a single cDNA template. The reaction mixture is incubated for 16 hr at 40°C (2.3).

cRNA is purified by adsorption of RNA on magnetic beads. cRNA is eluted by the beads using preheated (65°C) Nuclease-free Water (2.4). 15 µg of cRNA is required for 2nd-cycle sense single-strand cDNA synthesis. In this step, cRNA is the template and random primers and reverse transcriptase are used to synthesize sense-strand cDNA (**2.5**). RNase H hydrolyzes the cRNA template leaving single-stranded cDNA (**2.6**). After hydrolysis, the 2nd-cycle single-stranded cDNA is purified by adsorption to magnetic beads. cDNA concentration is measured by its absorbance at 260 nm. 15 µg of input cRNA provide 5.5 to 15 µg of single-strand cDNA. 5.5 µg of purified single-stranded cDNA are now required for

fragmentation and labeling (**2.7**). The single-strand DNA (ss-DNA) contains the unnatural uracil base. Uracil DNA Glycosylase (UDG) specifically removes the uracil residue from the ss-DNA molecules. In the same reaction, the apurinic/apyrimidinic endonuclease 1 (APE 1) cleaves the phosphodiester backbone at the abasic site. The sizes of DNA fragments are around 40 to 70 bases. The fragmented cDNA is labeled by terminal deoxynucleotidyl transferase (TdT) using the DNA Labeling Reagent that is covalently linked to biotin (**2.8**).

2.6.4 Synthesize First-Strand cDNA

Total RNA Sample (100 ng) and Diluted Poly-A RNA Controls	5 µl
First-Strand Buffer	4 µl
First-Strand Enzyme	1 µl
Total volume	10µl

Program the Thermal

Cycler: **Step**	**Temperature**	**Time**
1 Cycle	25°C	60 min.
1 Cycle	42°C	60 min.
1 Cycle	4°C	5 min.

2.2 Synthesize Second –Strand cDNA

First-strand cDNA sample	10 µl
Second-Strand Buffer	18 µl
Second-Strand Enzyme	2 µl
Total volume	30µl

Program the Thermal

Cycler **Step**	**Temperature**	**Time**
1 Cycle	16°C	60 min.
1 Cycle	65°C	10 min.
1 Cycle	4°C	5 min.
Total volume 30 µl.		

2.6.5 Synthesize cRNA by in Vitro

Transcription (IVT) second-strand cDNA sample	30 µl
IVT Buffer	24 µl
IVT Enzyme	6 µl
Total volume	60µl

Program the Thermal

Cycler **Step**	**Temperature**	**Time**
1 Cycle	40°C	16 hr.
Total 60 µl.		

2.6.6 Purify cRNA

In this procedure using Purification Beads, enzymes, salts, inorganic phosphates, and unincorporated nucleotides are removed to prepare the cRNA for 2nd-cycle single-stranded cDNA synthesis. The concentration of purify cRNA is determined by measuring its absorbance at 260 nm.

Synthesize 2nd-Cycle Single-Stranded cDNA

Purify cRNA in Nuclease-free Water (15 µg)	24 µl
2nd Cycle ss-cDNA Buffer	8 µl
2nd Cycle ss-cDNA Enzyme	4 µl
2nd-Cycle Primers	4 µl
Total volume	40 µl

Program the Thermal

Cycler **Step**	**Temperature**	**Time**
1 Cycle	25°C	10 min
1 Cycle	42°C	90 min
1 Cycle	70°C	10 min
1 Cycle	4°C	hold
Total 40 µl.		

Hydrolyze RNA

Using RNase H 2nd-cycle ss-cDNA sample	40 µl
RNase H	4 µl
Total volume	44µl

Program the Thermal

Cycler **Step**	**Temperature**	**Time**
1 Cycle	37°C	45 min
1 Cycle	95°C	5 min
1 Cycle	4°C	hold
Total volume 44 µl		

On ice, add 11 µL of the Nuclease-free Water to each (44 µL) hydrolyzed 2nd-cycle ss-cDNA sample for a final reaction volume of 55 µL.

2.6.7 Purify 2nd-Cycle Sense Single-Stranded cDNA

After hydrolysis, the 2nd-cycle single-stranded cDNA is purified using Purification Beads to remove enzymes, salts, and unincorporated dNTPs. This step prepares the cDNA for fragmentation and labeling. The concentration of sense single strand-cDNA samples is determined by measuring its absorbance at 260 nm.

Fragment Single-Stranded cDNA

ss-cDNA 5.5 µg	31.2 µl
RNAsi-free water	10 µl
10X cDNA Fragmentation buffer	4,8 µl
UDG, 10 U/µl	1 µl
APE1, 1000 U/µl	1 µl
Total volume	48 µl

Program the Thermal

Cycler **Step**	**Temperature**	**Time**
1 Cycle	37°C	60 min
1 Cycle	93°C	2 min
1 Cycle	4°C	2 min
Total 48 µl.		

Label Single-Stranded cDNA

fragmented ss-cDNA sample	45 µl
5X TdT buffer	12 µl
DNA labeling reagent, 5 mM	1 µl
TdT 30 U/µl	2 µl
Total volume	60 µl

Program the Thermal

Cycler **Step**	**Temperature**	**Time**
1 Cycle	37°C	60 min
1 Cycle	70°C	10 min
1 Cycle	4°C	5 min
Total 60 µl.		

2.6.8 WT Array Hybridization

Hybridization of fragmented and labeled target sense cDNA (fragmented and labeled ss-cDNA sample) to oligonucleotide probes on microarray surface and fluorimetric scan of the array.

In this step the fragmented and labeled target sense cDNA (fragmented and labeled ss-cDNA sample) is added to the hybridization mixture. The hybridization mixture is incubated at 99 °C for 5 min and then at 45°C for 5 min and is immediately loaded in the cartridge.

Fragmented and Labeled ssDNA (5,2 µg)	60 µl
Control oligo B2 (3nM)	3,7 µl
20X Hybridization Controls	11 µl
2X Hybridization Mix	110 µl
DMSO	15,4 µl
Nuclease-free water	19,9 µl
Total volume	220 µl

Program the Thermal

Cycler **Step**	**Temperature**	**Time**
1 Cycle	99°C	5 min
1 Cycle	45°C	hold
Total 220 µl.		

Table 3.2 Hybridization Cocktail for a Single Array

Component	49 or 64-Format	100 or 81/4-Format	169-Format
Hybridization Master Mix	160 µL	109 µL	73 µL
Fragmented and labeled ss-cDNA	~60 µL* (5.2 µg)	41 µL (3.5 µg)	27 µL (2.3 µg)
Total Volume	**220 µL**	**150 µL**	**100 µL**

** This volume is 58 µL if a portion of the sample was set aside for gel-shift analysis.*

After loading microarrays are incubated in an hybridization oven at 45°C for 16 hours with rotation at 60 rpm. During incubation sense target cDNAs will hybridize to the corresponding antisense oligoprobes.

After 16 hours the microarrays are removed from the oven.

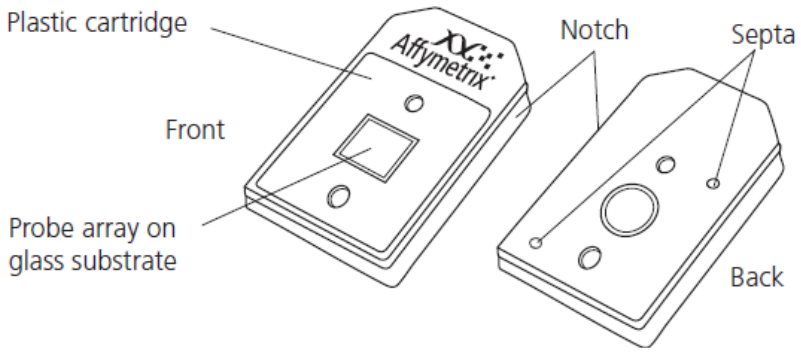

2.6.9 Processing of Hybridization Signals and Analysis of Gene Expression

The hybridization mix is removed from each array. Each array is filled completely with Wash Buffer A. The Fluidics Station is used to wash and stain the microarrays. The fluidics station will wash the cartridge with two different washing solution at selected temperature and with decreasing ionic strength. The first washing will be at low stringency with solution A and the second washing at high stringency with solution B. Then the station will perform the staining by three consecutive incubations with solutions contained in these tubes: the first incubation with streptavidin-phycoerythrin, the second incubation with biotinylated antibody against streptavidin and the third again with streptavidin-phycoerythrin. The fluidics station mix the staining solution by alternately draining and filling the cartridge.

During hybridization the sense cDNA hybridized to the antisense oligoprobe. In the staining step of the fluidic station the streptavidin-phycoerythrin binds to the biotin. At the end the fluidic station expel the staining solution to the waste line and fill the cartridge with holding buffer for scanning. Chip are now loaded in the autoloader for the fluorimetric scan.

Microarray scanning and data analysis have been performed using the following software: Affymetrix® Expression Console™ software (v.1.4). This procedure provides the signal estimation and the quality control functionality for the GeneChip Expression microarrays.

The software "Transcriptome Analysis Console (TAC)" performs statistical analysis and provides a list of differentially expressed genes. Robust Multi-array Average (RMA) (**Irizarry et al., 2003**) is the algorithm used as normalization method for the transcript level analysis.

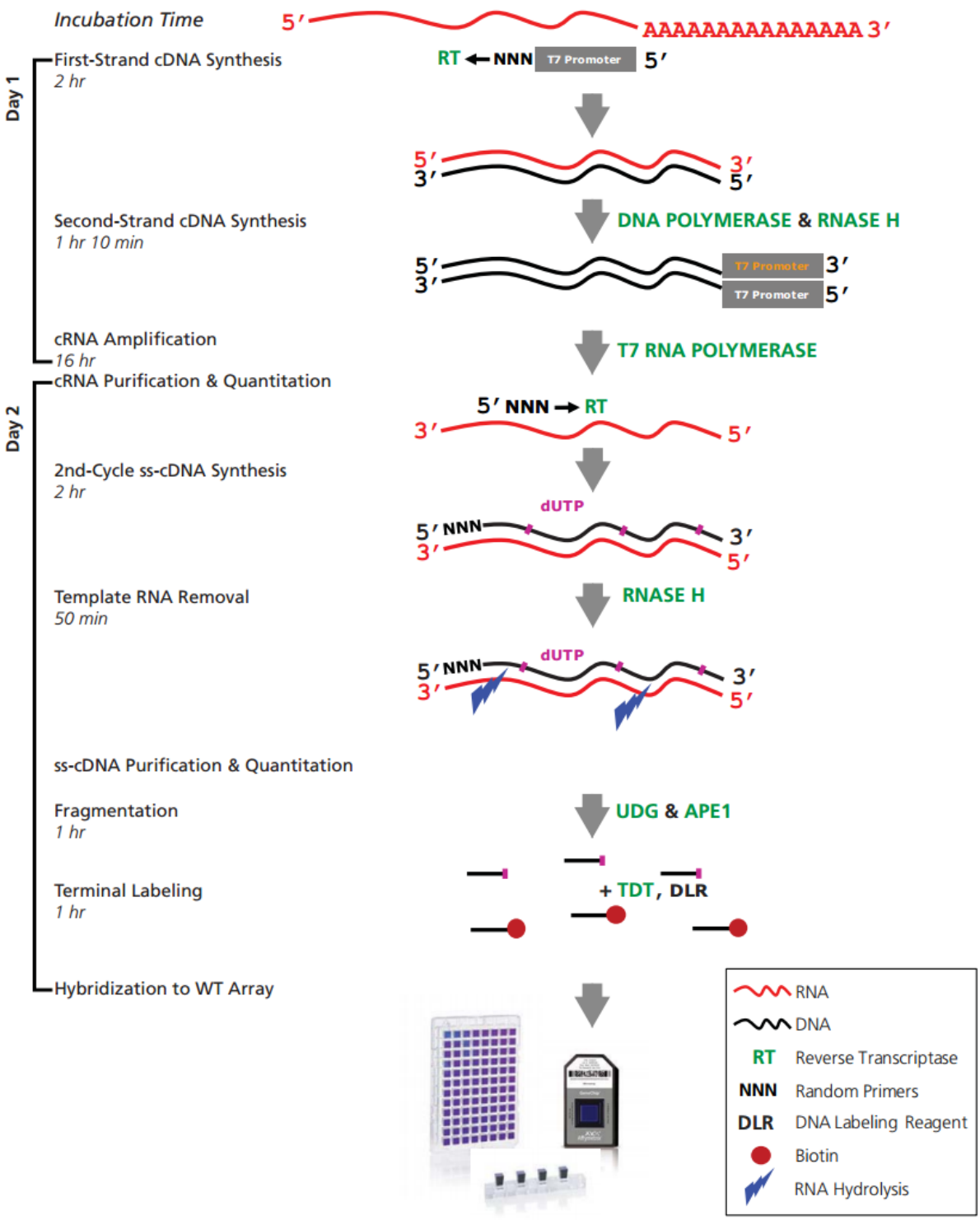

Human Transcriptome Array 2.0 workflow. Figure Source: www.affymetrix.com

3.RESULTS

3.1 Somatic point mutations of genes involved in copper homeostasis in colorectal tumors

In order to evaluate if inactivating point mutations can be responsible for dysfunctions of copper homeostasis, the exome sequencing of 228 tumours and normal pairs collected in "The Cancer Genome Atlas Dataset (TCGA) has been analysed. In Fig. 19 A,B the number of nonsense, frameshift and missense mutations for 21 transcripts involved in copper homeostasis, 3 transcripts coding for metal transcription factors (MTF) and 12 coding for several metallothioneins (MT) are reported.

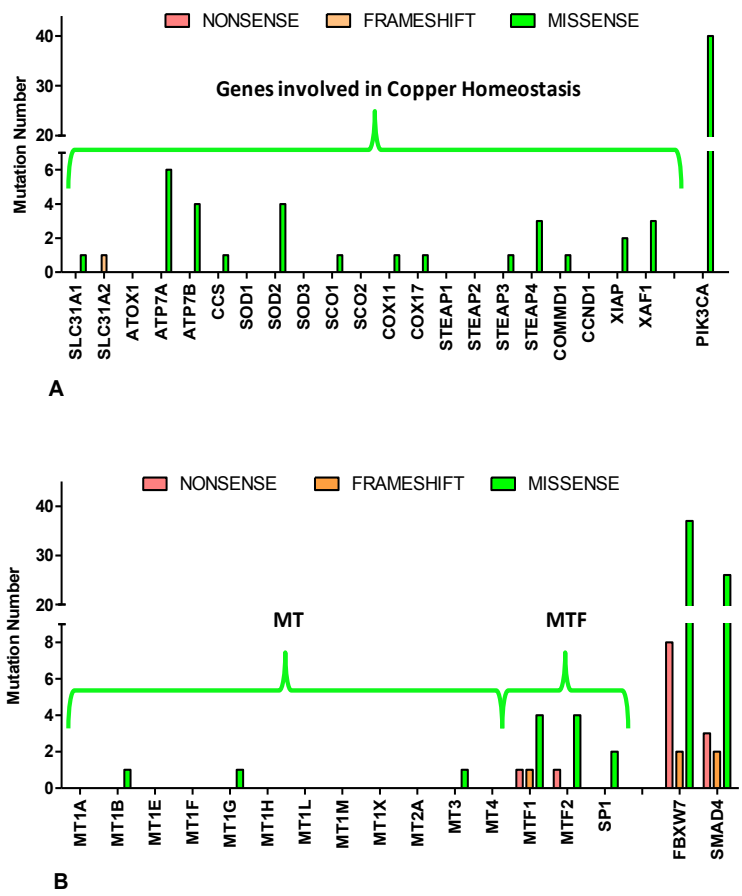

Figure 19. A,B Number of somatic point mutations (nonsense, frameshift, missesnse) in coding sequences of CHGs detected by exome sequencing in 228 CRC tumors and normal pairs reported in the data set published by "The Cancer Genome Atlas"

The point mutations in CHGs are infrequent when compared with typical oncogene and tumour suppressor genes (PIK3CA, FBW7 and SMAD4). These results suggest the assumption that accumulation of somatic mutations in CHGs cannot be responsible for a copper dyshomeostasis in colorectal tumors

3.2 mRNA levels of genes involved in copper homeostasis in colorectal cancer

The microarray technology based on Human Transcriptome Analysis (HTA) by Affymetrix gave us the possibility to analyze simultaneously 60.000 coding and non-coding transcripts.

In this thesis, the expression levels of 19 coding transcripts for genes involved in copper homeostasis (Copper Homeostasis Genes: CHGs), 12 coding transcripts for metallothioneins (MT) and three coding transcripts for metal transcription factors (MTFs) in 27 colorectal cancer (CRC) samples and in 19 matched normal colonic mucosae (Mu) have been evaluated.

In Fig. 20 (linear fold changes) and Fig. 21 A,B (RMA values) a strong increased of the copper transporter gene SLC31A1 has been reported with a value of 7.09 fold higher in CRC samples respect to matched normal colonic mucosae. However other CHGs showed a significantly increased expression in tumor samples compared to normal samples: the SOD1 cuproenzyme (4.85 times) and SOD2 manganese-enzyme (3.57 times). We, also, have been observed the upregulation of the pumps efflux ATP7A and B (1.55 and 1.37 times), the copper factors SCO1 (1.96 times) and COX11 (1.58 times), the metalloreductases STEAP1-2 and 3 (1.58, 1.40 and 1,52 times), the protein efflux of copper COMMD1 (1.35 times), the transcription factors MTF1 and MTF2 (1.87 and 1.64-fold) and SP1 (2.54). The value of cyclin D1 (CCND1) mRNA level has been reported (5.44 linear fold change) and is comparable with those observed for CTR1 (6.15-fold) and SOD1 (4.85-fold). On the contrary, STEAP4 showed a minor (-1.36-fold) and statically significant decrease of expression in the CRC sample group in comparison to normal matched colonic mucosae.

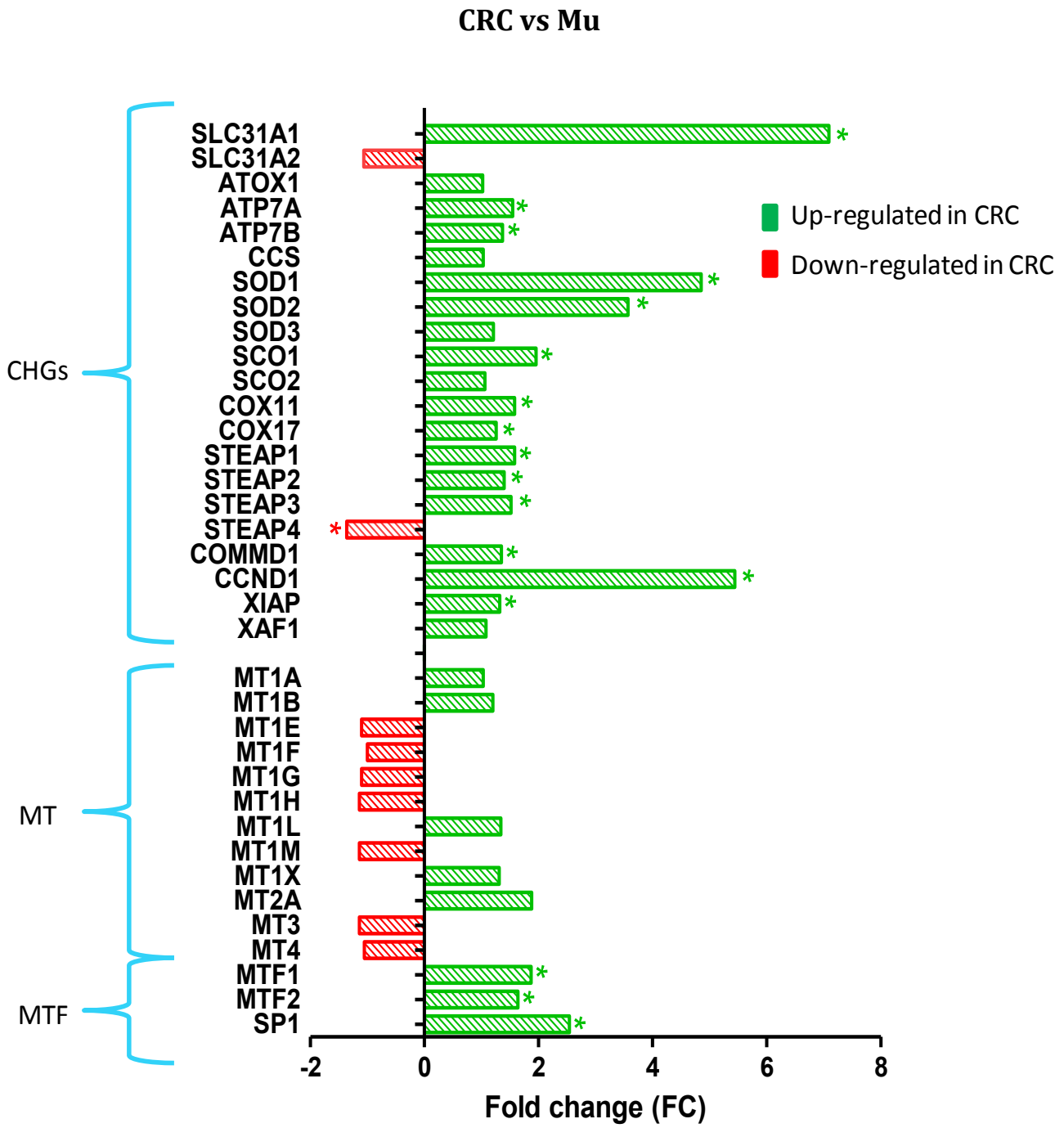

Figure 20. Differential expression of transcripts for copper homeostasis genes (CHGs), metallothioneins (MT) and metal transcription factors (MTF) in CRC versus normal matched mucosae (Mu). Values are expressed as linear fold changes calculated in the following way: $2^{[\text{CRC Average RMA} - \text{Mu average RMA}]}$ if CRC >Mu, or $-2^{[\text{Mu Average RMA} - \text{CRC average RMA}]}$ if CRC <Mu.* False Discovery Rate (FDR) p<0.004 and fold-change >1.25 or <-1.25

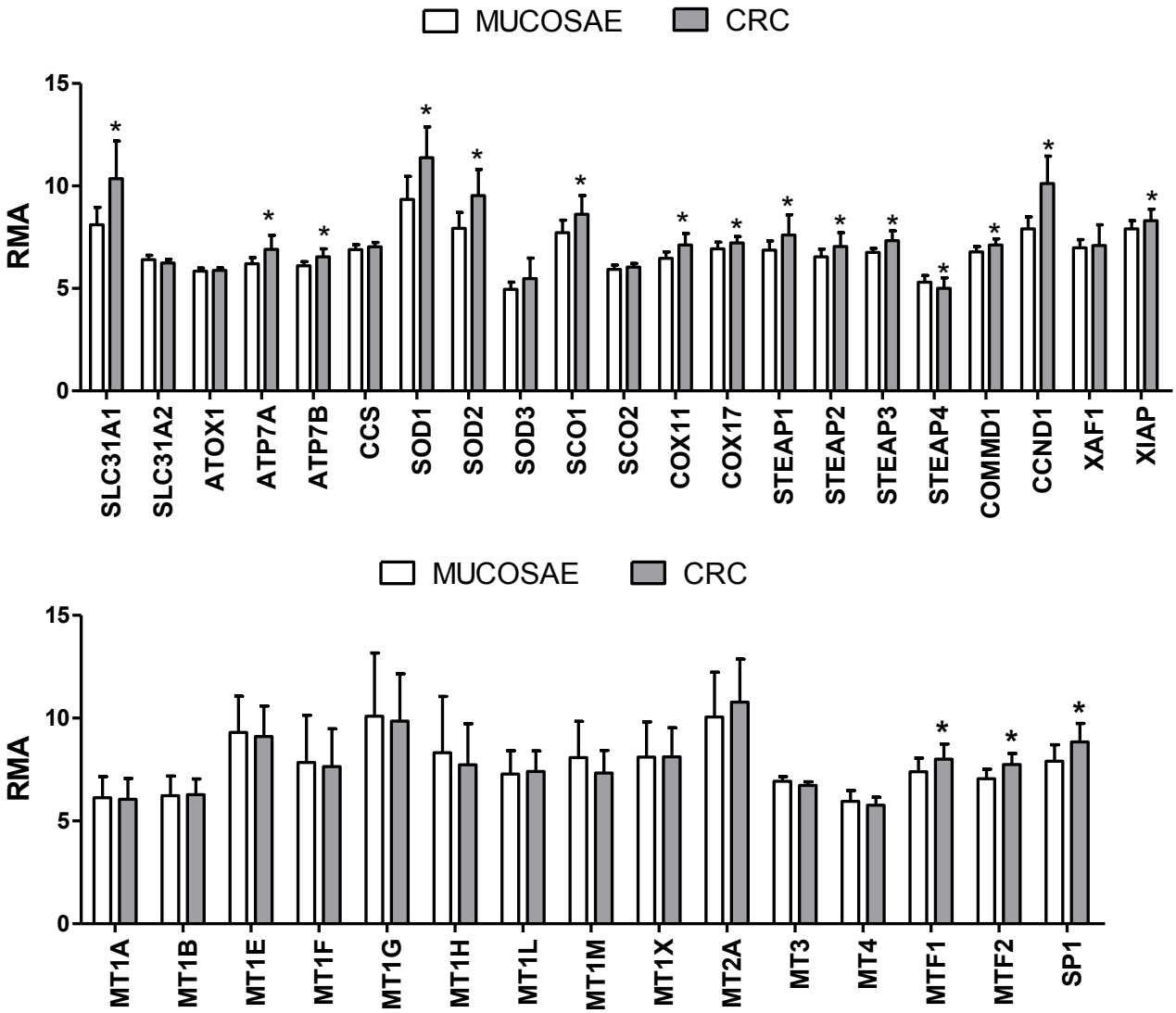

Figure 21. A,B Expression levels (RMA values) of transcripts coding for copper homeostasis genes (CHGs), metallothioneins (MT) and metal transcription factors (MTF) in 27 colorectal samples (CRC) and 19 matched normal colonic tissues. .* False Discovery Rate (FDR) p<0.002

Similar changes have been also detected in three colon cancer cell lines (Caco-2, HT29, HCT116) and in other different cancer cell lines: the breast cancer cell line, MCF7, and prostate cancer cell line, PC3 (Fig. 22). Our analysis revealed that in all tested cancer cell lines a strong increase of the following transcripts has been found: SLC31A1, SCO1 and COX11, as well as of the genes coding for the metal-regulatory transcription factors, MTF1 and MTF2. In conclusion the transcriptome analysis of copper homeostasis genes reveals a coordinated upregulation of SLC31A1, SCO1 and COX11 with the index of the proliferation status of the tumor (CCND1 mRNA level) in colorectal cancer tissues and in cancer cell lines.

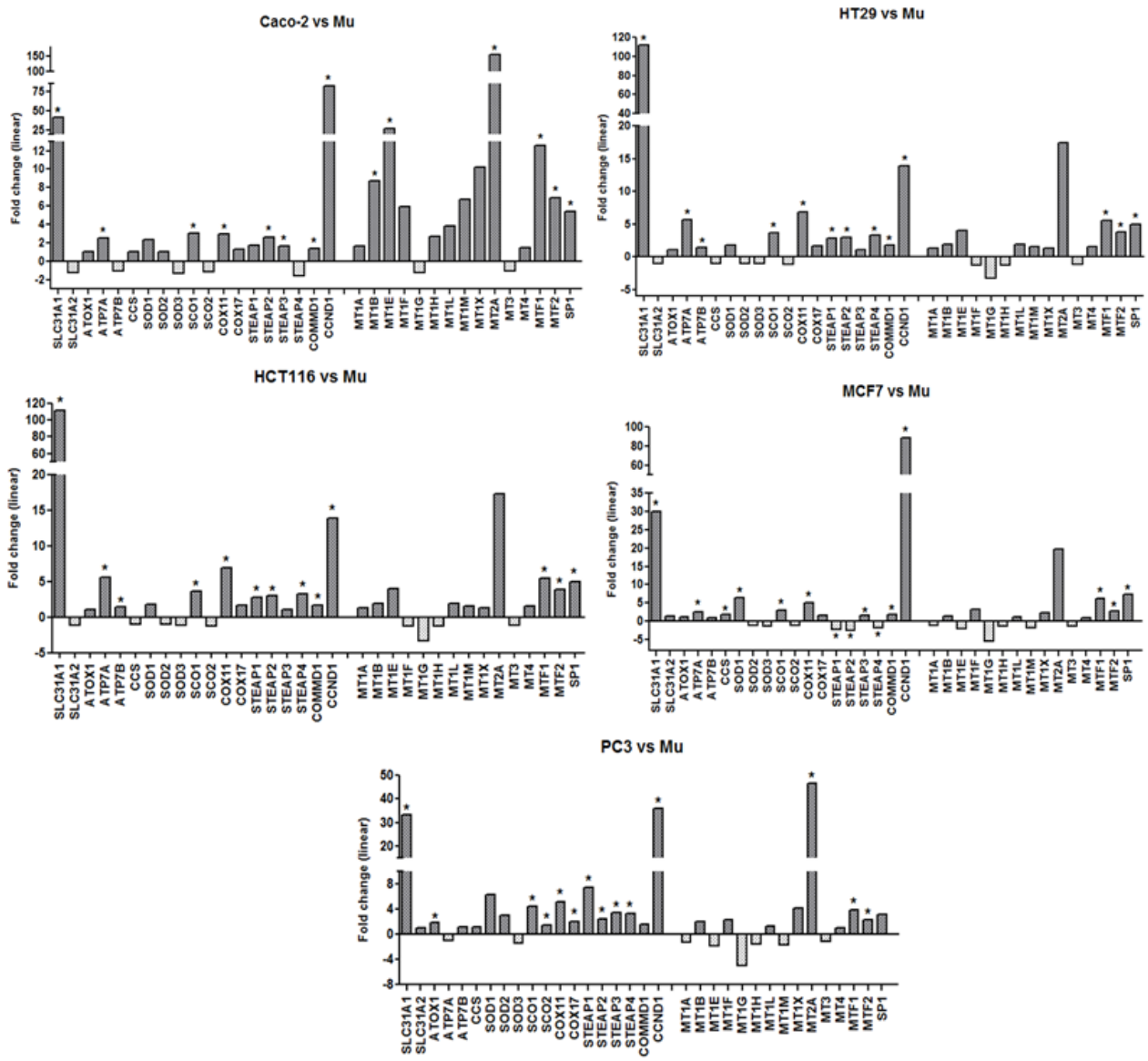

Figure 22. Differential expression of CHGs in different cancer cell lines versus normal mucosae (Mu). Linear fold changes are calculated in the following way: $2^{[\text{CRC Average RMA} - \text{Mu average RMA}]}$ if cell lines >Mu, or $-2^{[\text{Mu Average RMA} - \text{cell lines average RMA}]}$ if cell lines <Mu (●FDR p≤0.005)

3.3 Correlation analysis of CHG mRNA level in CRC samples

RMA-gene-full-signals obtained by HTA in 27 CRCs and 19 colonic mucosae allowed to reveal a significant correlation between SLC31A1 and CCND1 (Fig. 23), suggesting that the transcriptional up-regulation of CTR1 is part of a harmonized program of gene regulation associated with the proliferation status of the tumor. Interestingly a similar correlation with CCND1 mRNA has been also found for other up-regulated CHGs, such as SOD1, COX11, SCO1 and SOD2 indicating that the enhanced proliferative state of the tumor is correlated also with an increase of expression levels for some cuproenzymes and copper chaperones that play an important role in cellular defense to oxidative stress and in copper cellular distribution, respectively.

	CRC						
Gene Symbol	**SLC31A1**	**ATP7A**	**SOD1**	**SOD2**	**COX11**	**SCO1**	**CCND1**
SLC31A1		0.654	0.848	0.654	0.745	0.776	0.762
ATP7A	0.654		0.608	0.558	0.484	0.383	0.474
SOD1	0.848	0.608		0.655	0.657	0.578	0.613
SOD2	0.654	0.558	0.655		0.539	0.440	0.634
COX11	0.745	0.484	0.657	0.539		0.657	0.655
SCO1	0.776	0.383	0.578	0.440	0.657		0.692
CCND1	0.762	0.474	0.613	0.634	0.655	0.692	

Figure 23. Correlation analysis between mRNA levels for the indicated genes in 27 CRC samples. Pearson's correlation coefficients (R) are reported in the table, green $p<0.001$, purple not significant

3.4 Effect of copper treatments on CHGs expression

In order to evaluate the copper effect on gene expression levels of transcripts coding for CHGs, *Caco-2* cells were incubated for 2 hours in PBS (containing 0.9 mM Calcium Chloride, 0.5 mM Magnesium Chloride, and 5.6 mM DGlucose) and treated with copper nitrate at 10 and 100 µM. After 2-hours incubation in PBS, the standard growth medium (DMEM + 10% FBS) was restored and total RNA was extracted at 48 hours from the treatment and the gene expression levels were determined by microarray analysis (Human Transcriptome arrays). As reported in Fig. 24, the copper treatment at 100 µM showed, in comparison to control cells, a significantly decreased of RMA values for ATP7A, ATOX1, CCS, SCO1, COX11, and STEAP2 while the copper treatment at 10 µM showed the same expression levels respect to control cells.

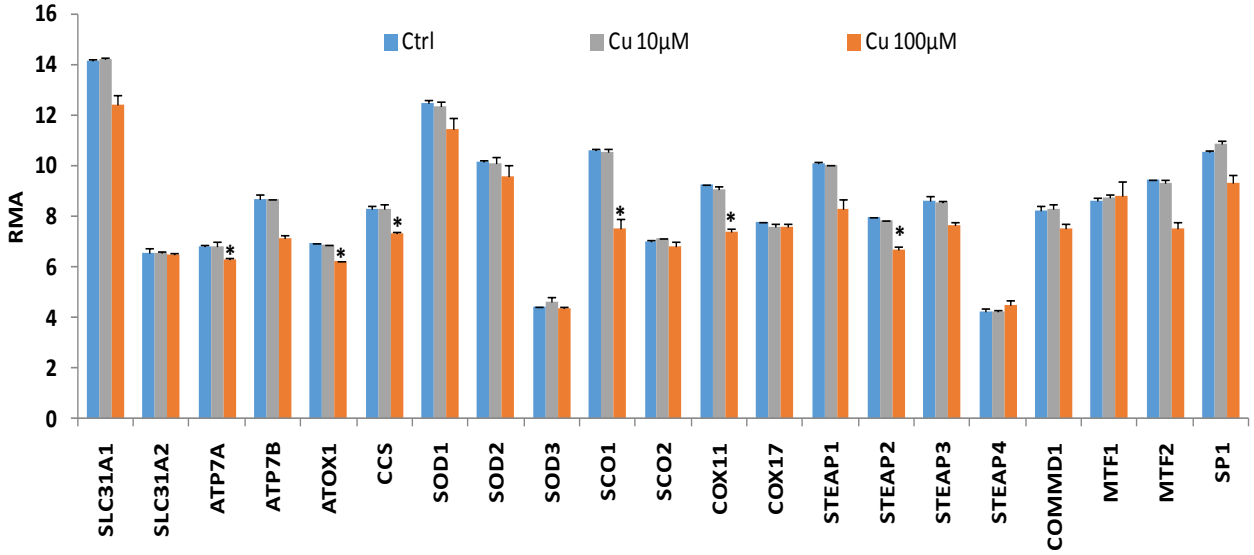

Figure 24. Expression levels (RMA values) of transcripts coding for copper homeostasis genes (CHGs), in *Caco-2* cells. Statistical differences were assessed using the Student's t test and were defined as * $p<0.005$

3.5 SLC31A1, SCO1 and COX 11 exon-level expression analysis

The GeneChip Human Transcriptome Array 2.0 (Affymetrix) was designed with approximately ten probes per exon and four probes per exon-exon splice junction, thus allowing an analysis of expression at the exon level. The software Transcriptome Analysis Console (TAC) 2.0 was used for the alternative splicing analysis using default parameters. The TAC software provides a comparison of the expression of each exon (corresponding to a probe selection region, PSR) in two different conditions (CRC versus normal colonic mucosae). Such comparison is obtained by algorithm called "splicing index". Splicing Index algorithm compares normalized signal estimates between normal and tumor condition: (Intensity of Exon X in CRC / Intensity of Gene Y in CRC) / (Intensity of Exon X in normal colonic mucosae / Intensity of Gene Y in normal colonic mucosae). Therefore a positive index is obtained for exons prevalently expressed in cancer cells, while a negative one indicates a prevalent expression in normal colonic cells. The exon levels (A) and alternative transcripts (B) for SLC31A1 determined by this high resolution array are shown in Fig. 25 and in Table 3A. The upregulation of SLC31A1 involves five exons (1, 2, 3, 4, 5) that have been included in the classical structure of this gene (Fig. 8) [**Lee et al. 2000, Kim et al 2013, Ohrvik and Thiele 2014**]. Differences in the expression level of the different exons (3, 4 and 5b) is also observed between CRC samples and Mu. The analysis revealed the presence of higher expression of exon 3,4 and 5b in CRC samples and of exon 1 and 2 in mucosae (Fold Change Table 3A). Fig. 25A and in Table 3A show a significant negative splicing index of exon 1,2 and 5d suggesting the possibility of this alternative transcript expressed prevalent in colonic mucosa respect to tumor samples. On the contrary, the positive splicing index for exon 3,4 and 5b indicate the possibility of a prevalent expression of the transcript containing these exons in CRC samples (Fig. 25A, Table 3A). Similar results were obtained by the comparison of cancer cell lines (Caco-2, HT29, HCT116) versus the same set of normal colonic mucosae (Table 3B).

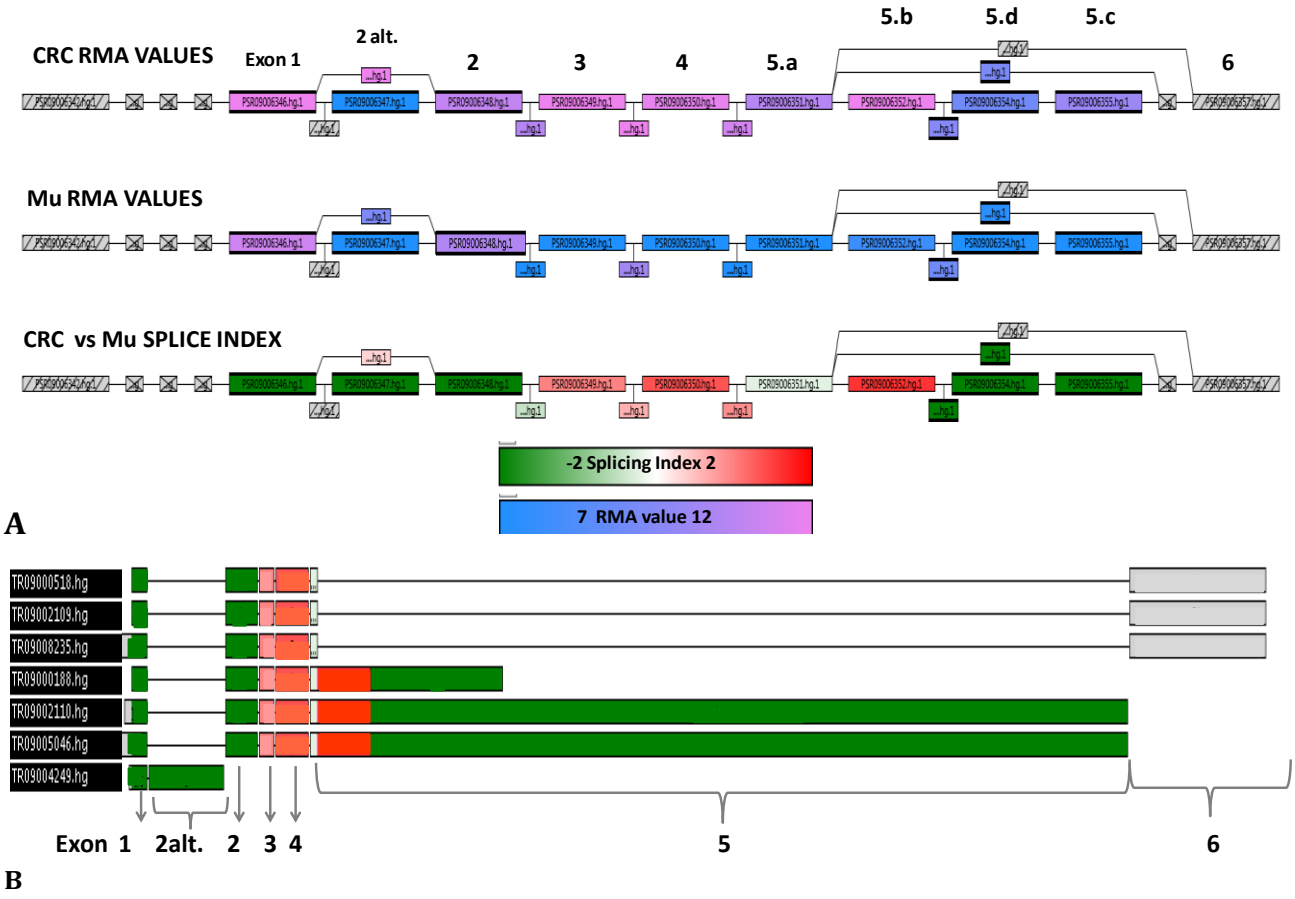

Figure 25. A Gene Structure View of SLC31A1 (TAC software). All PSRs and Junctions are represented with boxes. The first two lines from the top display, in pink/azure scale, the RMA values for each PSR and corresponding exons: top line for CRC and middle line for normal mucosae (Mu). The bottom line display the, in a green/red scale, the splicing index. **B Alternative transcripts for SLC31A1** on the basis of sequence data in public databases and in TAC (Affymetrix) database.

Table 3A

Exon	PSR	mRNA/PROTEIN	CRC RMA value	Mu RMA value	Fold change	Splicing Index	Splicing Index FDR
1	PSR09006346.hg.1	5' UTR	12.74	11.23	2.84	-5.02	0.0000004
2alt	PSR09006347.hg.1	?	6.2	6.48	-1.21	-17.97	0.000000001
2	PSR09006348.hg.1	5'UTR.CDS/aa 1-43	10.95	9.12	3.55	-3.56	0.000002
3	PSR09006349.hg.1	CDS/aa 44-68	12.25	6.9	40.78	1.49	0.005298
4	PSR09006350.hg.1	CDS/aa 69-124	11.82	6.67	35.50	1.68	0.000097
5a	PSR09006351.hg.1	CDS/aa 125-136	10.66	6.92	13.36	-1.11	0.518524
5b	PSR09006352.hg.1	CDS.3'UTR/ aa 137-190	12.99	7.73	38.31	1.8	0.000024
5d	PSR09006354.hg.1	3' UTR	8.99	6.99	4.00	-4.56	0.000008
5c	PSR09006355.hg.1	3' UTR	10.04	6.76	9.71	-2.1	0.000093

Table 3B

Exon	PSR	mRNA/PROTEIN	Cancer cell lines RMA value	Mu RMA value	Fold change	Splicing Index	Splicing Index FDR
1	PSR09006346.hg.1	5' UTR	15.36	11.23	17.50	-7.62	0.00000009
2alt	PSR09006347.hg.1	?	5.97	6.48	-1.42	-284.31	0.00000000000001
2	PSR09006348.hg.1	5'UTR.CDS/aa 1-43	13.33	9.12	18.50	-7.57	0.000000131
3	PSR09006349.hg.1	CDS/aa 44-68	16.62	6.9	843.35	2.61	0.000198
4	PSR09006350.hg.1	CDS/aa 69-124	15.57	6.67	568.09	1.99	0.001048
5a	PSR09006351.hg.1	CDS/aa 125-136	14.11	6.92	477.71	-1.19	0.459013
5b	PSR09006352.hg.1	CDS.3'UTR/ aa 137-190	16.4	7.73	407.3	1.44	0.132611
5d	PSR09006354.hg.1	3' UTR	10.1	6.99	8.63	-18.03	0.0000000007
5c	PSR09006355.hg.1	3' UTR	11.14	6.76	20.82	-6.78	0.000000003

Table 3. A Exon-level analysis of SLC31A1 gene: comparison between CRC samples and normal colonic mucosae (Mu). **B** Exon-level analysis of SLC31A1 gene: comparison between differential cancer cell lines and normal colonic mucosae (Mu).

Same analysis was performed on other two genes more expressed in tumor samples respect to normal colonic mucosae: SCO1, a cytochrome C oxidase assembly protein, and on COX11, a cytochrome c oxidase copper chaperone.

The SCO1 exon-level analysis and alternative transcripts are reported in Fig. 26 A-B. The RMA and Splice Index values are reported in Table 4A. Data showed that the exons 2, 3 and 4 of SCO1 were upregulation in CRC tumors respect to normal colonic mucosae while similar levels of expression were observed for exon 5 and 6 in both conditions. A significant positive splicing index of exon 2, 3, and 4 suggests the possibility of alternative transcripts containing these three genes, prevalent in CRC respect to normal colonic mucosae. Similar results were obtained comparing three cancer cell lines (Caco-2, HT29, HCT116) versus normal colonic mucosae (Table 4B), in this case only exon 3 revealed a significant splice index value. No variation of exon expression has been obtained for COX11.

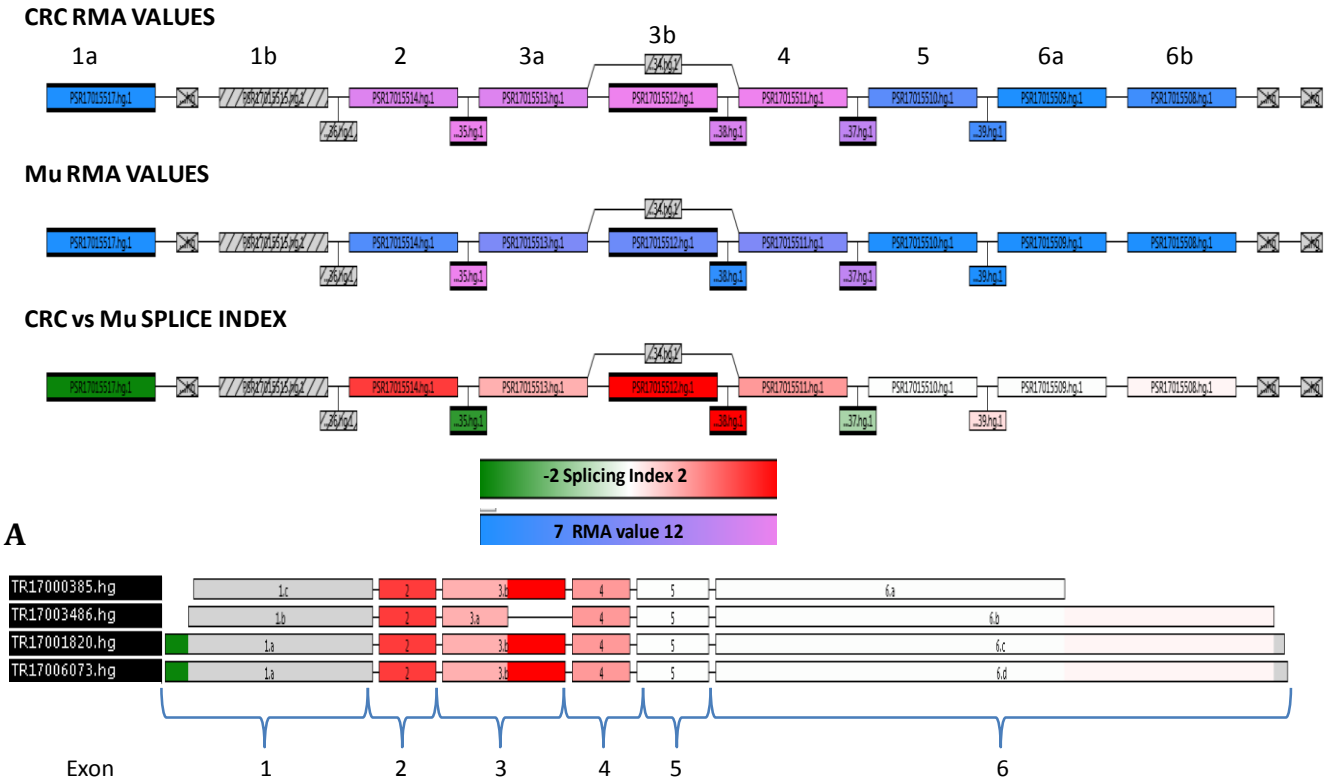

Figure 26. A Gene Structure View of SCO1 (TAC software). Probe Selection Regions (PSRs) and Junctions are represented with rectangles. The first two lines from the top display, in pink/azure scale, the RMA values for each PSR and corresponding exons: top line for CRC and middle line for normal mucosae (Mu). The bottom line display the, in a green/red scale, the splicing index. **B Alternative transcripts for SCO1** on the basis of sequence data in public databases and in TAC (Affymetrix) database.

Table 4A

Exon	PSR	mRNA/PROTEIN	CRC RMA value	Mu RMA value	Fold change	Splicing Index	Splicing Index FDR
1	PSR17015515.hg.1	5'UTR/CDS AAs 1-91	4.58	4.26	1.24	-1.65	0.000000001
2	PSR17015514.hg.1	CDS AAs 92-121	9.75	7.74	4.02	1.77	0.000009
3	PSR17015512.hg.1	CDS AAs 122-187	9.75	8.12	6	2.34	0.000017
4	PSR17015511.hg.1	CDS AAs 188-218	10.11	8.4	3.27	1.4	0.021419
5	PSR17015510.hg.1	CDS AAs 219-257	7.88	7.02	1.81	-1.03	0.081626
6	PSR17015508.hg.1	CDS AAs 258-301/3'UTR	7.48	6.33	2.22	1.04	0.938838

Table 4B

Exon	PSR	mRNA/PROTEIN	Cancer cell lines RMA value	Mu RMA value	Fold change	Splicing Index	Splicing Index FDR
1	PSR17015515.hg.1	5'UTR/CDS AAs 1-91	5.05	4.26	1.72	-2.49	0.000137
2	PSR17015514.hg.1	CDS AAs 92-121	10.43	9.12	6.48	1.77	0.16
3	PSR17015512.hg.1	CDS AAs 122-187	11.96	8.12	1.43	**2.99**	**0.000117**
4	PSR17015511.hg.1	CDS AAs 188-218	10.99	8.4	6.05	1.51	0.058
5	PSR17015510.hg.1	CDS AAs 219-257	8.65	7.02	3.09	-1.10	0.27
6	PSR17015508.hg.1	CDS AAs 258-301/3'UTR	8.15	6.33	3.53	-1.01	0.83

Table 4. A Exon-level analysis of SCO1 gene: comparison between CRC samples and normal colonic mucosae (Mu). **B** Exon-level analysis of SCO1 gene: comparison between differential cancer cell lines and normal colonic mucosae (Mu).

3.6 copper nitrate short treatment on Caco-2 cells growth

Caco-2 cells were incubated for 2 hours, respectively, in the DMEM medium with and without serum and in PBS (containing 0.9 mM Calcium Chloride, 0.5 mM Magnesium Chloride, and 5.5 mM D-Glucose) in order to investigate the chelating effect of molecules such as amino acids, vitamins and albumin contained in the culture medium and in the serum. After 2-hours incubation in DMEM or in PBS, the standard growth medium (DMEM + 10% FBS) was restored and cell viability was evaluated by MTT assay at various times (24h, 48h, 72h). As reported in Fig. 27, the 2-hours incubation in PBS or in DMEM without serum decreased the cellular growth in comparison to cells maintained in the presence of DMEM + 10% FBS. Since no significant difference was observed between PBS and DMEM, we concluded that this effect is mainly due to the short serum deprivation.

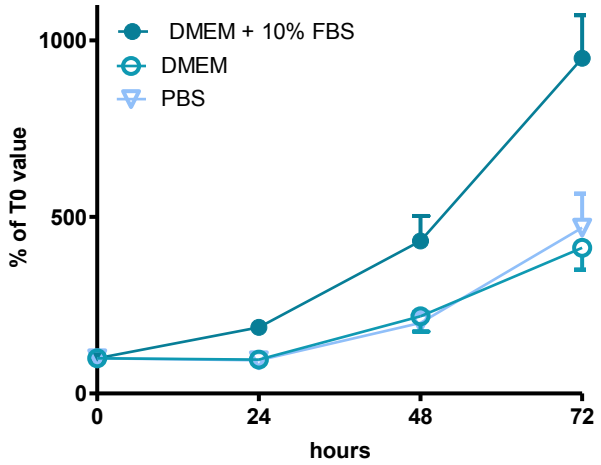

Figure 27. Effect of short serum-deprivation on cellular growth. Cells were incubated for 2 hours in PBS or in DMEM or in DMEM+10% FBS. Data are expressed as percentage of MTT assay values measured immediately before the two-hour incubation (T0 value).

Subsequently, it has been investigated the effects of a short treatment with copper nitrate, $Cu(NO_3)_2$ on cell growth and viability in the human colon cancer cells Caco-2. Cells were incubated for 2 hours with copper nitrate at increasing concentrations (0.01-100 μM) in three different incubation media: DMEM+10% FBS, DMEM without serum or PBS. Incubation media were replaced with standard growth medium (DMEM+10% FBS) at the end of the 2-hours copper treatment and MTT assay was performed after additional 48 hours.

Timeline of experimental procedure

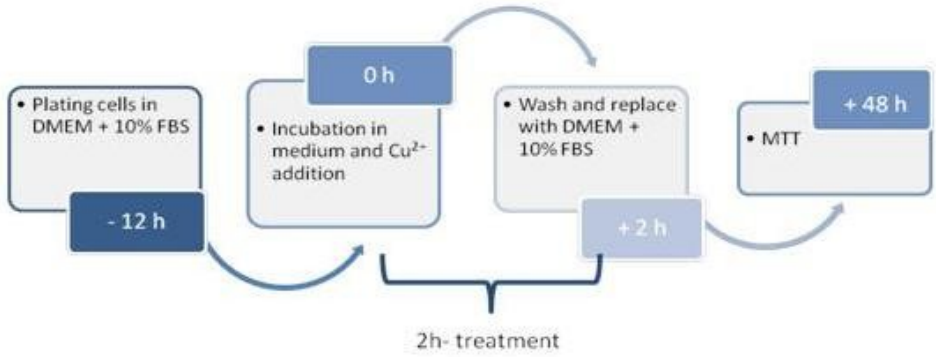

As reported in Fig 28, copper supplementation, at all tested concentrations, did not alter the Caco-2 cell viability in DMEM + 10% FBS or in DMEM alone. On the contrary, copper treatment produced a marked growth inhibition at higher concentrations (50-100 µM) when added in PBS. Moreover, a slight but significant increase of cell growth was observed with low copper concentrations (0.01-1 µM) when treatment was performed in PBS.

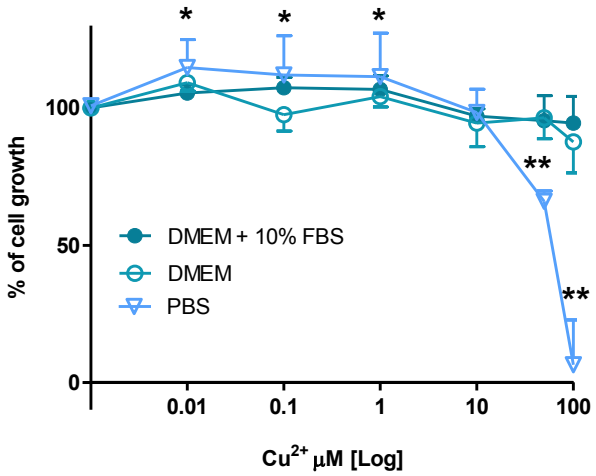

Figure 28. Copper treatment (2h) on Caco-2 cell growth in different incubation media (DMEM + 10%FBS, DMEM, PBS). Results are expressed as percentage of cell growth and are calculated as mean + S.E.M. for 4-5 independent experiments. Each experiment contains four-six samples for each treatment. Statistical differences were assessed using the Student's t-test. * $p \leq 0.002$, ** $p \leq 0.001$.

3.7 Copper increases the ionophores toxicity (OHQ compounds) in colorectal cancer cell lines

8-Hydroxyquinolines (OHQs) are metal binding compounds and are known to exhibit a variety of biological activities such as antibacterial and anticancer activities. Recently, these compounds have attracted interest as copper ionophores in fact the antiproliferative mechanism of hydroxyquinoline derivatives has been related to the complexation of copper ions and their intracellular transport. The Clioquinol (5-chloro-7-iodo-8-hydroxyquinoline, CQ) is the most known member of this family. In this scenario, Caco-2 and HT29 colorectal cancer cell lines were treated with three 8-Hydroxyquinoline derivatives: 5-chloro-7-iodo-8-hydroxyquinoline (CQ), 8-hydroxyquinoline (OHQ), 5-chloro-8-hydroxyquinoline (ClHQ), at increasing concentrations (from 0.01 to 100 µM) and two types of treatment have been planned: A short treatment which Caco-2 and HT29 cells have been incubated with OHQs in PBS for 2 hours and a prolonged treatment which the cells were incubated with OHQs in DMEM medium supplemented with 10% FBS for 72 hours.

Timeline of experimental procedures

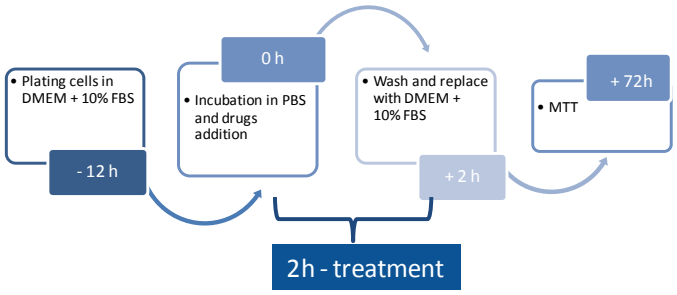

SHORT TREATMENT

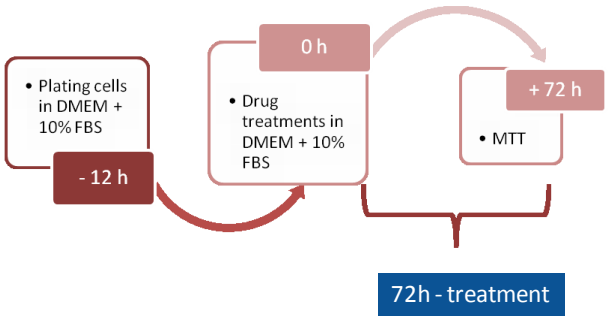

PROLONGED TREATMENT

As show in Fig. 29 the inhibition and cytotoxicity effects of ClHQ and OHQ were greater with prolonged treatment in both cell lines. The IC_{50}s calculated for short treatment ranging from

17.49 to 18.17 μM for CQ,, from 14.22 to 23.70 μM for ClHQ and from 17.77 to 26.94 μM for OHQ while IC_{50}s calculated for prolonged treatment ranging from 12.38 to 13.14 μM for CQ,, from 1.18 to 3.95 μM for ClHQ and from 0.81 to 1.52 μM for OHQ (IC_{50} values are reported in table 5). In addition, HT29 cell line showed a more sensitive to the same treatments with the OHQ compounds in comparison to Caco-2 cell line. In both cell lines, the OHQ and ClHQ showed a greater inhibition and cytotoxicity when the treatments were performed in 10% FBS for 72h, probably because the effect of these compounds was potentiated by copper contained in the culture medium. On the contrary the CQ revealed similar toxic effect in both treatments (short and prolonged).

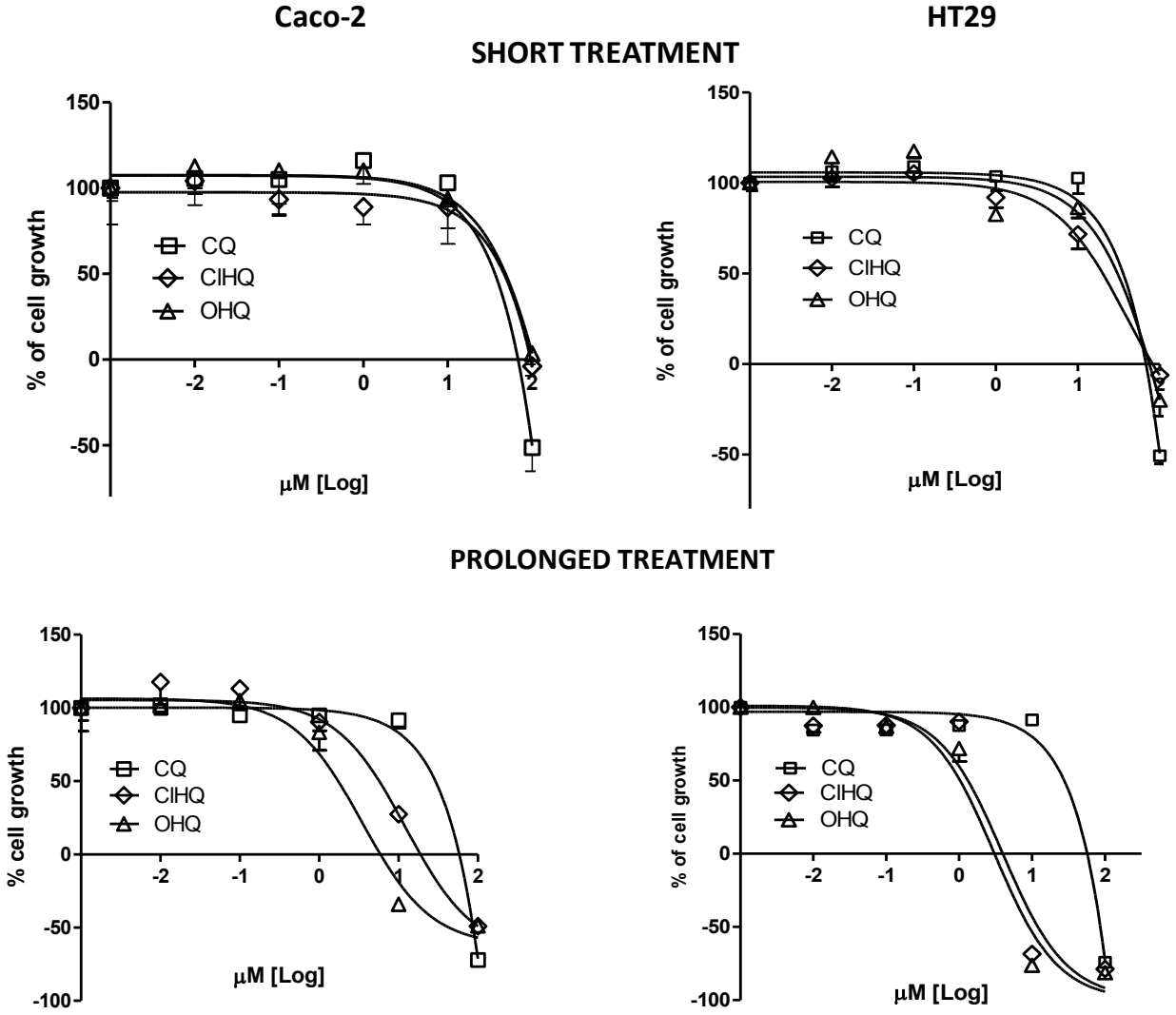

Figure 29. Concentration–response curves for "OHQ compounds" in colorectal cancer cell lines (Caco-2 and HT29 cells). Results are expressed as percentage of cell growth and are calculated as mean + S.E.M. for 4-5 independent experiments. IC50 values were calculated by the software GraphPad Prism v.5 with the equation log(inhibitor) vs. normalized response.

Table 5

	IC50 (95% Confidence Intervals)			
	Short		Prolonged	
	Caco-2	HT29	Caco-2	HT29
CQ	18.17 (6.82 to 48.40)	17.49 (4.57 to 66.94)	14.67 (6.46 to 33.29)	12.38 (3.70 to 41.39)
ClHQ	23.70 (13.79 to 40.75)	14.22 (8.40 to 24.06)	3.07 (1.63 to 5.78)	1.18 (0.27 to 5.04)
OHQ	26.94 (15.12 to 48.01)	17.77 (6.92 to 45.63)	1.52 (0.46 to 4.99)	0.81 (0.17 to 3.73)

Copper effects in combination with OHQs compounds have been evaluated in comparison to another essential trace element, the zinc in two colorectal cancer cell lines (Caco-2 and HT29). Cells have been treated, in DMEM, with 10% FBS or 2 hours in PBS, with OHQ compounds at increasing concentrations in the absence and in the presence of 20 μM $Cu(NO_3)_2$ and 50 μM $ZnCl_2$. MTT assays at 72 hours from the treatment (Fig. 30) have showed that growth-inhibition and cytotoxicity of ClHQ and OHQ were strongly increased by the short incubation with $Cu(NO_3)_2$ (20 μM) respect to the treatment with $ZnCl_2$ (50 μM), while CQ toxic effect was equally increased by both metals. On the contrary, in the prolonged treatment, the cytotoxic effect of ClHQ and OHQ on tested cell lines was enhanced by the copper addition but not zinc addition which showed a protective effect on cell growth. CQ toxic effect was potentiated by both metals. (IC_{50} values are showing in table 6).

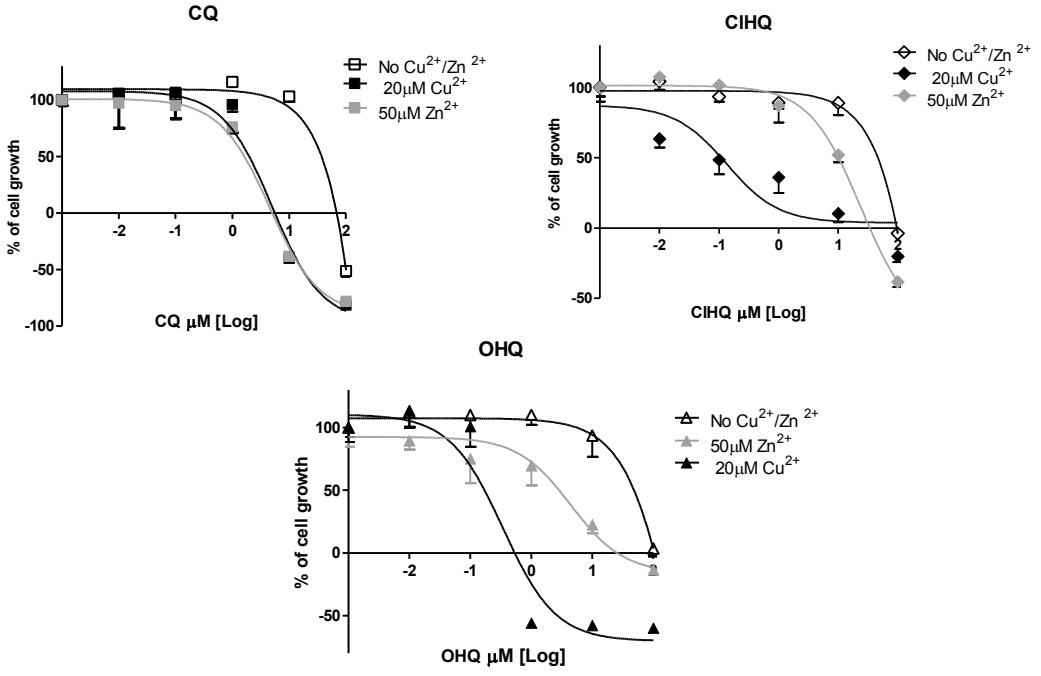

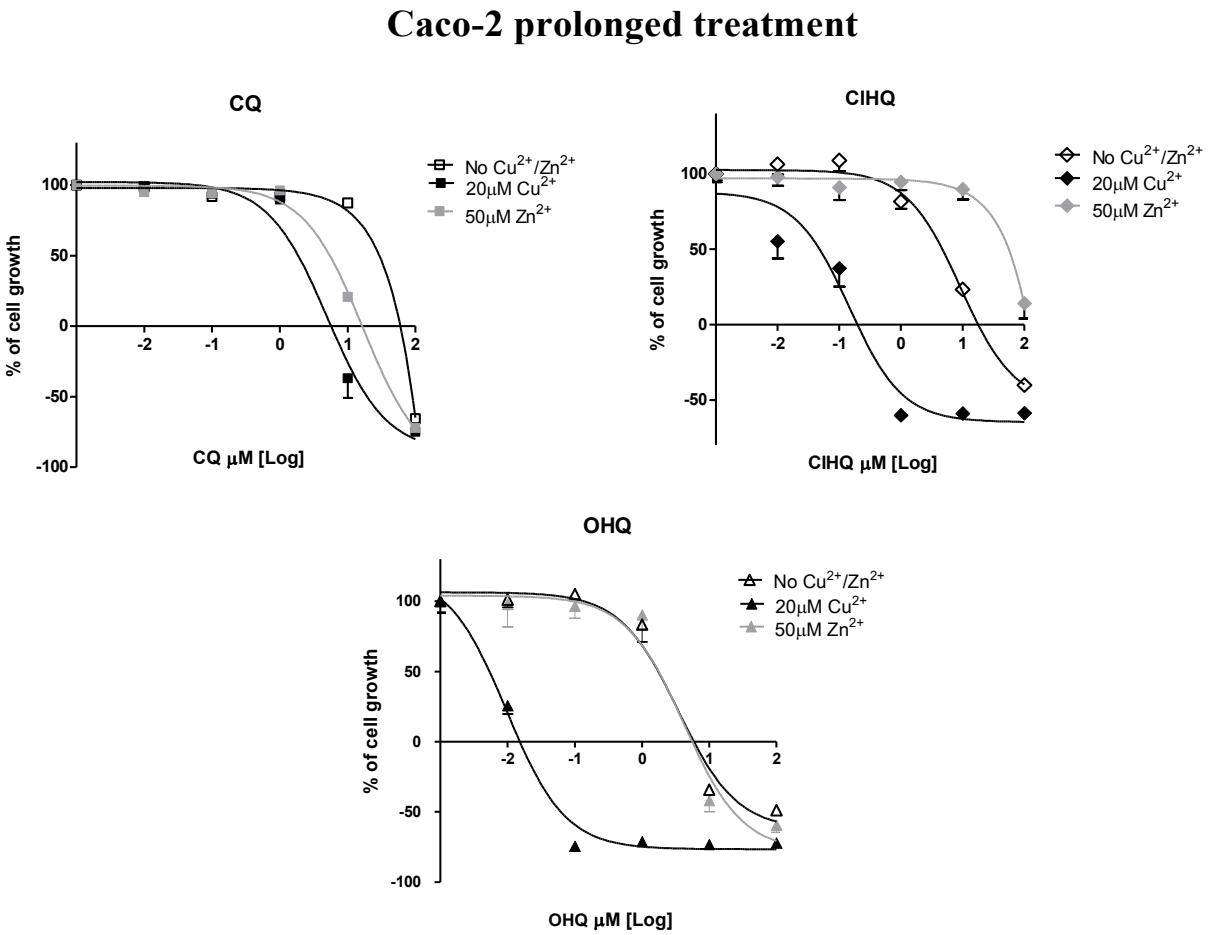

Figure 30. Comparison of concentration–response curves in Caco-2 cells treated for short and prolonged treatment with OHQs compounds. Results are expressed as percentage of cell growth and are calculated as mean + S.E.M. for 4-5 independent experiments. IC_{50} values were calculated by the software GraphPad Prism v.5 with the equation log(inhibitor) vs. normalized response

Table 6

CACO-2	IC_{50}(µM) (95% Confidence Intervals)		
Short treatment	**No Cu^{++} / Zn^{++}**	**20 µM Cu^{++}**	**50 µM Zn^{++}**
CQ	18.17 (6.82 to 48.40)	1.51 (0.23 to 9.79)	1.19 (0.23 to 6.05)
ClHQ	23.70 (13.79 to 40.75)	0.08 (0.03 to 0.19)	6.33 (2.38 to 16.70)
OHQ	26.94 (15.12 to 48.01)	0.17 (0.03 to 0.19)	2.01 (1.06 to 3.82)
Prolonged treatment	**No Cu^{++} / Zn^{++}**	**20 µM Cu^{++}**	**50 µM Zn^{++}**
CQ	14.67 (6.46 to 33.29)	1.43 (0.47 to 4.38)	3.54 (1.28 to 9.80)
ClHQ	3.07 (1.63 to 5.78)	0.02 (0.005 to 0.06)	29.69 (16.53 to 53.33)
OHQ	1.52 (0.46 to 4.99)	0.003 (0.0002 to 0.05)	1.55 (0.39 to 6.14)

Similar results were obtained with the other colorectal adenocarcinoma cell line HT29. In this dissertation we reported in Table 7 only IC_{50} values calculated by the software GraphPad Prism v.5 with the equation log(inhibitor) vs. normalized response.

Table 7

HT29	**IC_{50}(µM) (95% Confidence Intervals)**		
Short treatment	**No Cu^{++} / Zn^{++}**	**20 µM Cu^{++}**	**50 µM Zn^{++}**
CQ	17.49 (4.57 to 66.94)	0.82 (0.30 to 2.27)	1.31 (0.58 to 2.93)
ClHQ	14.22 (8.40 to 24.06)	0.03 (0.01 to 0.06)	1.80 (0.59 to 5.53)
OHQ	17.77 (6.92 to 45.63)	0.009 (0.002 to 0.03)	1.58 (0.43 to 5.79)
Prolonged treatment	**No Cu^{++} / Zn^{++}**	**20 µM Cu^{++}**	**50 µM Zn^{++}**
CQ	12.38 (3.70 to 41.39)	1.59 (0.39 to 6.45)	12.00 (4.52 to 31.85)
ClHQ	1.18 (0.27 to 5.04)	0.18 (0.04 to 0.89)	6328 (5.56 to 197)
OHQ	0.81 (0.17 to 3.73)	0.01 (0.001 to 0.11)	12.92 (4.25 to 39.33)

3.8 Copper converses the chelating effect of TPEN

TPEN (N.N.N'.N-tetrakis (2-pyridylmethyl) ethylenediamine) is a cell permeable high-affinity zinc and copper chelator. Several studies demonstrated that at lethal concentrations (>1μM), directly induces apoptosis of cultured human RPE cells (retinal pigment epithelium) in 48 hours. Although TPEN can chelate all the endogenous transition metals such as zinc, iron, and copper. TPEN-induced apoptosis is most likely caused by chelating and thus depleting intracellular zinc, and possibly copper. This conclusion can be deduced from the result that addition of equimolar copper or zinc. but not iron, blocked TPEN-induced apoptosis. and from the affinities of metals with TPEN (copper > zinc >iron) [**Hyun. Sohn et al., 2001**].

In order to test the activity of TPEN on cell growth, Caco-2 cells were treated in PBS, for 2 hours, and in D-MEM supplemented with 10% of FBS for 48 hours with the chelator at increasing concentrations (0.01-100 μM) then cell growth was evaluated after 48 hours by MTT assay (Fig. 31).

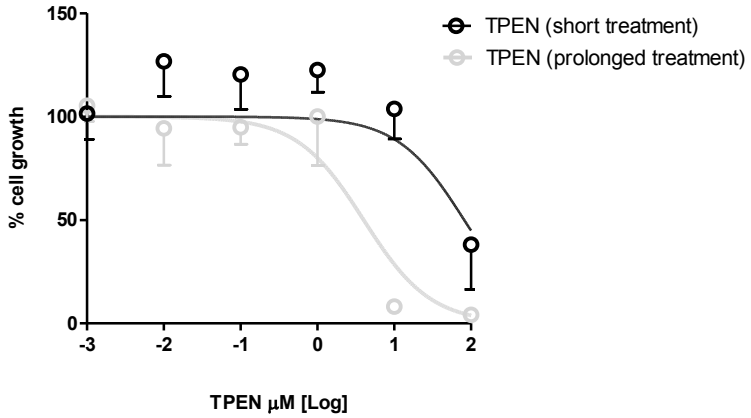

Figure 31. Caco-2 colon cancer cell line treated with TPEN for 48h in DMEM medium supplemented with FBS 10% and in PBS for only 2h. After 48h, MTT assays showed that TPEN is toxic at 100 μM in PBS and in DMEM medium at 10 μM. TPEN IC_{50} (μM) in cultured Caco-2 cells treated with TPEN at increasing concentrations.

Table 8

48h	TPEN in PBS 2h	TPEN in FBS10%
IC_{50} (μM)	62.67	1.25
95%ConfidenceIntervals	(16.83 to 233.3)	(0.2432 to 6.436)

MTT assays revealed that the TPEN treatment had different effects in PBS and in D-MEM. In PBS the treatment with TPEN was limited to a short time of 2h, then DMEM plus 10% FBS was replaced. MTT assay, at 48 hours from the treatment, showed that the chelator at lowest concentrations (0.01 to 1 μM) preserved the cell vitality but the growth-inhibiting activity

appeared at 100 µM (IC_{50} 62.67 µM) while in D-MEM supplemented with 10% of FBS, the TPEN treatment showed a cytotoxic effect at the concentration of 10 µM (IC_{50} 1.25 µM).

To establish whether copper depletion is involved in the TPEN-induced cytotoxicity, copper nitrate, at increasing concentrations (0.01-100 µM), was added to the incubation medium during TPEN treatment. Similar experiments were performed to evaluate the effect on TPEN toxicity of another metal: the Zinc, therefore the zinc chloride at increasing concentration was added in the culture medium.

For the short treatment, the TPEN has been used at the toxic concentrations of 100 µM while for prolonged treatment in DMEM, supplemented with 10% FBS, the TPEN has been added at 10 µM. After 48 hours from the treatment, The results showed (Fig. 32) that the TPEN toxic effect of TPEN was completely abrogated by addition of Copper or Zinc at equimolar concentration.

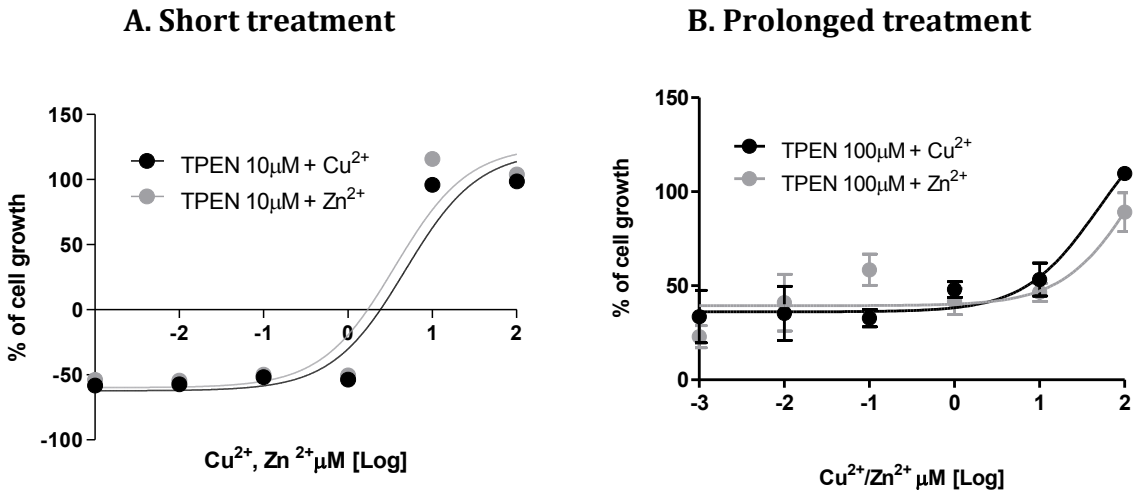

Figure 32. Concentration response curves of TPEN in Caco-2 cell line. Caco-2 cells were exposed at increasing concentrations of TPEN for2 hours in PBS (A) and for 48 hours in DMEM plus 10% FBS (B). Data were calculated as mean + S.E.M. for 2 independent experiments performed in quadruplicate.

3.9 GENE COPY NUMBER AND ATOX1 expression IN *Caco-2* CELL LINE

The Caco-2 is a cell line derived from a colon cancer with a strong aneuploidy. The long arm of chromosome 5, where is located the ATOX1 gene (5q33.1), is frequently deleted in colon cancer and in colon cancer cell lines [**Sheffer *et al*, 2009**]. In order to establish that the ATOX1 gene is not deleted in such cell model, *a high-resolution molecular cytogenetic* analysis by SNP array has been previously performed in Prof. D.F. Condorelli and Prof.ssa V. Barresi laboratories (University of Catania). Molecular analysis confirmed the presence of several chromosomal aberrations but showed a diploid copy number for chromosome 5 (Fig. 33A). Moreover, the mRNA level for ATOX1 was obtained by microarray analysis. As shown in Fig. 33B the RMA value for ATOX1 mRNA in Caco-2 cells is not significantly different from value observed in normal colonic mucosae. Data suggest the idea that this gene if altered in its expression, could represent a "Achilles' heel" of cancer cells becoming a good target for specific drug treatments.

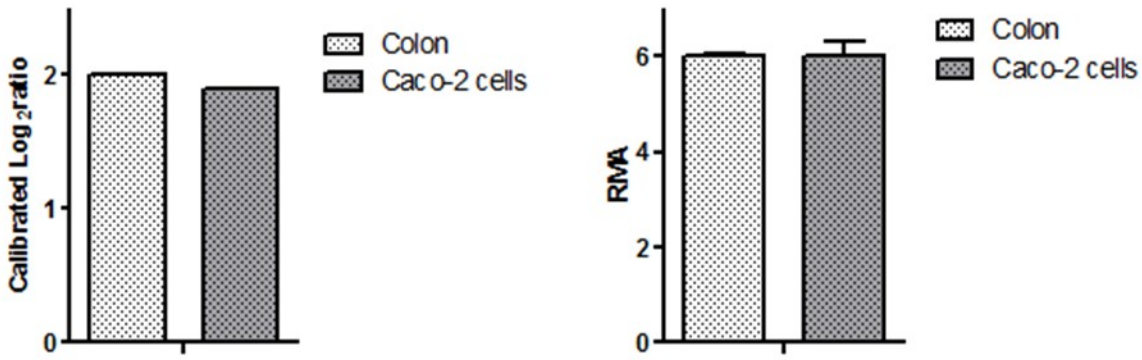

Figure 33 A) **ATOX1 gene copy number values** are reported in Caco-2 Cells (1.89) and in Colon mucosa (2.0) . The smoothed log2ratio is calibrated to copy number and anti-logged. B) **Expression levels of the ATOX1** in Caco-2 cells and in Colon Mucosa show the same amounts of ATOX1 transcripts, in both.

3.10 Silencing of copper chaperone ATOX1 in Caco-2 cell line

The expression of ATOX1 in Caco-2 cells was selectively silenced by short interference RNA (siRNA) at 25nM for 10 hours in Optimem as described in materials and methods. The efficiency of siRNA silencing was assessed by measuring ATOX1 transcript level by quantitative real time RT-PCR 24 and 48h hours after siRNA transfection. The mRNA expression of ATOX1 gene was normalized to GAPDH levels.

Timeline for silencing experimental procedure

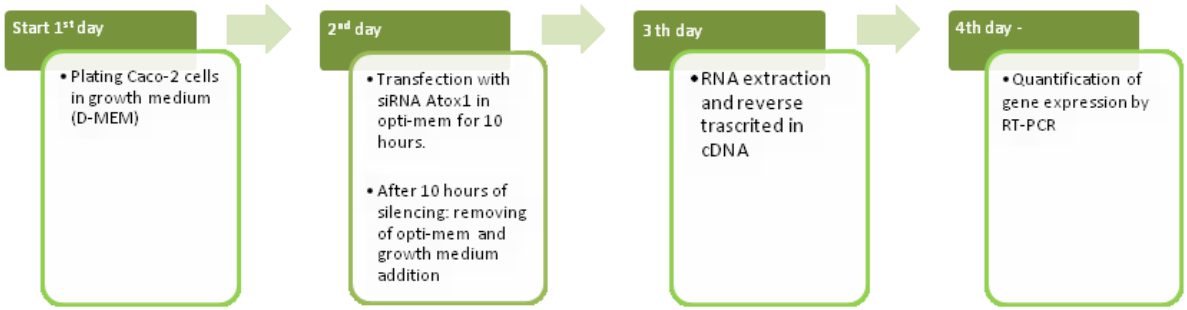

As shown in Fig.8 ATOX1 mRNA level was strongly decreased (-75%) in Caco-2 cells 24 hours after transfection with 25 nM ATOX1 siRNA. A significant decrease of ATOX1 mRNA level (-50%) persisted at 48 hours from siRNA transfection. In the same conditions the CCND1 transcript level was measured and the significant reduction of its expression was observed only 48 hours after siATOX1 transfection (Fig. 34).

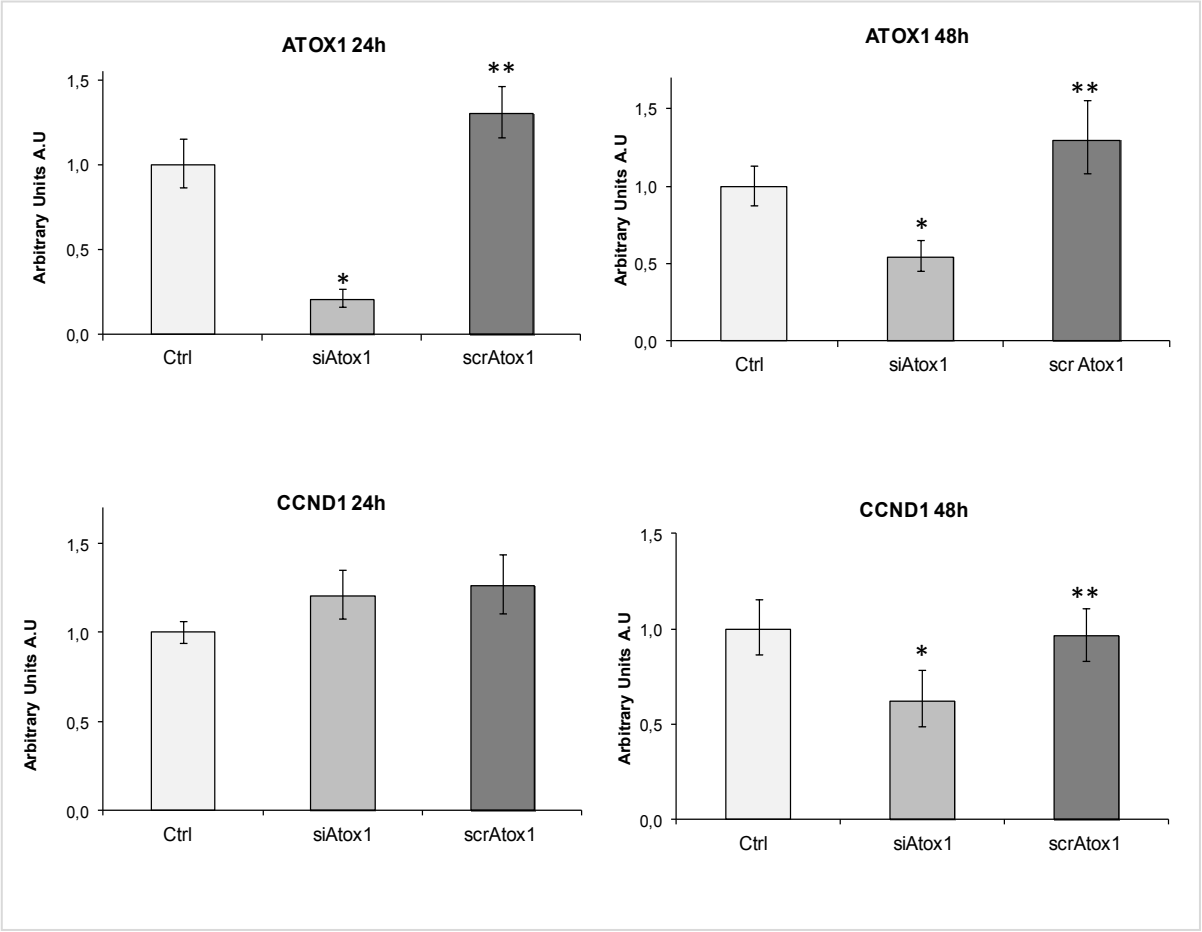

Figure 34. Effects of *specific siRNA* on ATOX1 gene expression evaluated by RT-PCR assay. Data were calculated as mean + S.E.M. for 3-4 independent experiments performed in quadruplicate. Statistical differences were assessed using the Student's t test and were defined as * siRNA vs Ctrl $p < 0.01$ and ** siRNA vs ScrRNA $p < 0.05$

As previously described ATOX1, alternatively, can assume a different function as a copper-dependent transcription factor able to regulate the expression of Cyclin D1 [**Itoh et al., 2008**]. These data could reflect the absence of ATOX1 transcript observed in the first 24 h and responsible, in the second time (after 48 from ATOX1 silencing), of the low levels of Cyclin transcript.

3.11 ATOX1 silencing enhances the sensitivity to copper

In order to evaluate if the silencing of Atox1 modulated the copper effect on cellular growth, Caco-2 cells were transfected with siAtox1 and scrAtox1 at 25nM for 10 hours. At 24 hours from transfection, cells were incubated for 2 hours in PBS containing copper nitrate at increasing concentrations (0.01-100 μM).

After replacing PBS with standard growth medium (DMEM+10% FBS), cells were incubated for additional 48 hours and MTT assays were performed. As shown in Fig. 35 ATOX1 silenced cells were more sensitive to toxic effects of high copper concentrations (50-100 μM) than control cells treated with scrambled RNA. In Atox1 silenced cells IC50 for copper decreased significantly in comparison to scrambled RNA treated cells. IC_{50} and 95% Confidence Intervals values are reported in table 9.

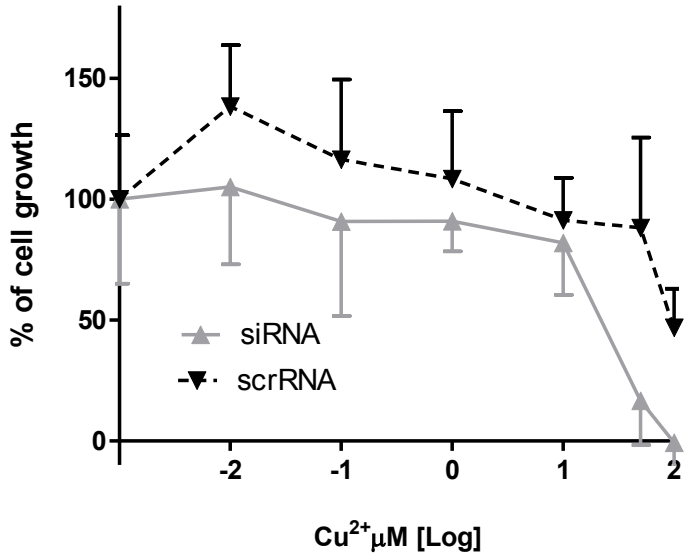

Figure 35. Effects of copper on ATOX1-silenced Caco-2 cells. Effects of siAtox-1 on cell growth were examined at 48 hours in comparison with scrATOX1 transfected cells.

Table 9

	IC_{50} (μM)	95% Confidence Intervals
siRNA + Cu^{2+}	19.33	9.005 to 41.49
scrRNA + Cu^{2+}	131.90	55.17 to 315.30

3.12 ATOX1 silencing enhances the sensitivity to ClHQ and TPEN

In this paragraph, the contribute of Atox-1 silencing on cellular growth in Caco-2 cells treated with OHQ compounds at increasing concentrations has been evaluated. Caco-2 cells were transfected with SiAtox1 and ScrAtox1 at 25nM for 10 hours. At 24 hours from the transfection, OHQs compounds were added at increasing concentration (0.01-100µM) in PBS for 2 hours. After the short-treatment, medium was replaced with standard DMEM+10% FBS and cell growth was evaluated after 48 hours by MTT assay. Data obtained showed that siAtox-1 was not able of increasing significantly the toxicity of cells treated with OHQ and CQ while the ClHQ toxicity was increased in silenced cells in comparison to control cells but a significant toxicity was obtained also in cells treated with the relative scramble (Fig. 36 and Table 10).

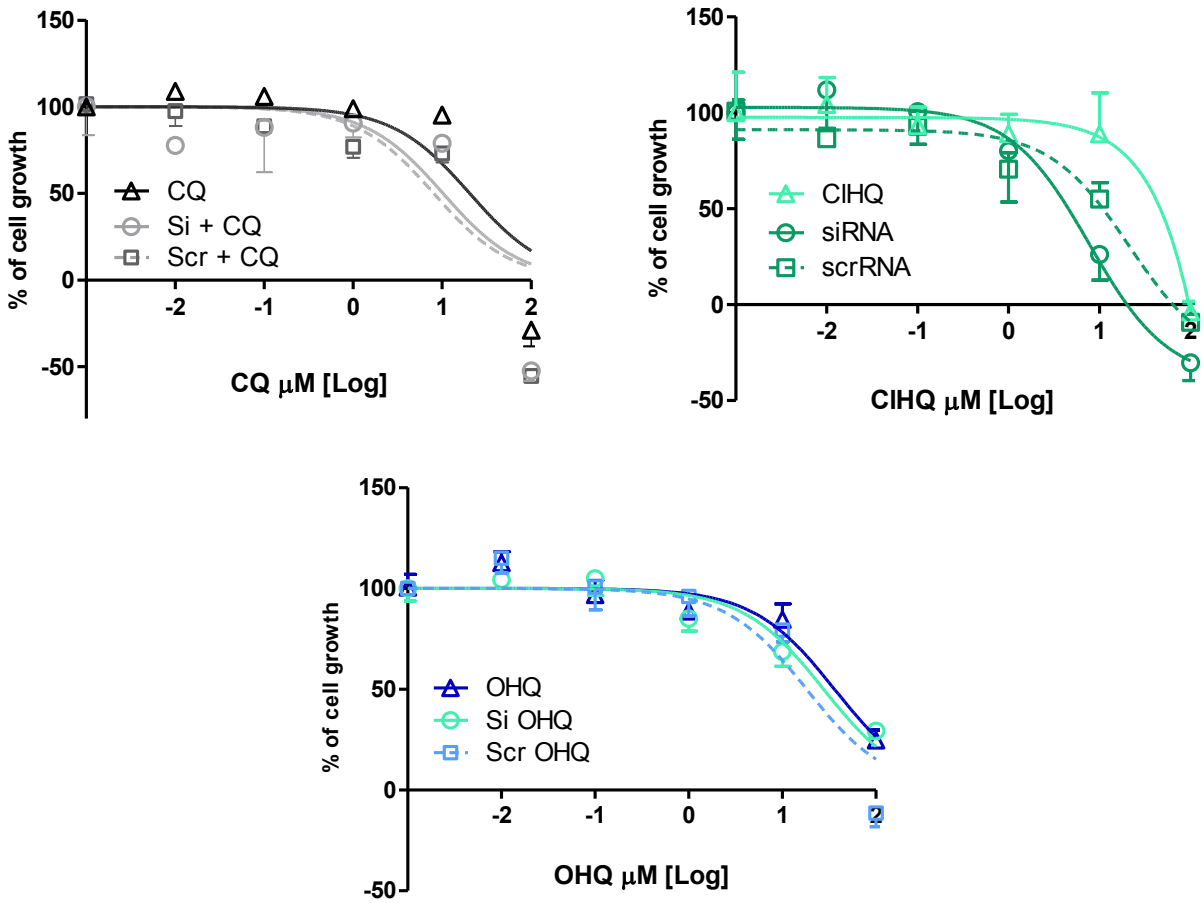

Figure 36. Concentration–response curves for short treatment with OHQs complexes on ATOX1-silenced Caco-2 cells

Table 10

Caco-2 in PBS	CQ	ClHQ	OHQ
IC_{50}	20.40	29.98	36.05
95% Confidence Intervals	9.129 to 45.57	20.10 to 44.70	21.05 to 61.74
	Si + CQ	**Si+ClHQ**	**Si+OHQ**
IC_{50}	10.23	3.300	27.57
95% Confidence Intervals	2.385 to 43.87	**1.733 to 6.284**	16.56 to 45.89
	Scr + CQ	**Scr+ClHQ**	**Scr+OHQ**
IC_{50}	8.040	**7.**628	18.14
95% Confidence Intervals	2.088 to 30.95	5.101 to 11.41	8.612 to 38.22

Subsequently, the copper contribution on cellular growth in Caco-2 cells silenced by siAtox-1 has been tested. Caco-2 cells were transfected with siAtox1 and scrAtox1 at 25nM for 10 hours after 24 hours the cells were treated with complexes of OHQs compounds, at increasing concentrations, and copper nitrate at 10 µM, in PBS for 2 hours. MTT assays at 48 hours from the treatment (Fig. 37 and Table 11), have shown that the combined effect of Atox1 silencing and the addition of copper nitrate increased the cytotoxicity of the only ClHQ, on the contrary the Caco-2 cells transfected with relative scramble did not show this enhancement of cytotoxicity. In the same experimental conditions the effect of ATOX1 silencing on cellular sensitivity to TPEN toxicity has been tested. As shown in Fig. 37 TPEN toxicity, was significantly enhanced in ATOX1-silenced cells (IC_{50} values in Table 11).

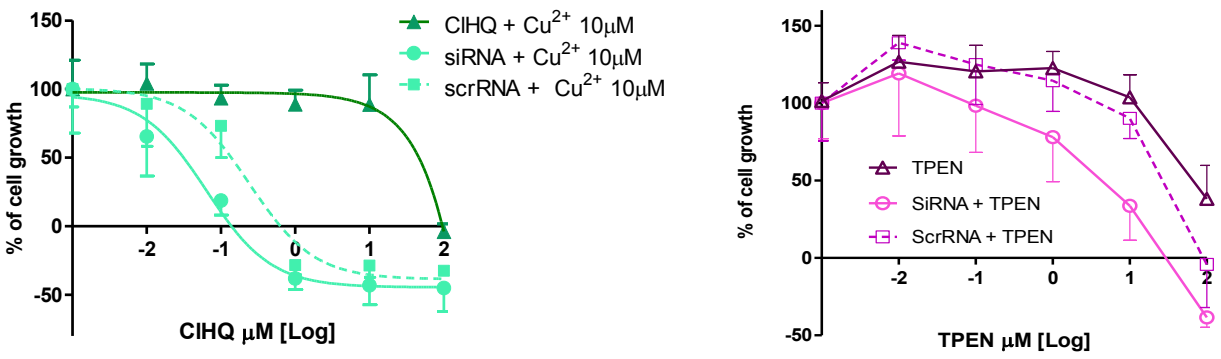

Figure 37. Effect of ATOX1 silencing in Caco-2 cell line treated with ClHQ/Cu complexes and TPEN for 2 hours in PBS. ATOX1 silencing increased the sensitivity of Caco-2 cells to copper-dependent effects of ClHQ and to TPEN treatment. Data were calculated as mean ± S.E.M. for 4-5 independent experiments. Each experiment contains four-six samples for each treatment.

Table 11

Caco-2 cells	ClHQ+ Cu 10µM	siRNA + ClHQ + Cu 10µM	scrRNA + ClHQ + Cu 10µM	TPEN	siRNA + TPEN	scrRNA + TPEN
IC_{50}(µM)	23.70	0.01	0.12	81.63	3.61	30.61
95% Confidence Intervals	13.05 to 43.04	0.006 to 0.053	0.055 to 0.27	44.29 to 150.50	1.29 to 10.06	10.46 to 89.57

These data demonstrated that a copper ionophores, ClHQ, is able to exert a copper-dependent cell toxicity in Caco-2 cells and the its effect is largely potentiated by ATOX1 silencing. On the contrary, the copper chelator T-PEN produces a form of cell toxicity that is reversed by the addition of Cu^{2+}. However, ATOX1 silencing, by RNA interference, potentiates TPEN toxicity in a way similar to what has been observed with ClHQ/Cu^{2+} complexes.

Discussion and conclusions

Copper plays essential roles in mammalian bioenergetics and it is critical in controlling cellular ROS levels. At the same time, excess copper concentrations are extremely toxic. A balance between copper necessity and toxicity is therefore crucial for cellular survival. To this purpose a conserved machinery has evolved to tightly regulate cellular Cu uptake and efflux. Disturbances in this balance could be crucial to the occurrence of genetic alterations and consequent development of cancer.

The public database Cancer Genome Atlas Network (2012) has been consulted, in this thesis, to investigate the presence of somatic mutations in Colorectal Cancer (CRC) and data obtained showed that genes encoding proteins involved in copper homeostasis, rarely harbor inactivating mutations suggesting that these mutations are negatively selected during the cancerogenesis process since these proteins play a fundamental role in cell survival.

The Human Transcriptome Array technology has enabled the analysis of CHGs expression in our series of colorectal carcinoma samples, showing an upregulation of several components of this functional pathway. In particular, we found a strong increase of mRNA levels for the copper transporter CTR1 (SCLC31A1 gene). CTR1 is a high-affinity copper transporter and an important regulator in response to environmental Cu stresses. Recently, it has been demonstrated that variations of copper levels into the cell can modulate the SCL31A1 expression. Indeed, Cu deficiency induced by treating human cancer cells with copper chelators up-regulates hCtr1 expression; whereas Cu sufficiency achieved by treating cells with $CuSO_4$, down-regulates endogenous hCtr1 expression [**Liang *et al.,* 2012. Song *et al.,* 2008**].

Differently from mRNA levels obtained for CTR1, the transcript for the low-affinity copper transporter, CTR2, did not show any significant change in CRC samples in comparison to normal colonic mucosae. This observation is in agreement with the difference in function and regulation of expression between the two copper transporters [**Blair *et al.,* 2010**]. The up-regulation of CTR1 in tumor samples respect to mucosae can be interpreted suggesting that the cancer cell proliferation and the cancer development are supported by a greater requirement for copper than normal cells.

It is important to remark that conclusions of the present thesis are not supported by analysis at the protein level. However, several studies show a correlation between

transcriptional activation of the CTR1 gene, its protein levels and the intensity of copper uptake [**Lin *et al.,* 2014; Song *et al.,* 2008; Kuo *et al.,* 2012**]. Moreover, an upregulation of CTR1 protein has been observed in a mouse model of HPV16-induced cervical carcinoma. In this model the CTR1 protein is highly expressed in tumoral cells but not in the normal cells of the tissue of origin of the tumor [**Ishida *et al.,* 2010**].

Our results have revealed that the increased CTR1 mRNA level is accompanied by a parallel increase of transcript levels for copper efflux pump ATP7A, the copper assembly factor SCO1 and COX11, the cupric reductases STEAP2 and STEAP3, and the metal transcription factors MTF1, MTF2 and Sp1. The high level of correlation of these mRNA changes might be explained by the existence of a coordinated transcriptional program.

In this sense, the significant correlations between SLC31A1 (encoding CTR1), SCO1, COX11 and CCND1 (cyclin D1) mRNA levels suggest that such transcriptional up-regulation is part of a gene regulation program associated with the proliferation status of the tumor and with a functional hyperactivity of copper trafficking pathways. Indeed, the observed transcriptional upregulation of the cuproenzyme SOD1 gene is coherent with an increase requirement and delivery of copper to intracellular sites. The observation that such results are also observed in the artificial growth conditions of the colon cancer cell lines suggests that the functional hyperactivity of copper trafficking pathways might represent a basic feature of this carcinogenesis process.

On the contrary, the copper chaperones ATOX1 and CCS showed a normal expression levels between the two conditions tested, suggesting that different mechanisms of post-translational regulation might be involved [**van den Berghe *et al.,* 2010; Dong *et al.,* 2014**]. Moreover, it has been reported that CTR1 silencing increases and copper supplementation decrease the protein level of ATOX1 and CCS [**Dong *et al.,* 2014**]. It is, therefore, conceivable that CTR1 over-expression in CRC is not accompanied by a parallel increase of ATOX1 and CCS mRNAs.

Several studies confirm that gene or protein expression levels of CTR1 could be regulated by several components of copper homeostasis pathway. In particular, recent papers have revealed that human Cu homeostasis is tightly controlled by inter-regulatory circuitry involving Cu, Sp1 and hCtr1. This circuitry uses Sp1 transcription factor as a Cu sensor in modulating hCtr1 expression which in turn controls cellular Cu and Sp1 levels in a three-way mutual regulatory loop [**Kuo *et al.,* 2012**]. Not only hCtr1, but also Sp1 itself, is regulated by Cu bioavailability (Fig. 9) The highest demand for copper by the

tumor cells could increase the expression level of Sp1 and consequentially those of SLC31A1.

Interestingly, in the present thesis we found a parallel transcriptional upregulation of CTR1 and the metallochaperones SCO1 and COX11 involved in the assembly of cytochrome c oxidase [**Cobine *et al.*, 2006**]. COX11 and SCO1 are co-metallochaperones assisting Cox17 in the copper insertion in cytochrome c oxidase. Copper metallation of the CuB site in the subunit 1 of cythocrome oxidase (Cox1) requires Cox11, while the metallochaperone SCO1 interacts with the subunit 2 of cythocrome oxidase (Cox2) to facilitate the maturation of its CuA site. It has been postulated that SCO1 mediates Cu(I) transfer from Cox17 to Cox2. In a recent paper [**Hlynialuk *et al.*, 2015**] it has been demonstrated that SCO1 is integral to a mitochondrial signalling pathway that regulates copper homeostasis by controlling the abundance and plasma membrane localization of CTR1, the high-affinity permease responsible for importing copper into the cell. Results obtained by Hlynialuk and colleagues suggest that SCO1 is implicated in the post-translational regulation of the high-affinity Cu importer CTR1 (Fig. 38). First, liver-specific deletion of SCO1 caused a severe Cu deficiency associated with a lack of the mature, glycosylated form of CTR1. Second, reductions in SCO1 in mouse embryonic fibroblasts abundance attenuated the localization of CTR1 on the plasmatic membrane, leading to a profound reduction in CTR1 protein levels. Therefore, a functional synergy between CTR1 and SCO1 may meet the higher copper demand by CRC cells.

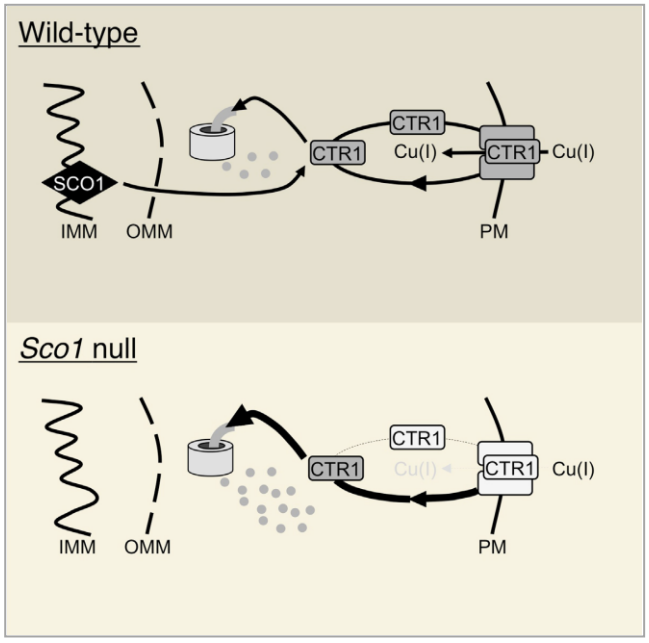

Figure 38. Schematic rappresentation of CTR1 regulation by SCO1 in wild-type mouse embryonic fibroblasts and in Sco1-/- mouse.

Our results provides fundamental information on the transcript-level expression of CHGs in colorectal cancer and further support the hypothesis that a subgroup of such cancers are characterized by a higher copper demand [**Ishida *et al.,* 2013**].

Furthermore, oligonucleotide microarrays have provided fundamental information on the exon-level expression of CHGs in colorectal cancer supporting, in particular, the hypothesis that specific alternative transcripts for SLC31A1 gene are prevalent in a condition respect to other.

It is well known that ATOX1 is an abbreviation of Antioxidant Protein 1, deriving from initial studies which have characterized this protein, for the importance its role in the defense against reactive oxygen species. Atox-1 is a copper chaperone with the ability to bind free copper ions protecting thus cells from generation of oxygen free radicals. Recent studies have showed that the lack of ATOX1 produces an abnormal distribution of intracellular copper, [**Miyayama *et al.,* 2009**] this probably determines an increase of intracellular copper-catalyzed toxic redox reactions, and therefore induces oxidative stress.

Probably, the cellular functions of ATOX1 are not limited solely to its copper-trafficking role but may include storage of labile copper, modulation of transcription, and antioxidant defense [**Klomp *et al.,*1997. Miyayama *et al.,* 2009**]. Recent data show that loss of ATOX1 or its inactivation, in mammalian cells, affects the intracellular copper amount depending whether or not cells express metallothioneins, small intracellular metal buffering proteins. [**Safaei *et al.,* 2009**]

Miyayama and colleagues [2009] demonstrated that the ATOX1 knockdown, in fibroblasts, was associated with an enhancement in intracellular copper levels, probably due to reduced copper export by Cu-ATPases (ATP7A/B). Cells, featured by both ATOX1 and metallothioneins downregulation, accumulated considerably more copper probably sequestered in cytosolic vesicles. This intracellular confinement is coherent with the data obtained previously **[Safaei *et al.,* 2009**, **Van den Berghe *et al.,* 2007**] which report that late endosomes and lysosomes act as a copper pool for the maintenance of cellular metallostasis in HEK-293T, HeLa, and U2OS cell lines. Safaei and colleagues [**2009**] have demonstrated that the silencing of ATOX1 in fibroblasts showed a significant enhance in the sensitivity of cells to copper treatment in comparison to ATOX1$^{+/+}$ fibroblasts.

In this thesis, data obtained by gene expression analysis and mutation profile in colorectal cancer have showed that the gene coding for copper chaperone Atox1 is highly stable as mRNA level in comparison to normal mucosae. These results suggest the idea that this gene could be a good target for specific anticancer treatments.

Therefore, in this thesis the effect of a down expression of Atox1 has been tested on cancer cell growth. The ATOX1 silencing has been performed using *RNA interference* (*RNAi*) in human colorectal adenocarcinoma cell line Caco-2. Our results have demonstrated that *ATOX1* silencing in Caco-2 increased the cellular toxicity during a short treatment with high concentrations of Cu^{2+} (Fig. 39) administrated in the extracellular medium. In this thesis, it has been also hypothesized that such modification in copper homeostasis might modify the sensitivity of tumor cells to anticancer drugs which act as copper ionophores or copper chelators (Fig. 39). For this purpose, Caco-2 cell line was silenced by short interfering for Atox1 and after 10 hours the cells were treated with 8-Hydroxyquinoline (OHQ) and two its derivatives such as ClHQ and CQ, all classified as copper ionophores. In cell line tested, these compounds have exhibited a copper-dependent cell toxicity and the copper dyshomeostasis induced by ATOX1 silencing has significantly enhanced the ClHQ toxic effect.

It is known that, CQ directly induces cell death in malignant cells at micromolar concentrations and also exhibits anti-cancer activity in vivo [Ding et al., 2005]. CQ induces apoptosis in cancer cells through a caspase dependent apoptotic pathway [Daniel et al., 2005; Ding et al., 2006]. Other OHQ derivatives have also been tested as anticancer compounds and it has been reported that the interaction with copper(II) ion is a prerequisite for their anticancer activity, as well as for CQ [**Zhai *et al.,* 2010**]. Experimental evidences suggest that OHQ and CQ act as anticancer agents through proteasome inhibition in the presence of copper [Schimmer et al., 2011]. It has recently been reported that CQ treatment caused cytoplasmic XIAP [X-linked IAP (inhibitor of apoptosis protein)] [**Fulda and Vucic 2012**], rapidly relocation to the nucleus in multiple human transformed (hyperplasic and carcinoma) prostate lines [**Cater and Haupt 2011**]. In the same work, the authors claimed that CQ also caused the cytoplasmic clearance of other IAP family members (cIAP1 and cIAP2) and that copper ion, and no other relevant bivalent metal ion (e.g. zinc or iron), was exclusively required for clioquinol to elicit an effect on XIAP. CQ in the presence of exogenous copper exerts an increased toxicity in comparison with the wild type Caco-2 cells probably by a more efficient degradation of

XIAP, the primary function of which is to hinder caspase activity and suppress apoptotic cell death.

On the other hand, cancer cells are known to accumulate more copper than normal cells. To deplete cellular copper, copper chelator, such as TPEN, was used to study cell responses under copper ''starvation'' conditions. Data obtained showed that TPEN produced a form of cell toxicity that is reversed by the addition of Cu^{2+} or Zn^{2+}, probably this particular toxic effect of TPEN was due to removal of metals, in particular copper and zinc, from their biologically active role. As reported by Fatfat and colleagues [**2014**] TPEN induces cell death by chelating intracellular copper and producing a TPEN-copper complex that engages in redox cycling. In particular TPEN ability to extract essential metals, particularly copper from mitochondrial electron carriers, facilitated the generation of superoxide and H_2O_2. Interestingly both the cytotoxic effect of co-treatment of ClHQ/copper complex than that TPEN were significantly potentiated by ATOX1 silencing because the down regulation of copper chaperone alters the normal intracellular balance making the cell more sensitive to copper biding compounds.

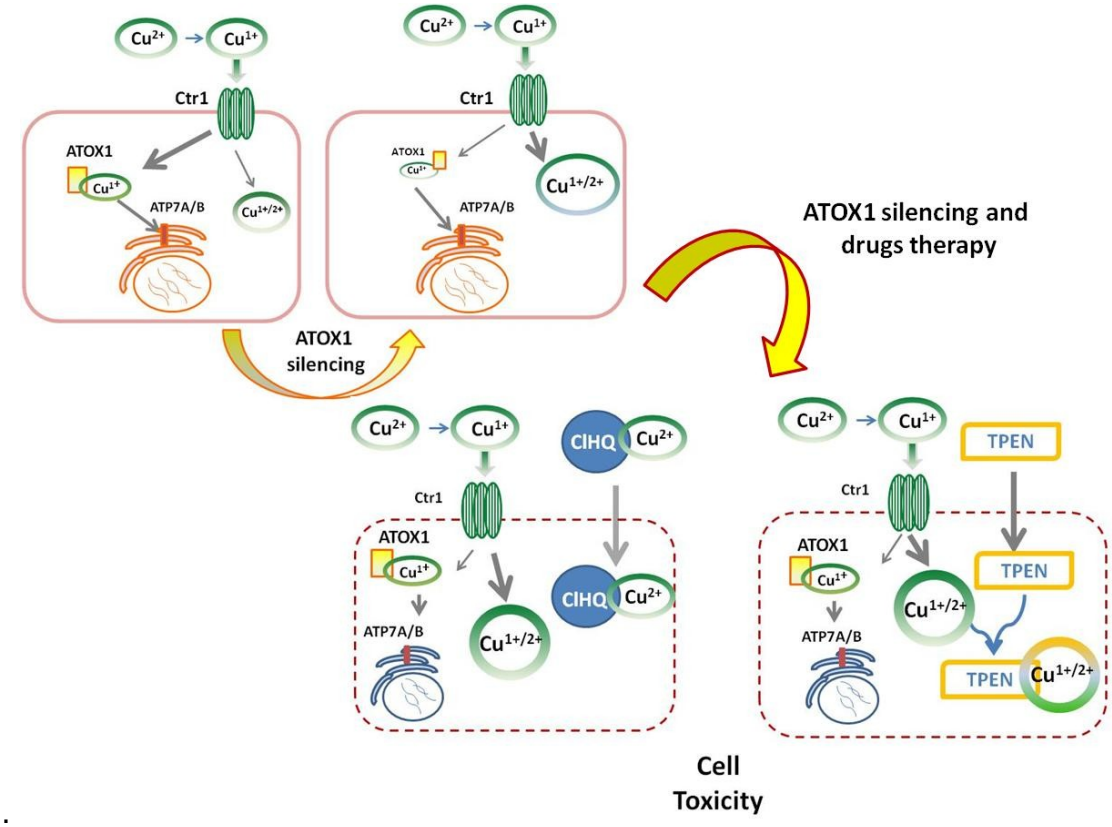

Figure 39. Copper dyshomeostasis induced by Atox1 silencing enhances toxicity of copper overload or treatments with ClHQ (5-chloro-8-hydroxyquinoline)/Cu^{II} complexes or with copper chelator TPEN (N,N,N',N-tetrakis (2-pyridylmethyl) ethylenediamine).

New data have recently been reported showing a protective effect of ATOX1 on cells grown in low GSH [**Kelner *et al.,* 2012**], along with the studies illustrating the dual role of ATOX1 in maintaining the mRNA levels for the secreted Cu/Zn dependent superoxide dismutase 3, SOD3 along with transferring copper to SOD3 during biosynthesis [**Jeney *et al.,* 2005**]. It has been found that in proliferating cells, the C*XX*C metal binding site of ATOX1 is mostly reduced and that high glutathione level assists the maintenance of this state. Changes in GSH/GSSG balance altered: i) the redox status of ATOX1, indicating that glutathione balance is essential for normal activity of the copper secretion pathway; ii) the cooperative relationship of copper export and glutathione homeostasis in maintaining cell viability.

In the attempt to answer to the question concerning the reasons for which the ATOX1-/- cells lose viability in low glutathione, also affecting the two pathways that characterize normal cellular copper homeostasis, it has been suggested that metallostasis alteration "would have several metabolic consequences [**Hatori and Lutsenko 2013**]: (i) the loss of functional maturation of oxidoreductases in the secretory pathway, (ii) copper overload in inappropriate cellular compartments such as the nucleus [**Burkhead *et al.,* 2011**] and cytosol vesicles [**Miyayama *et al.,* 2009**] and (iii) potential induction [**Suzuki *et al.,* 2002**] and sequestration of bioavailable copper by metallothioneins [**Nartey *et al.,* 1987**].

The mechanisms of actions proposed for TPEN-dependent cell killing are quite varied [51 **Makhov *et al.,* 2008**], including the ability to induce cell death by chelating copper to produce TPEN-copper complexes that engage in redox cycling to selectively eliminate colon cancer cells [**Safaei *et al.,* 2009**]. Furthermore, TPEN treatment results in depletion of glutathione causing increased redox stress [**Nakatani *et al.,* 2000**], thus allowing for rationalizing the results here reported on the increased toxicity of this chelating molecule in ATOX1 silenced Caco-2 cells where the glutathione depletion weakens the cellular defense to oxidative stress.

The demonstration that ATOX1 is a determinant factor for the sensitivity to such ionophore and chelating therapy could stimulate further research aimed to assess the expression level of this chaperone in different form of tumors. While this thesis was submitted, Wang and colleagues on Nature chemistry [2015] have reported the possibility to adopt small molecules to inhibit the human copper chaperones ATOX1 and CCS in order to provide a selective approach to disrupt copper cellular transporter and attenuate tumor growth in mouse models. Wang and colleagues affirmed that the cell proliferation inhibition demonstrated though the knockdown of ATOX1 and CCS establishes these copper chaperons as potential new targets for future anticancer biomedical research and therapeutic developments. On the basis of the data obtained

in this thesis, it is proposed a new therapeutic strategy, based on copper-dependent cytotoxic drugs in combination with therapeutic strategies aimed to decreasing ATOX1 activity.

Concluding Remarks

In this thesis the following specific aims have been discussed:

1. The public database: Cancer Genome Atlas Network has been consulted in order to reveal the presence of somatic mutations in copper homeostasis genes (CHGs) in colorectal cancer, and such analysis, performed on 228 colorectal tumor samples, has revealed that inactivating mutations are extremely rare in CHGs.
2. The collection of whole transcriptome profiles by oligonucleotide microarrays represents the second aim of the thesis. CHGs mRNA levels have been measured in 37 colorectal carcinoma samples in comparison to matched normal colonic mucosae. The transcriptome analysis has been perfomed using the last Human Transcriptome Array (HTA 2.0, Affymetrix) which allows to analyze simultaneously 40.000 coding transcripts and 20.000 non-coding transcripts and to reveal variations of mRNA levels between in colorectal cancer samples respect to normal colonic mucosae. The gene expression analysis has showed an up-regulation of several transcripts involved in copper homeostasis pathway (such as SLC31A1, SLC31A2, COX11, SCO1, SOD1) in two different conditions. On the contrary, some genes did not show variations of expression between two tested conditions suggesting the idea that these genes, if experimental altered in their expression, could represent the good targets for specific drug treatments. The transcriptome analysis by the last generation on oligonucleotide microarrays gives a possibility to analyse gene expression levels and single exon expression levels. In the 37 human colorectal samples, the exon-level expression analysis has been revealed the presence of alternative transcripts prevalent in a condition respect to other.

3. In this part of thesis the experimental down-regulation, by short interfering, of a copper chaperone ATOX1, significantly reduced the tumor growth in a Caco2 colorectal cell line. It has been demonstrated that the copper addition increase the toxic effects of some copper binding compounds, in particular, the ionophore copper-ionophore 5-chloro-8-hydroxyquinoline (ClHQ) and the copper chelator (N,N,N'N',-tetrakis (2-pyridylmethyl)ethylenediamine (TPEN) in two human colorectal cancer cell lines (Caco-2 and HT29). Moreover, the Atox1 silencing has enhanced the toxic effects of copper-ClHQ complexes and TPEN in Caco-2 cells confirming that the inhibition of copper chaperone

Atox1 could be a good strategy to attenuate the cancer cell proliferation and to increase the anticancer effects of some copper binding drugs.

REFERENCES

- **Aaltonen L.A., Peltomaki P., Leach F.S., et** al. Clues to the pathogenesis of familial colorectal cancer. Science 1993;260:812–816.
- **Aicha Ba L., Doering M., Burkholz T., Jacob C.** Metal trafficking: from maintaining the metal homeostasis to future drug design. Metallomics, 2009, 1, 292–311
- **Alvarez, H. M.** *et al.* Tetrathiomolybdate inhibits copper trafficking proteins through metal cluster formation. *Science* 2010; **327,** 331–334.
- **Ba L.A., Doering M., Burkholz T., Jacob C.** Metal trafficking: from maintaining the metal homeostasis to future drug design. *Metallomics.* 2009; 1(4):292-311.
- **Banci L., Bertini I., Ciofi-Baffoni S., Hadjiloi T., Martinelli M., Palumaa P.** Mitochondrial copper(I) transfer from Cox17 to Sco1 is coupled to electron transfer. PNAS 2008**;** 6803–6808.
- **Bisgaard M.L., Fenger K., Bulow S., Niebuhr E., Mohr J.** Familial adenomatous polyposis (FAP): frequency, penetrance, and mutation rate. *Hum Mutat* 1994; **3**: 121–5
- **Brewer, G. J.** Anticopper therapy against cancer and diseases of inflammation and fibrosis. *Drug Discov Today* 2005; **10,** 1103–1109.
- **Burstein E., Hoberg J.E., Wilkinson A.S., Rumble J.M., Csomos R.A., Komarck C.M., Maine G.N., Wilkinson J.C., Mayo M.W., Duckett C.S.** COMMD proteins, a novel family of structural and functional homologs of MURR1. J Biol Chem 2005; 280:22222–22232.
- **Cancer Genome Atlas Network** Comprehensive molecular characterization of human colon and rectal cancer. *Nature* 2012 **487**, 330–337.
- **Cao B., Li J., Zhu J., Shen M., Han K., Zhang Z., Yu Y., Wang Y., Wu D., Chen S., Sun A., Tang X., Zhao Y., Qiao C., Hou T. and Mao X.**. The antiparasitic clioquinol induces apoptosis in leukemia and myeloma cells by inhibiting histone deacetylase activity, The journal of biological chemistry. 22, (2013), vol. 288, no. 47, pp. 34181–34189.
- **Carraway R.E. and Dobner P.R..** Zinc pyrithione induces ERK- and PKC-dependent necrosis distinct from TPEN-induced apoptosis in prostate cancer cells. BiochimBiophysActa. (2012);1823(2):544-57.
- **Chen D., Cui Q.C., Yang H., Barrea R.A., Sarkar F.H., Sheng S., Yan B., Reddy G.P., and Dou Q.P.** Clioquinol, a therapeutic agent for Alzheimer's disease, has proteasome-inhibitory, androgen receptorsuppressing, apoptosis-inducing, and antitumor activities in human prostate cancer cells and xenografts, Cancer Res (2007) 67, 1636-1644.

- **Cleary S.P., et al.** Germline MutY human homologue mutations and colorectal cancer: a multisite case-control study. Gastroenterology 2009;136(4):1251–60.
- **Cottrell S., Bicknell D., Kaklamanis L., Bodmer W.F**. Molecular analysis of APC mutations in familial adenomatous polyposis and sporadic colon carcinomas [see comments]. *Lancet* 1992;340: 626–30.
- **Daniel K.G., Chen D., Orlu S., Cui Q.C., Miller F.R., Dou Q.P.** Clioquinol and pyrrolidinedithiocarbamate complex with copper to form proteasome inhibitors and apoptosis inducers in human breast cancer cells. Breast Cancer Res. (2005); 7(6):R897-908.
- **De Feo C.J., Aller S.G., Siluvai G.S., Blackburn N.J., Unger V.M.** Three-dimensional structure of the human copper transporter hCTR1. Proc Natl Acad Sci U S A. 2009; 106:4237–4242.
- **Dìez M., Cerdàn F.J., Arroyo M., Balibrea J.L.**, Use of the copper/zinc ratio in the diagnosis of lung cancer. Cancer. (1989) 15;63(4):726-30.
- **Ding W.Q. and Lind S.E.**, Metal Ionophores – An Emerging Class of Anticancer Drugs. IUBMB Life, (2009), 61(11): 1013–1018.
- **Ding W.Q., Liu B., Vaught J.L.,** Anticancer Activity of the Antibiotic Clioquinol. Cancer Res 2005;65:3389-3395 (2005).
- **Ding W.Q., Liu B., Vaught J.L., Palmiter R.D. and Lind S.E.,** Clioquinol and docosahexaenoic acid act synergistically to kill tumor cells. Mol. Cancer Ther. (2006) 5. 1864–1872.
- **Fatfat M., Merhi R.A., Rahal O., Stoyanovsky D.A., Zaki A., Haidar H., Kagan V.E., Gali-Muhtasib H., Machaca K.**, Copper chelation selectively kills colon cancer cells through redox cycling and generation of reactive oxygen species. BMC Cancer. (2014) 21;14:527. doi: 10.1186/1471-2407-14-527.
- **Fearon ER, Vogelstein B.** A genetic model for colorectal tumorigenesis. Cell 1990;61:759
- **Fishel R.** Mismatch repair, molecular switches, and signal transduction. Genes Dev 1998;12:2096–2101.
- **Fishel R. & , Kolodner R. D**. Identification of mismatch repair genes and their role in the development of cancer. *Curr. Opin. Genet. Dev.* 1995. **5**, 382–395.
- **Formigari A., Gregianin E., Irato P.** The effect of zinc and the role of p53 in copper-induced cellular stress responses. *J Appl Toxicol*. 2013; 33(7):527-36.
- **Franklin R.B., Costello L.C.** The important role of the apoptotic effects of zinc in the development of cancers. *J Cell Biochem*. 2009; 106(5):750-7.

- **Goel A., Nagasaka T., Arnold C.N., Inoue T., Hamilton C., Niedzwiecki D., Compton C., Mayer R.J., Goldberg R., Bertagnolli M.M., Boland C.R**. The CpG island methylator phenotype and chromosomal instability are inversely correlated in sporadic colorectal cancer. *Gastroenterology* 2007; **132**: 127-138
- **Gollin S.M.** Mechanisms leading to chromosomal instability. Semin Cancer Biol 2005; 15:33–42.
- **Grady W. and Carethers J**. Genomic and Epigenetic Instability in Colorectal Cancer Pathogenesis. Gastroenterology. 2008 135(4): 1079–1099.
- **Grady W.M**. Genomic instability and colon cancer. Cancer Metastasis Rev 2004;23:11–27.
- **Grady WM**.. Genetic testing for high-risk colon cancer patients. Gastroenterology 2003. 124(6):1574–94.
- **Guo Y., Smith K., Lee J., Thiele D.J., Petris M.J.** Identification of methionine-rich clusters that regulate copper-stimulated endocytosis of the human Ctr1 copper transporter. J Biol Chem 2004; 279:17428–17433.
- **Gupta S.K., Singh S.P., Shukla V.K.** Copper, zinc, and Cu/Zn ratio in carcinoma of the gallbladder. *J Surg Oncol.* 2005; 91(3):204-8.
- **Hampel H**, et al. Screening for Lynch syndrome (hereditary nonpolyposis colorectal cancer) among endometrial cancer patients. Cancer Res 2006;66(15):7810–7.
- **Hampel H**., et al. Feasibility of screening for Lynch syndrome among patients with colorectal cancer. J Clin Oncol 2008;26(35):5783–8.
- **Hamza, I., Schaefer, M., Klomp, L. W. & Gitlin, J. D.** Interaction of the copper chaperone HAH1 with the Wilson disease protein is essential for copper homeostasis. *Proc Natl Acad Sci USA* 1999; **96,** 13363–13368 (.
- **Hanahan D, Weinberg RA**. The hallmarks of cancer. Cell 2000;100:57–70.
- **Harrison M.D., Jones C.E., Solioz M., Dameron C.T.,** Intracellular copper routing: the role of copper chaperones. Trends in biochemical sciences (2000) 25: 29–32.
- **Hatori Yuta and Svetlana Lutsenko**. An Expanding Range of Functions for the Copper Chaperone/Antioxidant Protein Atox1. Antioxidants & redox signaling 2013 Volume 19, Number 9,
- **Hemminki A.***, et al.* Loss of the wild type *MLH1* gene is a feature of hereditary nonpolyposis colorectal cancer. *Nature Genet.* (1994) **8**, 405–410.

- **Horng Y.C., Cobine P.A., Maxfield A.B., Carr H.S., Winge D.R.** Specific copper transfer from the Cox17 metallochaperone to both Sco1 and Cox11 in the assembly of yeast cytochrome *c* oxidase. J Biol Chem 2004; 279:35334–35340.
- **Hyun H.J., Sohn J.H., Ha D.W., Ahn Y.H., Koh J.Y. and Yoon Y.H.**, Depletion of intracellular zinc and copper with TPEN results in apoptosis of cultured human retinal pigment epithelial cells. Investigative Ophthalmology & Visual Science. (2001). Vol. 42. No. 2.
- **Itoh S., Kim HW., Nakagawa O., Ozumi K., Lessner S.M., Aoki H., Akram K., McKinney R.D., Ushio-Fukai M., Fukai T.** Novel Role of Antioxidant-1 (Atox1) as a Copper-dependent Transcription Factor Involved in Cell Proliferation. The journal of biological chemistry 2008 VOL. 283, NO. 14, pp. 9157–9167.
- **Jasperson K. W.**, **Tuohy T.M.**, **Neklason D.W.**, **Burt Randall W**. Hereditary and Familial Colon Cancer. Gastroenterology. 2010 138(6): 2044–2058.
- **Jemal A., Bray F., Center M.M., Ferlay J., Ward E., Forman D**. Global cancer statistics. *CA Cancer J Clin* 2011;**61**:69-90.
- **Kastrinos F**., et al. Risk of pancreatic cancer in families with Lynch syndrome. JAMA 2009;302(16):1790–5.
- **Klomp A.E., et al.** The N-terminus of the human copper transporter 1 (hCTR1) is localized extracellularly, and interacts with itself. Biochem J. 2003; 370(Pt 3):881–889.
- **Klomp L.W., Lin SJ., Yuan D.S., Klausner R.D., Culotta V.C., Gitlin J.D.** Identification and Functional Expression of *HAH1*, a Novel Human Gene Involved in Copper Homeostasis. The journal of biological chemistry. 1997; 9221–9226
- **Knudson, A. G. Jr** Hereditary cancer, oncogenes, and antioncogenes. *Cancer Res.* **45**, 1437–1443 (1985). **This paper is important historically, as it contains Knudson's two-hit hypothesis of carcinogenesis.**
- **Kuo M. T.**, **Fu S.**, **Savara N.**, **Chen H. H. W.** Role of the Human High-Affinity Copper Transporter (hCtr1) in Copper Homeostasis Regulation and Cisplatin Sensitivity in Cancer Chemotherapy. Cancer Res. 2012. 15; 72(18): 4616–4621.
- **Leary S.C., *et al*.** Human SCO1 and SCO2 have independent, cooperative functions in copper delivery to cytochrome *c* oxidase. Hum Mol Genet 2004; 13:1839–1848.
- **Lee J., Prohaska J.R., Thiele D.J.** Essential role for mammalian copper transporter Ctr1 in copper homeostasis and embryonic development. Proc Natl Acad Sci U.S.A 2001; 98:6842–6847.

- **Lengauer C., Kinzler K., Vogelstein B**. Genetic instabilities in human cancers. Nature 1998; 396:643 649.
- **Liang Z.D., Tsai W.B., Lee M.Y., Savaraj N., Kuo M.T.** Specificity protein 1 (Sp1) oscillation is involved in copper homeostasis maintenance by regulating human high-affinity copper transporter 1 expression. Mol Pharmacol. 2012; 81:455–64.
- **Lichtenstein P., Holm N., Verkasalo P., Iliadou A., Kaprio J., Koskenvuo M., Pukkala E., Skytthe A., Hemminki K.** Environmental and heritable factors in the causation of cancer. New England Journal of Medicine 2000;343:78–85.
- **Livak K.J., Schmittgen T.D.**, Analysis of relative gene expression data using real-time quantitative PCR and the 2(-Delta Delta C(T)) Method. Methods. (2001);25(4):402-8.
- **Loeb, L. A., Springgate, C. F. & Battula, N.** Errors in DNA replication as a basis of malignant changes. *Cancer Res.* 1974. **34**, 2311–2321.
- **Lutsenko S.** Human copper homeostasis: a network of interconnected pathways. *Curr Opin Chem Biol.* (2010);14(2):211-7.
- **Lutsenko S., Efremov R.G., Tsivkovskii R., Walker J.M.** Human copper-transporting ATPase ATP7B (the Wilson's disease protein): biochemical properties and regulation. J Bioenerg Biomembr 2002; 34:351–362
- **Lynch H.T., de la Chapelle A**. Hereditary colorectal cancer. N Engl J Med 2003; 348(10):919–32
- **Lynch H.T., Snyder C.L., Shaw T.G., Heinen C.D., Hitchins M.P.** Milestones of Lynch syndrome: 1895–2015. Nature reviews. Volume 15. 2015
- **Mao X. and Schimmer A.D.,** The toxicology of Clioquinol, Toxicol Lett (2008) 182,1-6.
- **Mao X., Li X., Sprangers R., Wang X., Venugopal A., Wood T., Zhang Y., Kuntz D.A., Coe E., Trudel S., Rose R. Batey D.A., Kay L.E., and Schimmer A.D.,** Clioquinol inhibits the proteasome and displays preclinical activity in leukemia and myeloma, Leukemia (2009) 23, 585-590.
- **Margalioth E.J., Schenker J.G., Chevion M.,** Copper and zinc levels in normal and malignant tissues. Cancer. (1983) 1;52(5):868-72.
- **Marra G.,Boland C.R**. DNA repair and colorectal cancer. Gastroenterol Clin North Am 1996; 25:755–772.
- **Miyayama T., Suzuki K.T., Ogra Y.** Copper accumulation and compartmentalization in mouse fibroblast lacking metallothionein and copper chaperone, Atox1-Toxicology and Applied Pharmacology 237 (2009) 205–213

- **Mosmann T.,** Rapid Colorimetric Assay for Cellular Growth and Survival: Application to Proliferation and Cytotoxicity Assays. Journal of lmmunological Methods, 65 (1983) 55-63 55.
- **Mufti A. R., Burstein E. and Duckett C. S.**. XIAP: cell death regulation meets copper homeostasis. Arch Biochem Biophys. 2007 15; 463(2): 168–174.
- **Mufti A.R., Burstein E., Duckett C.S.** XIAP: cell death regulation meets copper homeostasis. Arch Biochem Biophys. 2007; 463(2):168-74.
- **Muller P., Klomp L.** ATOX1: A novel copper-responsive transcription factor in mammals? The International Journal of Biochemistry & Cell Biology 2009; 1233–1236.
- **Nevitt T, Ohrvik H, Thiele DJ.** Charting the travels of copper in eukaryotes from yeast to mammals. *Biochim Biophys Acta*. 2012 ;1823(9):1580-93.
- **Ozumi, K. *et al.*** Role of copper transport protein antioxidant 1 in angiotensin II-induced hypertension: a key regulator of extracellular superoxide dismutase. *Hypertension* 2012; **60,** 476–486
- **Pang W.**, **Leng X., Lu H., Yang H., Song N., Tan L., Jiang Y., Guo C.,** Depletion of intracellular zinc induces apoptosis of cultured hippocampal neurons through suppression of ERK signaling pathway and activation of caspase-3. Neurosci Lett. (2013) 27;552:140-5.
- **Parsons, R.** *et al.* Hypermutability and mismatch repair deficiency in RER+ tumor cells. *Cell* (1993). **75**, 1227–1236
- **Peltomaki P. and Vasen H.** Mutations associated with HNPCC predisposition --Update of ICGHNPCC/ INSiGHT mutation database. Dis Markers 2004;20(4–5):269–76.
- **Petris, M. J., Mercer, J. F., Culvenor, J. G., Lockhart, P., Camakaris, J.** Ligand-regulated transport of the Menkes copper P-type ATPase efflux pump from the Golgi apparatus to the plasma membrane: a novel mechanism of regulated trafficking, *EMBO J.* 1996 *15*, 6084-6095
- **Puig S., Lee J., Lau M., Thiele D.J**. Biochemical and genetic analyses of yeast and human high affinity copper transporters suggest a conserved mechanism for copper uptake. J Biol Chem. 2002; 277(29):26021–26030.
- **Puig S., Thiele D.J.** Molecular mechanisms of copper uptake and distribution. Curr Opin Chem Biol 2002; 6:171–180.
- **Rees E.M., Lee J., Thiele D.J.** Mobilization of intracellular copper stores by the ctr2 vacuolar copper transporter. J Biol Chem 2004; 279:54221–54229

- **Ribic C.M.,** et al. Tumor microsatellite-instability status as a predictor of benefit from fluorouracil based adjuvant chemotherapy for colon cancer. N Engl J Med 2003;349(3):247–57.
- **Robinson N.J. and Winge D.R,** Copper metallochaperones. Annual review of biochemistry (2010) 79: 537–562.
- **Rowland L.P., Shneider N.A**. Amyotrophic lateral sclerosis. N Engl J Med 2001; 344:1688–1700.
- **Rustgi A.K**. The genetics of hereditary colon cancer. Genes Dev 2007;21(20):2525–38.
- **Sheffer M., Bacolod M., Zuk O., Giardina S., Pincas H., Barany F., Paty P., Gerald W., Nottermanf D., Domany E.** Association of survival and disease progression with chromosomal instability: A genomic exploration of colorectal cancer. PNAS, 2009 vol. 106 no. 17 (7131–7136)
- **Shui Ping Tu, Yun Wei Sun, Jian Tao Cui, Bing Zou, Marie C. M. Lin, Qing Gu, Shi Hu Jiang, Hsiang Fu Kung, Robert G. Korneluk, Benjamin C. Y. Wong.** Tumor Suppressor XIAP-Associated Factor 1 (XAF1) Cooperates with tumor necrosis factor-related apoptosis-inducing ligand to suppress colon cancer growth and trigger tumor regression. Cancer 2010;116:1252–63.
- **Skrzycki M., Majewska M., Podsiad M., Czeczot H**. Expression and activity of superoxide dismutase isoenzymes in colorectal cancer. ABP Vol. 56 No. 4/2009, 663–670
- **Song I.S., Chen H.H., Aiba I., Hossain A., Liang ZD, Klomp L.W**., et al. Transcription factor Sp1 plays an important role in the regulation of copper homeostasis in mammalian cells. Mol Pharmacol. 2008; 74:705–13.
- **Sperandio S., de Belle I., Bredesen D.E.,** An alternative, nonapoptotic form of programmed cell death. Proc. Natl. Acad. Sci. U.S.A. (2000), 97, 14376.
- **Stephen B. Howell, Roohangiz Safaei, Christopher A. Larson, and Michael J. Sailor**. Copper Transporters and the Cellular Pharmacology of the Platinum-Containing Cancer Drugs.MOLECULAR PHARMACOLOGY Vol. 77, No. 6 77:887–894, 2010
- **Stoffel E**., et al. Calculation of risk of colorectal and endometrial cancer among patients with Lynch syndrome. Gastroenterology 2009;137(5):1621–7.
- **Strausak D, Howie MK, Firth SD, Schlicksupp A, Pipkorn R, Multhaup G, Mercer JF.** Kinetic analysis of the interaction of the copper chaperone Atox1 with the metal binding sites of the Menkes protein. J Biol Chem. 2003 6;278(23):20821-7

- **Tao T.Y., Liu F., Klomp L., Wijmenga C., Gitlin J.D.** The copper toxicosis gene product Murr1 directly interacts with the Wilson disease protein. J Biol Chem 2003; 278:41593–41596.
- **Tardito S., Barilli A., Bassanetti I., Tegoni M., Bussolati O., Franchi-Gazzola R., Mucchino C., and Marchiò L.** Copper-dependent cytotoxicity of 8-Hydroxyquinoline derivatives correlates with their hydrophobicity and does not require caspase activation dx.doi.org/10.1021/jm301053a J. Med. Chem. (2012), 55, 10448−10459.
- **Tsao J.L., Yatabe Y., Salovaara R., et al.** Genetic reconstruction of individual colorectal tumor histories. Proc Natl Acad Sci U S A 2000;97:1236–1241.
- **Voskoboinik I. and Camakaris J.** Menkes copper-translocating P-type ATPase (ATP7A): biochemical and cell biology properties, and role in Menkes disease. J Bioenerg Biomembr 2002; 34:363–371.
- **Wang J., Luo C., Shan C., You Q., Lu J., Elf S., Zhou Y., Wen Y., Vinkenborg J.L., Fan J., Kang H., Lin R., Han D., Xie Y., Karpus J., Chen S., Ouyang S., Luan C., Zhang N., Ding H., Merkx M., Liu H., Chen J., Jiang H., He C.** Inhibition of human copper trafficking by a small molecule significantly attenuates cancer cell proliferation. Nat Chem. (2015);7(12):968-79.
- **Wernimont A.K., Huffman D.L., Lamb A.L., O'Halloran T.V., Rosenzweig A.C**. Structural basis for copper transfer by the metallochaperone for the Menkes/Wilson disease proteins. Nat Struct Biol. 2000.
- **Yannone S. M.**, **Hartung S.**, **Menon A. L.**, **Adams M. W. W.**, **Tainer J. A.** Metals in biology: defining metalloproteomes. *Curr Opin Biotechnol*. (2012); 23(1):89-95.
- **Zalewska M., Trefon J., Milnerowicz H.,** The role of metallothionein interactions with other proteins. Proteomics. 2014; 14(11):1343-56.
- **Zhai S., Yang L., Cui Q.C., Sun Y., Dou Q.P., Yan B.,** Tumor cellular proteasome inhibition and growth suppression by 8-hydroxyquinoline and clioquinol requires their capabilities to bind copper and transport copper into cells. J BiolInorg Chem. (2010) Feb;15(2):259-69.